

การควบคุมคุณภาพของระบบคอมพิวเตอร์ควบคุมการแสดงภาพรังสี



นางเพ็ชรลีย์ สุวรรณประดิษฐ์

สถาบันวิทยบริการ
วิทยานิพนธ์นี้เป็นส่วนหนึ่งของการศึกษาตามหลักสูตรปริญญาวิทยาศาสตรมหาบัณฑิต
สาขาวิชาฉายาเวชศาสตร์ ภาควิชารังสีวิทยา
คณะแพทยศาสตร์ จุฬาลงกรณ์มหาวิทยาลัย
ปีการศึกษา 2547
ISBN 974-17-6531-2
ลิขสิทธิ์ของจุฬาลงกรณ์มหาวิทยาลัย

**QUALITY CONTROL PROGRAM OF THE COMPUTED RADIOGRAPHY
SYSTEM**



Mrs. Petcharleeya Suwanpradit

A Thesis Submitted in Partial Fulfillment of the Requirements

For the Degree of Master of Science in Medical Imaging

Department of Radiology

Faculty of Medicine

Chulalongkorn University

Academic Year 2004

ISBN 974-17-6531-2

Thesis Title Quality control program of the computed radiography system.
By Mrs. Petcharleeya Suwanpradit
Field of Study Medical Imaging
Thesis Advisor Associate Professor Anchali Krisanachinda, Ph.D.
Thesis Co-advisor Assistant Professor Sukalaya Lerdlum, M.D.
 Assistant Professor Kiat Arjhansiri, M.D.

Accepted by the Faculty of Medicine, Chulalongkorn University in Partial
Fulfillment of the Requirements for the Master's Degree

..... Dean of the Faculty of Medicine
(Professor Pirom Kamol-ratanakul, M.D., M.Sc.)

THESIS COMMITTEE

..... Chairman
(Associate Professor Somjai Wangsuphachart, M.D., M.Sc.)

..... Thesis Advisor
(Associate Professor Anchali Krisanachinda, Ph.D.)

..... Thesis Co-advisor
(Assistant Professor Sukalaya Lerdlum, M.D., M.Sc.)

..... Thesis Co-advisor
(Assistant Professor Kiat Arjhansiri, M.D.)

..... Member
(Mrs. Weeranuch Kitsukjit, M.Sc.)

เพ็ชรสิทธิ์ สุวรรณประดิษฐ์ : การควบคุมคุณภาพของระบบคอมพิวเตอร์ควบคุมการแสดงผลภาพรังสี (Quality Control Program of the Computed Radiography System) อาจารย์ที่ปรึกษา : รองศาสตราจารย์ ดร.อัญชลี กฤษณจินดา, อาจารย์ที่ปรึกษาร่วม : ผู้ช่วยศาสตราจารย์แพทย์หญิงสุกัลยา เลิศล้ำ, ผู้ช่วยศาสตราจารย์นายแพทย์เกียรติ อัจฉาญศิริ, 122 หน้า ISBN : 974-17-6531-2

วัตถุประสงค์ : เพื่อประเมินความสัมพันธ์ระหว่างปริมาณรังสีที่ผิว (ESD) กับคุณภาพของภาพรังสี หลังจากการนำวิธีการควบคุมคุณภาพ (QC) ระบบคอมพิวเตอร์ควบคุมการแสดงผลภาพรังสี (CR) ที่ได้มาตรฐานมาใช้ในการทดสอบระบบดังกล่าวในฝ่ายรังสีวิทยา โรงพยาบาลจุฬาลงกรณ์ สภากาชาดไทย

รูปแบบการวิจัย : การวิจัยโดยการทดลองแบบเก็บข้อมูลไปข้างหน้ากับกลุ่มตัวอย่าง 2 กลุ่มที่ยินยอมรับการตรวจแล้ว คือกลุ่มก่อน และกลุ่มหลังการทำการ QC ระบบ CR

สถานที่ทำการวิจัย : หน่วยบริการถ่ายภาพรังสีผู้ป่วยนอก ดึก ภปร. ชั้น 4 ฝ่ายรังสีวิทยา โรงพยาบาลจุฬาลงกรณ์ สภากาชาดไทย

ประชากรที่ศึกษา : ผู้ป่วยนอกทั่วไปจำนวนทั้งสิ้น 1,384 การตรวจ ซึ่งเป็นผู้ป่วยผู้ใหญ่ที่มีอายุอยู่ระหว่าง 16 ถึง 75 ปี มีน้ำหนักร่างกายอยู่ระหว่าง 35 ถึง 114 กิโลกรัม ที่ยินยอมให้ศึกษาใน 8 ชนิดการตรวจ ได้แก่ skull PA, lateral cephalometry, cervical spine AP, chest PA, abdomen AP, lumbo-sacral spine AP และ lateral view และ pelvis AP

เครื่องมือที่ใช้ในการศึกษา : เครื่องเอกซเรย์ชนิดไฟ 1 เฟส 2 เครื่องยี่ห้อฮิตาชิ รุ่น DR-155HM จากบริษัทฮิตาชิ จำกัด ประเทศญี่ปุ่น ภายในห้องเอกซเรย์ หมายเลข 4 และหมายเลข 5 ถูกใช้ร่วมกับเครื่อง CR ยี่ห้อฟูจิ รุ่น FCR 5000 จากบริษัทฟูจิ ไรต์ฟิล์ม จำกัด ประเทศญี่ปุ่น จำนวน 1 เครื่อง ใช้อุปกรณ์รับภาพชนิดเรืองแสงชนิดเบเรียมฟลูออโรเฮไลด์เจือสารยูโรเปียม ประเภทความไวแบบมาตรฐาน ขนาด 24 x 30 ซม และ 35 x 43 ซม ภาพรังสีแบบ soft copy จะถูกวิเคราะห์บนจอภาพ LCD ยี่ห้อ Totoku รุ่น ME 201L ชนิดแสดงรายละเอียดของภาพสูง บน HI- C 655 workstation ส่วน hard copy ได้พิมพ์ภาพลงฟิล์มชนิดเคลเซอร์แบบล้างเปียกยี่ห้อฟูจิ รุ่น FL-IMD ร่วมกับฟิล์มไวต่อแสงเลเซอร์ ยี่ห้อฟูจิ ขนาด 25.7 x 36.4 ซม รุ่น 780-H และขนาด 35 x 43 ซม รุ่น LI-LM นำมาสร้างภาพ RD-20 และนำมาสกรภาพ RF-15 เครื่องมือและอุปกรณ์ในการควบคุมคุณภาพของระบบ CR

วิธีการศึกษา : ในการศึกษาครั้งนี้ได้ทำการเก็บข้อมูล 8 ชนิดการตรวจทางรังสี ด้วยเครื่อง CR ร่วมกับส่วนของน้ำหนัก ส่วนสูง ค่าดัชนีมวลกาย ความหนาแน่นกระดูกกลางบริเวณที่ทำการตรวจ เพื่อใช้กำหนดการตั้งค่าปริมาณรังสี โดยกลุ่มก่อนการ QC นักรังสีการแพทย์เป็นผู้ตั้งค่าปัจจัยต่างๆ ส่วนในกลุ่มหลังการทำการ QC ได้กำหนดปัจจัยค่าปริมาณรังสีตามตารางปริมาณรังสีที่กำหนดให้ หลังจากถ่ายภาพรังสีแล้ว ค่า ESD ของผู้ป่วยได้ถูกคำนวณ ภาพรังสีที่ได้ของทั้ง 2 กลุ่ม ได้ถูกจับคู่เพื่อการวิเคราะห์คุณภาพของภาพแบบสุ่มโดยรังสีแพทย์ที่มีประสบการณ์ทัดเทียมกัน 2 ท่าน

การวัดผล : ค่าเฉลี่ยของ ESD ที่ได้จากการคำนวณในแต่ละการตรวจเมื่อเปรียบเทียบกับเกณฑ์มาตรฐาน และมีความแตกต่างในเปอร์เซ็นต์การถ่ายภาพรังสีระหว่างกลุ่มก่อนและหลังการควบคุมคุณภาพระบบ CR ค่าแตกต่างกันอย่างมีนัยสำคัญหรือไม่

ผลการวิจัย : กลุ่มตัวอย่างที่ได้ทำการเก็บข้อมูลทั้ง 2 กลุ่ม มีความคล้ายคลึงกันดีทั้งในเรื่องของ อายุ เพศ น้ำหนัก และส่วนสูง ผลของเปอร์เซ็นต์การถ่ายภาพรังสีซ้ำเปรียบเทียบกับกันระหว่างกลุ่มก่อนและหลังการควบคุมคุณภาพระบบ CR มีความแตกต่างกันอย่างมีนัยสำคัญ ($P < 0.05$)

สรุป : การควบคุมคุณภาพระบบ CR เป็นวิธีที่มีประสิทธิภาพที่ช่วยลดอัตราการถ่ายภาพรังสีซ้ำ (54.55%, $P < 0.05$) อันเนื่องมาจากความบกพร่องผิดพลาดของระบบ CR ได้ โดยสามารถลดปริมาณรังสีลงได้ 17.69 % ใน chest PA และ 16.22 % ใน lumbo-sacral spine AP แต่ยังคงคุณภาพของภาพเพื่อการวินิจฉัยโรคไว้ได้ ในการศึกษาครั้งนี้พบว่า เครื่องเอกซเรย์ทั้งสองเครื่องให้ปริมาณรังสีที่แตกต่างกัน

ภาควิชา รังสีวิทยา
สาขาวิชา ฉายาเวชศาสตร์
ปีการศึกษา 2547

ลายมือชื่อนิสิต
ลายมือชื่ออาจารย์ที่ปรึกษา
ลายมือชื่ออาจารย์ที่ปรึกษาร่วม
ลายมือชื่ออาจารย์ที่ปรึกษาร่วม.....

4674755030: **MAJOR MEDICAL IMAGING**

KEY WORD: QUALITY CONTROL / COMPUTED RADIOGRAPHY / REJECT AND RETAKE RATE / ESD

PETCHARLEEYA SUWANPRADIT: QUALITY CONTROL PROGRAM OF THE COMPUTED RADIOGRAPHY SYSTEM. THESIS ADVISOR: ASSOC.PROF. ANCHALI KRISANACHINDA, Ph.D. THESIS CO-ADVISOR: ASST.PROF. SUKALAYA LERDLUM, M.D., M.Sc., ASST.PROF. KIAT ARJHANSIRI, M.D., M.Sc. 122 pp ISBN: 974-17-6531-2

Objectives: To evaluate the correlation between the patient radiation dose and the image quality after implement the quality control program to the computed radiography system at the Department of Radiology of King Chulalongkorn Memorial Hospital, Thai Red Cross Society.

Design: Experimental prospective study, prospective, before and after design by using the control (before) and experimental (after) group for QC program intervene to the CR system.

Setting: Department of Radiology, King Chulalongkorn Memorial Hospital, Thai Red Cross Society.

Samples: 1,384 examinations of the adult patients, age ranged from 16 to 75 years, body weight ranged from 35 to 114 kilogram of 8 types of x-ray examination, skull PA, lateral cephalometry, cervical spine AP, chest PA, abdomen AP, lumbo-sacral spine AP and lateral view and pelvis AP.

Materials: Two sets of single-phase x-ray machine (Hitachi DR-155HM, Hitachi, Japan) in Room No. 4 and 5, one set of the computed radiography system, a Fuji computed radiography system model FCR 5000 (Fuji Photo Film Co. Ltd., Japan) were used during the study. Imaging phosphors were of europium doped barium fluorohalide in standard type (ST-V_N). All soft copies were observed on Fuji CR Workstation model HI-C 655 by using Totoku high resolution monochrome liquid crystal display model ME 201L. Hard copies were made on Fuji film type 780-H (25.7 x 36.4 cm) and type LI-LM (35 x 43 cm) on Fuji wet laser imager model FL-IM D with developer (RD-20) and fixer (RF-15) were used. QC accessories were Ionization chamber (Victoreen 4000 M⁺ and Farmer model type 2670), FL18 phantom, wiremesh, steel ruler, resolution test tool, Sensitometer, Densitometer, Tape measurement, copper and aluminum plates and lead block.

Methods: In this study, eight projections of CR images were performed under patient consent form before body weight and height measurement. The body mass index was calculated before setting the exposure factors by the radiological technologists. The radiographic dose was defined as the comparison of the reject and retake rate for the before and after QC of equipment were recorded, calculated the entrance skin dose (ESD) by application of the backscatter factor. Each machine energy entrance surface air kerma (ESAK), mAs, focus-skin-distance and focus-film distance. The matching the before and after QC CR image quality evaluation had been followed the European Commission Quality Criteria Guideline for Diagnostic Radiographic Images on CR workstation monitor by two of equivalent experience radiologists.

Outcome measurements: Entrance skin dose (ESD) was determined from each general radiograph, the calculation of average radiation dose of patient would be corresponded to the reject and retake percentage and used in the statistical analysis.

Results: In 1,384 examinations of the computed radiography, the examinations in two groups of study were well matched for number, age, sex, weight and height for each group. There was a significantly differences of the reject and retake rate after the quality control of the computed radiography system ($P < 0.05$).

Conclusion: The reject and retake rate of the x-ray procedures in this study was reduced 54.55% ($P < 0.05$) after the implementation of the quality control of the CR system. Likewise, the patient skin dose was reduced 17.69 % in chest PA and 16.22 % in lumbo-sacral spine AP view. The result from the QC of x-ray equipment was shown the discrepancy of the entrance skin dose between two x-ray systems. As the QC program of the CR system was initiated using phantom, measuring devices, the result obtained shows the useful parameters benefit for the optimization of the patient dose and the image quality.

| | | |
|----------------|------------------------|------------------------------|
| Department | Radiology | Student's signature..... |
| Field of study | Medical Imaging | Advisor's signature |
| Academic year | 2004 | Co-advisor's signature |
| | | Co-advisor's signature |

ACKNOWLEDGEMENT

The success of this thesis depends on the contributions of many people. In particular, I wish to express gratitude to my advisor, Assoc. Prof. Anchali Krisanachinda, Ph.D., my co-advisors, Asst. Prof. Sukalaya Lerdlum, M.D., M.Sc., and Asst. Prof. Kiat Arjhansiri, M.D., for their guidance, encouragement, hospitality and assessment the image quality of the sample during the whole study. Special thanks are also delivered to Asst. Prof. Somrat Lertmaharit, Mrs. Weeranuch Kitsukjit, M.Sc., and Mr. Wasan Panyaseang, M.Sc., for their invaluable comments and suggestions on biostatistics, to Prof. Kwan Hoong Ng, Ph.D., Prof. Peter Homolka, Ph.D., Prof. Lee Collins, M.Sc., MARPS, FACPSEM, Mr. Napapong Pongnapang, Ph.D., and Assoc. Prof. Sivalee Suriyapee, M.Sc., for their invaluable comments, materials and methods in the quality control of the computed radiography system.

I would like to acknowledge the enthusiastic support from all radiological technologists and all staff at the Out-patient Department of Radiology of King Chulalongkorn Memorial Hospital, Thai Red Cross Society for their sacrifice to complete the study for months, especially Mr. Bunchai Nitayasupaporn and Mrs. Chawee Luechapan for their management. I also would like to thank to Mr. Taweap Sanghangthum, M.Sc., and Mr. Sornjarod Oonsiri for their valuable dose measurement during the computed radiography control program.

Finally I would like to thank to Assoc. Prof. Somjai Wangsuphachart, M.D., M.Sc., Head of Department of Radiology for her kind support through my study and particular thanks to King Chulalongkorn Memorial Hospital, Thai Red Cross Society and Faculty of Medicine, Chulalongkorn University for granting me the scholarship to study in this Medical Imaging Program of Department of Radiology.

CONTENT

| | Page |
|---|-------------|
| ABSTRACT (THAI) | iv |
| ABSTRACT (ENGLISH) | v |
| ACKNOWLEDGEMENTS | vi |
| LIST OF TABLES | x |
| LIST OF FIGURES | xiii |
| LIST OF ABBREVIATIONS | xv |
| CHAPTER I INTRODUCTION | |
| Background and rationale | 1 |
| Assumption | 1 |
| Definition | 2 |
| CHAPTER II REVIEW OF RELATED LITERATURE | |
| Physics of the computed radiography | |
| 2.1. Introduction | 3 |
| 2.2. Historical background | 3 |
| 2.3. The CR System Overview | 4 |
| 2.3.1. Image acquisition | |
| 2.3.1.1. Photostimulable phosphors | 5 |
| 2.3.1.1.1. Types of photostimulable phosphors | 6 |
| 2.3.1.1.2. PSP receptor characteristics | 7 |
| 2.3.1.1.3. Mechanisms of trapping and photostimulation..... | 8 |
| 2.3.1.2. X-ray properties of photostimulable phosphors..... | 11 |
| 2.3.1.3. CR imaging plates (IPs)..... | 11 |
| 2.3.2. Image processing | |
| 2.3.2.1. The CR reader | 11 |
| 2.3.2.2. Image Data Pre-Processing..... | 21 |
| 2.3.2.3. Image Data Post-Processing..... | 23 |
| 2.3.2.4. Exposure indicators | 26 |
| 2.3.2.5. CR Exposure Recommendations..... | 27 |
| 2.3.2.6. PSP image characteristics | 28 |
| 2.3.3. Image presentation | 29 |
| 2.3.3.1 Laser Film Printers..... | 30 |
| 2.3.3.2 CRT and LCD Monitors..... | 30 |
| 2.3.4. Image data managing | |
| 2.3.4.1. System configurations and digital soft copy interfaces | 31 |

CONTENT (continued)

| | page |
|---|-----------|
| 2.4. Clinical application of complete CR systems | |
| 2.4.1. Portable | 32 |
| 2.4.2. General radiography | 33 |
| 2.4.3. Mammography | 33 |
| 2.5. Quality assurance and quality control for computed radiography system | |
| 2.6. Dose Reference Level (DRL)..... | 35 |
| Review the related literatures | 36 |
| CHAPTER III CONCEPTUAL FRAMEWORK, RESEARCH QUESTIONS AND RESEARCH OBJECTIVES | |
| 3.1. Conceptual Framework | 37 |
| 3.2 Research Questions | 37 |
| 3.3 Research Objectives | 38 |
| 3.4 Hypothesis | 38 |
| CHAPTER IV RESEARCH METHODOLOGY | |
| 4.1. Research Design | |
| 4.1.1 Research Design Model | 39 |
| 4.2. The Sample | |
| 4.2.1. Target Population | 40 |
| 4.2.2. Sample Population | 40 |
| 4.2.3. Eligible criteria | |
| 4.2.3.1 Inclusion criteria | 40 |
| 4.2.3.2 Exclusion criteria | 40 |
| 4.2.4. Sample Size Estimation | 40 |
| 4.3. Experimental Maneuver | |
| 4.3.1. Study Methodology | 41 |
| 4.3.2. Materials | 43 |
| 4.3.3. Computed Radiography System Quality Control Method | 44 |
| 4.4. Measurement | 51 |
| 4.5. Data Collection | 51 |
| 4.6. Data Analysis | |
| 4.6.1. Summarization of Data | 52 |
| 4.6.2. Data Presentation | 52 |
| 4.6.3. Hypothesis Testing | 52 |
| 4.6.4. Problem from Protocol Deviation | 53 |
| 4.7 Ethical Consideration | 53 |
| 4.8. Limitations | 53 |
| 4.9. Benefit of the Study | 53 |
| 4.10. Administration and Time Schedule | 54 |

CONTENT (continued)

| | page |
|--|---------|
| CHAPTER V RESULT ANALYSIS | |
| 5.1. Result analysis | 55 |
| 5.1.1. Patient Data | 55 |
| 5.1.2. Exposure Conditions | 58 |
| 5.1.3. Patient doses and image quality | 60 |
| 5.2. Result comparison | 64 |
| 5.3. Analysis result factor | 65 |
| CHAPTER VI CONCLUSION DISCUSSION AND RECOMMENDATION | |
| 6.1. Conclusion | 66 |
| 6.2. Discussion | 66 |
| 6.3. Recommendation | 66 |
| REFERENCES | 67 |
| APPENDICES | |
| Appendix A | 69-79 |
| Appendix B | 80-112 |
| Appendix C | 112-113 |
| Appendix D | 114-118 |
| Appendix E | 119-121 |
| VITAE | 122 |

สถาบันวิทยบริการ
จุฬาลงกรณ์มหาวิทยาลัย

LIST OF TABLES

| TABLE | page |
|--|-------------|
| 1. Recommended “S” number limits for general “adult” imaging procedures..... | 27 |
| 2. The total sample size and total number of each examination group used to collect the patient data..... | 42 |
| 3. The items of x-ray machine QC and list of test tools to be used..... | 43 |
| 4. The items of CR machine QC and list of test tools to be used for Commissioning Tests | 44 |
| 5. Time table for the study..... | 54 |
| 6. Comparison of the reject and retake rate data in the period of before and after QC program of 8 examinations..... | 55 |
| 7. Shown the percentage of the reject and retake by causes | 56 |
| 8. Shown the percentage of reject and retake by the types of examination. | 57 |
| 9. Comparison of affect exposure factors data in the period of before and after QC program by body part thickness | 58 |
| 10. Comparison of affect exposure factors data in the period of before and after QC program by body mass index (BMI)..... | 58 |
| 11. Comparison of exposure factor data in the period of before and after QC program of 8 examinations. | 59 |
| 12. Comparison of the entrance skin dose (mGy) data in the period of before and after QC program | 60 |
| 13. Comparison of the image quality data in the period of Before and After QC program of 4 examinations..... | 61 |
| 14. Relationship between the body part thickness (cm) and BMI to the entrance skin dose (mGy) and the image quality of 4 main examinations in both groups were matched by using P value presentation. | 61 |
| 15. Main report of x-ray machine performance room number 4..... | 62 |
| 16. Main report of x-ray machine performance room number 5..... | 63 |
| 17. Main report of CR system performance | 64 |
| APPENDIX A | |
| 18. Patient characteristic details colleted by Technologists for each examination..... | 70 |

LIST OF TABLES (continued)

| TABLE | page |
|---|-------------|
| 19. Case record form..... | 71 |
| 20. Comparison of the Reject and Retake rate data in the period of Before and After QC program intervention for Skull PA view (from paranasal sinuses series)... | 72 |
| 21. Comparison of the Reject and Retake rate data in the period of Before and After QC program intervention for Lateral Cephalometry view..... | 73 |
| 22. Comparison of the Reject and Retake rate data in the period of Before and After QC program intervention for C-spine AP view..... | 74 |
| 23. Comparison of the Reject and Retake rate data in the period of Before and After QC program intervention for Chest PA view..... | 75 |
| 24. Comparison of the Reject and Retake rate data in the period of Before and After QC program intervention for Abdomen AP view..... | 76 |
| 25. Comparison of the Reject and Retake rate data in the period of Before and After QC program intervention for L-S spine AP view..... | 77 |
| 26. Comparison of the Reject and Retake rate data in the period of Before and After QC program intervention for L-S spine lateral view..... | 78 |
| 27. Comparison of the Reject and Retake rate data in the period of Before and After QC program intervention for Pelvis AP view..... | 79 |
| APPENDIX B | |
| 28. X-ray Machine Calibration Room No. 4..... | 80 |
| 29. X-ray Machine Calibration Room No. 5..... | 87 |
| 30. Common backscatter factor data for each x-ray energy..... | 94 |
| 31. Normalized the Entrance Skin Dose ($\mu\text{Gy/mAs}$) from backscatter factor and Entrance Skin Air Kerma at 100 cm of Focus to skin distance for large focal spot of Room No. 4. | 94 |
| 32. Normalized the Entrance Skin Dose ($\mu\text{Gy/mAs}$) from backscatter factor and Entrance Sin Air Kerma at 100 cm of Focus to skin distance for large focal spot of Room No. 5. | 95 |
| 33. Tolerance -The Established Criteria for CR system..... | 96 |
| 34. Computed Radiography Systems Performance..... | 97 |
| 35. Image Display Device Constancy Test Report..... | 110 |
| 36. Viewbox Constancy Test Report..... | 111 |

LIST OF TABLES (continued)

| TABLE | page |
|--|-------------|
| APPENDIX C | |
| 37. Approaches to Reference Levels (September 2001)..... | 112 |
| 38. Listing of Dose Reference Level (DRL; September 2001)..... | 113 |
| APPENDIX D | |
| 39. Image Quality Grading Forms..... | 114 |
| 40. Exposure factors chart | 117 |
| APPENDIX E | |
| Patient Information Sheet..... | 119 |
| Consent form..... | 121 |

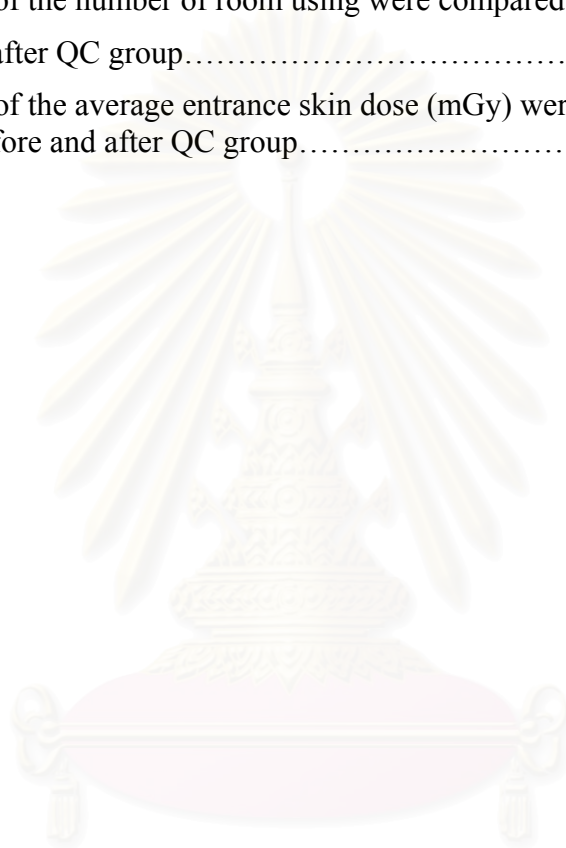

 สถาบันวิทยบริการ
 จุฬาลงกรณ์มหาวิทยาลัย

LIST OF FIGURES

| FIGURE | page |
|---|-------------|
| 1. Representation of CR image acquisition and dataflow..... | 4 |
| 2. PSP image acquisition and processing | 5 |
| 3. Absorption characteristics of BaFBr, CsI, and Gd ₂ O ₂ S phosphors..... | 6 |
| 4. Crystal structure of BaFX | 7 |
| 5. Shows energy levels expressing the PSL mechanism of the photostimulable phosphor..... | 8 |
| 6. An energy diagram of the excitation and photo-stimulated luminescence processes in a BaFBr:Eu ²⁺ phosphor..... | 9 |
| 7. Stimulation and emission spectra for BaFBr:Eu ²⁺ and BaFBr _{0.85} I _{0.15} :Eu ²⁺ storage phosphors..... | 10 |
| 8. Overall concept of CR readout systems..... | 12 |
| 9. Major components of a PSP reader..... | 13 |
| 10. Component-level illustration of a line-scan CR detector..... | 15 |
| 11. A diagram of the raster-scan of the phosphor detector indicates the fast scan (laser scan) direction and the sub-scan (plate scan) direction..... | 16 |
| 12. Flying spot CR readout scanner..... | 17 |
| 13. The characteristic curve of rare-earth screen-film (400 speed) and the PSP receptor are compared..... | 19 |
| 14. The phosphor plate cycle..... | 20 |
| 15. One-dimensional flat field methods correct for “shading” variations caused by the repetitive variations in laser-beam output and light-guide pick-up characteristics..... | 21 |
| 16. Illustrates the data “finding” and “scaling” steps..... | 22 |
| 17. Simplified edge-enhancement example using a single bandpass frequency Kernel..... | 24 |
| 18. Multi-scale, multi-frequency approach for simultaneous contrast and Frequency enhancement of images across all frequency ranges of the image..... | 25 |
| 19. Conceptual Framework of research..... | 37 |
| 20. Research Design Model..... | 39 |
| 21. Set-up for exposure index calibration..... | 46 |
| 22. Positions of the ROI’s for uniformity tests..... | 47 |
| 23. Scaling assessment..... | 48 |

LIST OF FIGURES (continued)

| FIGURE | page |
|--|-------------|
| 24. Calculated the aspect ratio $x1/y1$ | 48 |
| 25. Bar graph was shown the reject and retake rate by causes | 56 |
| 26. Bar graphs was shown the reject and retake rate by types of examination..... | 57 |
| 27. Bar graphs of the number of room using were compared between before and after QC group..... | 59 |
| 28. Bar graphs of the average entrance skin dose (mGy) were compared between before and after QC group..... | 60 |



สถาบันวิทยบริการ
จุฬาลงกรณ์มหาวิทยาลัย

LIST OF ABBREVIATIONS

| | |
|-------------------|---|
| AAPM | American Association of Physicists in Medicine |
| Abd | Abdomen |
| ACR | American college of Radiology |
| ADC or a/d | Analogue-to-digital converter |
| AEC | Automatic exposure control |
| ALARA | As Low As Reasonably Achievable |
| AP | Antero-posterior |
| A_Q | Quantum efficiency |
| BaFBr | Barium fluoro-bromide |
| BaFBrI | Barium fluoro-bromo-iodide |
| BaFX | Barium fluoro-halide family |
| BMI | Body mass index |
| BSF | Backscatter factor |
| CCD | Charge- coupled-device |
| Ceph | Cephalometry |
| CR | Computed radiography |
| CRCPD | The Conference of Radiation Control Program Directors, Inc. |
| CRT | Cathode ray tube |
| CsI | Cesium Iodide |
| C-spine | Cervical spine |
| CTDI | Computed Tomographic Dose Index |
| CXR | Chest x-ray |
| 1-D | one dimension |
| 2-D | two dimensions |
| DAP | Dose Area Product |
| DICOM | Digital Imaging and Communications in Medicine |
| DQE | Detective quantum efficiency |
| DR | Digital radiography |
| DRL | Dose reference level |
| EC | European commissioning |
| E_{Fuji} | Fuji indicated exposure |
| ESAK | Entrance Surface Air Kerma (mGy) |
| ESD | Entrance Skin Dose (mGy) |
| ESE | Entrance Skin Exposure (mR) |
| Eu^{2+} | Europium divalent |
| eV | Electron volt |
| EVP | Enhanced visualization processing |
| exam. | Examination |
| FCR | Fuji computed radiography |
| f_d | Frequency of digitization rate |
| FDD | Focus-detector-distance |
| FFD | Focus-film-distance |
| FSD | Focus-skin-distance |

LIST OF ABBREVIATIONS (continued)

| | |
|----------------------------------|---|
| G | The intensity gain response |
| Gd ₂ O ₂ S | Gadolinium di-oxysulfide |
| G(n) | The intensity gain response averaged over n independent lines |
| G(x) | The intensity gain response at each position x along the scan |
| Gy | Gray |
| HA | Hospital accreditation |
| HeNe | Helium Neon |
| HL-7 | Health Level Seven |
| H.N. | Hospital number |
| Ht. | Body height in centimeter unit |
| HVL | Half Value Layer |
| IAEA | International Atomic Energy Agency |
| ICRP | International Commission on Radiological Protection |
| ICRU | International Commission of Radiation Units and Measurements |
| I _c (x) | The corrected data point |
| ID | Identification |
| IEC | The International Electrotechnical Commission |
| IMACS | Image and information management system |
| I _{uc} (x) | The dark current offset |
| IP | Imaging plate |
| IPSM | The Institute for Preventative Sports Medicine |
| JICA | Japan International Cooperation Agency |
| kVp | kilo voltage peak |
| L | Latitude |
| Lat | Lateral |
| LCD | Liquid crystal display |
| lp/mm | line pairs per millimeter |
| L-S spine | Lumbo-sacral spine |
| M | the mean value of the denominator |
| mAs | milli ampere-second |
| MBq | Mega Baquerel |
| MFP | Multi-objective frequency processing |
| mGy | milli Gray |
| mR | milli Roentgen |
| MTF | Modulation transfer function |
| MUSICA | Multi-scale image contrast amplification |
| NCRP | Nation Council of Radiation Protection and Measurement |
| N _d | the number of x-rays detected |
| NEMA | National Electrical Manufacturers Association |

LIST OF ABBREVIATIONS (continued)

| | |
|----------------|--|
| NEQ | Noise Equivalent Quanta |
| N_i | the number of x-rays incident on the detector |
| NRPB | National Radiological Protection Board |
| NPS | Noise power spectra |
| O | the dark-level offset variations |
| ODA | The Official of Development Assistant |
| $O_m(x)$ | the dark-level offset variations averaged over m the independent lines |
| $O(x)$ | the dark-level offset variations at the same position (x) along the scan |
| PA | Postero-anterior |
| PACS | Picture Archiving and Communication System |
| Pel | Pelvis |
| PET | Polyethylene terephthalate |
| PMT | Photomultiplier tube |
| pns | Paranasal air sinuses |
| PSL | Photostimulable luminescence |
| PSL | Photostimulable luminescence complex |
| PSP | Photostimulable phosphor |
| PV | Pixel value |
| QA | Quality assurance |
| QC | Quality control |
| IQF | Image quality factor |
| RIS | Radiology information system |
| ROC | Receiver Operating Characteristics |
| ROI | Region of interest |
| RSNA | Radiological Society of North America |
| RTs | Radiological technologists |
| SCD | Source-chamber-distance |
| SD | Standard deviation |
| SID | Source-image-distance |
| SMPTE | Standard of the motion picture and television engineer |
| SNR | Signal-to-noise ratio |
| SNR_{in} | Signal-to-noise ratio at the input of a detector |
| SNR_{out} | Signal-to-noise ratio at the output of a detector |
| SSK | Strahlenschutzkommission |
| Sv | Sievert |
| S-value | Sensitivity value |
| $S(x)$ | Shading corrections |
| $S_n(x)$ | the normalized shading correction array |
| TCDD | Threshold contrast detail detectability |
| μGy | micro Gray |
| μs | micro second |
| UV | Ultraviolet |
| Wt. | Body weight in kilogram unit |

CHAPTER I

INTRODUCTION

Background and rationale

Computed Radiography (CR) is a process for capturing digital radiographic images. A storage phosphor plate is placed in the x-ray cassette instead of a piece of film. The phosphor plate captures and "stores" the x-rays. The image is "developed" in a CR reader instead of a film processor. The CR reader extracts the information stored in the plate and produces a digital image. The fundamental innovation in the development of CR was by Kodak who conceived the storage of an x-ray image in a phosphor screen. It required significant technical steps and conceptualization of the application by Fuji (FCR 101) to produce the first medical x-ray images in 1983. With two passing decades since CR worldwide introduction, it has become a mainstream technology for acquiring ordinary radiographic projections in digital form that produces images equivalent or better than conventional x-ray film-screen systems. CR, photostimulable phosphor (PSP) imaging system, is extremely flexible, promising to replace virtually all conventional screen-film radiography. Its wide latitude and automatic density adjustment dramatically improve the consistency of radiographs after acquisition. The CR image can be distributed virtually anywhere electronically, viewed simultaneously by multiple care providers, and reprinted, as necessary. The CR image is acquired on reusable image media, which can be erased and imaged thousands of times. Some hospital can eliminate the need for film and chemicals. CR is especially suited to bedside radiographic examinations including scoliosis, and panoramic studies. The success of CR leads to the misconception that quality assurance (QA) and quality control (QC) processes are no longer necessary. In actual fact, QA and QC processes for CR are no less important than they are for conventional screen-film radiography, and must be modified to take into consideration the unique characteristics of CR technology [1]. A good QC program utilizes tests that are sensitive and frequent enough to detect degradation in equipment performance before diagnostic information is lost, with a special focus on potential dose reduction [2]. In the year 2000, Department of Radiology of King Chulalongkorn Memorial Hospital, Thai Red Cross Society had already installed the first CR system (Fuji FCR 5000 with standard resolution phosphor imaging plates ST-V_N, Fuji Photo Film Co., Ltd.). The system was donated by the Office of Development Assistant (ODA); Japanese Government. In clinical use, several problems have been found such as Moiré patterns, too dark, too bright, too noisy images, superimposed appearances, post-processing parameter mismatch, reject and retake rate over 9 percent for 6 examinations (84 cases from total 934 cases in 6 months), incorrect imaging plate handle, lack of QC protocol for routine job, etc. For the long term result, it is expected that the reject and retake rate should be reduced to 5 percent or less, the unnecessary patient radiation doses could be reduced, the costs reduction, and such the mentioned problem could be reduced if the CR system is maintained properly using the standard quality control protocol. The better image quality which is the increasing validity of diagnostic information for the radiologists and clinicians will be obtained.

Key words: Quality control program, Computed Radiography.

Assumption:

In this study, the patient radiation dose reduction will be represented by means of the reduction of reject and retake rate that will directly affect the patient dose. The dose

reference level of general radiography is recommended by the Committee 3 Advice of the International Commission on Radiological Protection (ICRP) [3].

Definition

| | |
|-----------------------------|--|
| Back scatter factor | The ratio between a dose quantity measured at a phantom or material surface which is facing the source of radiation and the same dose quantity at the same position free in air. |
| Computed Radiography (CR) | A system uses an imaging plate instead of film to capture an image. The plate is made of a storage phosphor that absorbs x-ray energy. When scanned with a laser, the plate emits light, captured by the plate reader to build up an image from the energy released. |
| Dose, Absorbed dose | Energy imparted to matter per unit mass of the irradiated matter, expressed in units of rads or Grays. |
| Dose Reference level (DRL) | The reference dose value quantifying patient dose of standard radiographic exposures (for standard patients). |
| Entrance Skin Dose (ESD) | Absorbed dose in the skin of the patient surface including backscatter. |
| Exposure | A radiation quantity of ionization in air from x-rays or gamma rays. Units are expressed in Roentgen (R) or coulomb per kilogram of air. Also a conversational term was meaning simply exposure to radiation or radioactive material. |
| External exposure | Radiation exposure from a source outside the body. |
| Quality control program | Techniques used in the monitoring (or testing) and maintenance of the components of the system. The quality control techniques thus are concerned directly with the equipment. |
| Radiation | The emission and propagation of energy through space. |
| Radiation-producing Machine | Any high voltage machine capable of producing ionizing radiation, usually X-rays, but may be any nuclear reaction, e.g. neutrons, protons. |
| Sievert | an international unit of dose equivalent, represented as Sv. 1 Sievert = 100 rem |
| X-rays | A photon that originates outside the nucleus of an atom. |

CHAPTER II

REVIEW OF RELATED LITERATURE

PHYSICS OF THE COMPUTED RADIOGRAPHY

2.1. Introduction

The conventional radiography using the film-screens combination is roughly 70 % of the diagnostic service in an x-ray department [4]. The film-screens combination has some advantages i.e. low costs and adaptation to the existing radiographic units, use at bedside and operating room. The disadvantages are: a narrow range of response, cassettes manipulation, delay of display, storage and retrieval problems. Many radiological imaging departments both small and large are moving rapidly into the electronic management of information. Images in radiology are captured, processed, displayed and stored electronically by using photostimulable phosphor, x-ray detectors based on imaging plate technology have become very popular. Nowadays, CR can be used in conventional x-ray equipment, needs the same manipulations as conventional radiography and the technology is well established. CR was initially used for portable chest radiography, overcoming inconsistent image quality from errors in exposure. With manufacturers' ongoing improvements to make the systems easy to use and improve image quality, CR use has expanded to chest, musculoskeletal, abdominal, paediatric examinations and mammography.

2.2. Historical background

The fundamental innovation in the development of CR was by Kodak who conceived the storage of an x-ray image in a phosphor screen. It required significant technical steps and conceptualization of the application by Fuji (FCR 101) to produce the first medical x-ray images in 1983. Fuji, the main developer of CR in the eighties, used BaFBr:Eu²⁺ phosphor and a cassette-based approach [5]. During this time, Agfa and Kodak performed research and development on the same method but were constrained from commercialization by patent issues and ambivalence due to the fear of damaging their installed base of screen-film, respectively. In this era the storage effect was also being observed in screen-film applications where it caused the unwanted effect of *print through*, i.e. a ghost image of a prior exposure to the screen that appears on a subsequent film exposed in the same cassette. The storage effect is related to the phenomenon of thermally induced luminescence of irradiated materials, i.e. thermoluminescence. Since that time (and particularly in the 1990s), several manufacturers have realized the opportunities and the importance of CR clinical acquisition systems as necessary to the implementation of Picture Archiving and Communications Systems (PACS). These manufacturers have provided a wide range of capabilities—from large, high-throughput, multi-plate stackers to cassetteless and high-speed automated CR acquisition devices to small, desktop-sized, single-plate readers—to address the needs of the largest hospitals to the smallest outpatient clinics. A shift to an all-digital, filmless environment has also stimulated progress in the application of CR to pediatric and mammographic imaging and has brought added

importance to image pre- and post-processing to take advantage of the flexibility provided by the digital format.

2.3. The CR system overview [6]

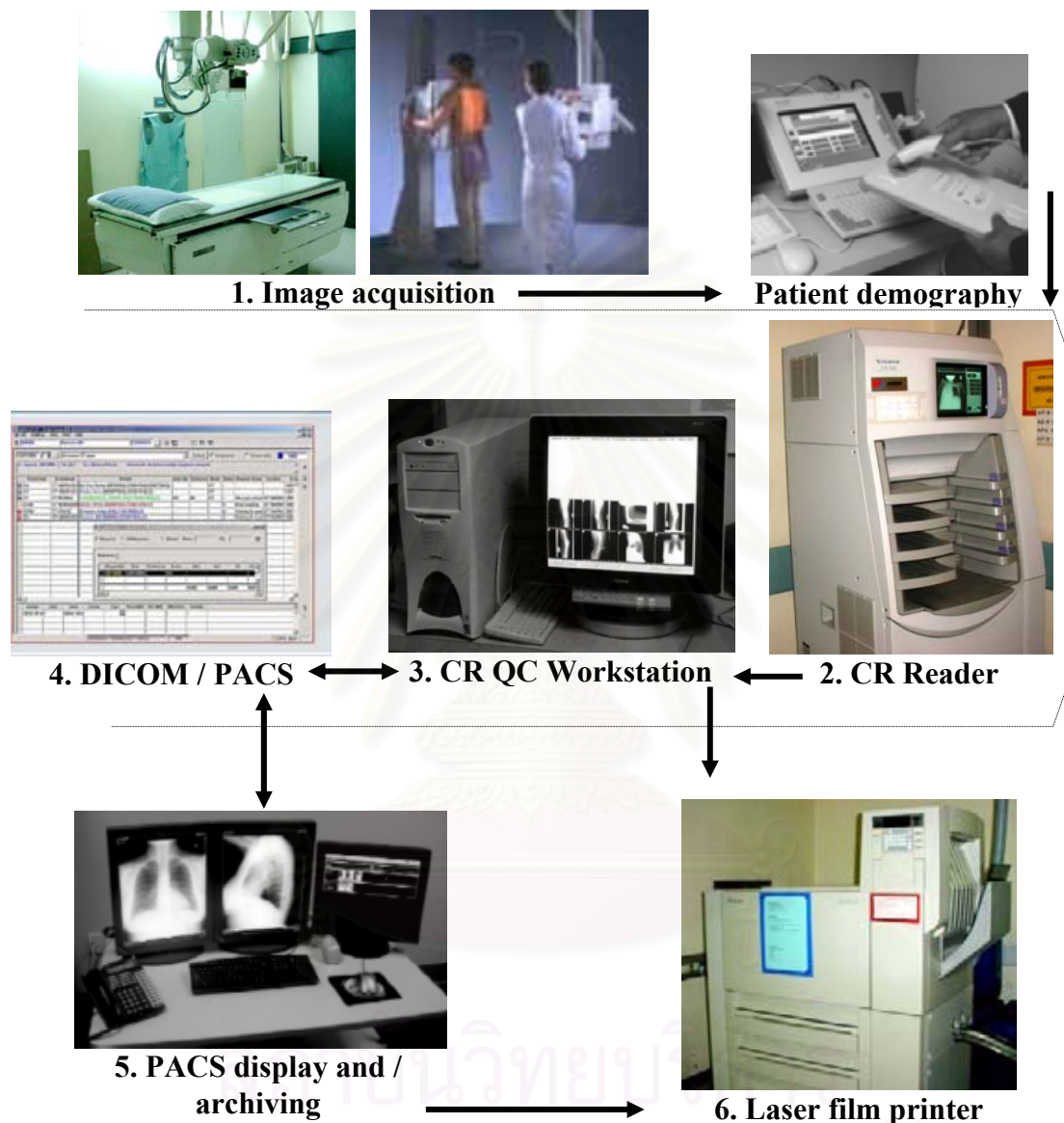


Figure 1. Representation of CR image acquisition and dataflow: 1. acquisition and identification; 2. processing; 3. quality control; 4. electronic transfer; 5. soft copy display and digital archiving; and 6. laser film printer (option).

Present day computed radiography (CR) device is composed of an independent, passive x-ray detector (a cassette-based photostimulable phosphors (PSP) detector of various dimensions that is similar to conventional screen-film cassettes), which are also known as storage phosphors and an image processor (also known as a CR “reader”), which processes the latent x-ray image captured by the detector. The PSP detector, which is commonly referred to as an imaging plate (IP), resides in a protective cassette is most often

in the barium fluorohalide family in powder form and deposited onto a substrate to form an imaging plate or screen. X-ray absorption mechanisms are identical to those of conventional phosphor screens used with film. They differ in that the useful optical signal is not derived from the light emitted in prompt response to the incident radiation, but rather from subsequent emission when the latent image, consisting of trapped charge, is optically stimulated and released from metastable traps. This triggers a process called *photostimulated luminescence* (PSL) resulting in the emission of shorter wavelength (blue) light in an amount proportional to the original x-ray irradiation and then read out by raster scanning with a laser to release the PSL. After latent image readout and digital signal conversion, the image data are accumulated, stored into a digital, two-dimensional (2-D) matrix, and transferred to a Quality Control (QC) review workstation. Patient demographic information is appended, and contrast/spatial frequency enhancement algorithms are applied to the digital image and/or adjusted before transfer to the PACS. Subsequent image viewing, diagnosis, and archiving are achieved outside of the direct interaction with the CR system, as illustrated in figure 1 and 2. This process is notably similar to the 100-year-old screen-film paradigm, which are both a blessing and a curse. Blessings are in the form of positioning flexibility and the ubiquitous cassette form factor. The curse is in the extra handling and time required for processing the IP, which reduces workflow efficiency and patient throughput expected of a “digital” detector system.

CR or PSP imaging employs reusable imaging plates and associated hardware and software includes the entire process of creating a digital projection radiographs, e.g. acquisition, processing, image presentation, and managing image data. The following section provides a basic of those principles [7]:⁷

2.3.1. Image acquisition

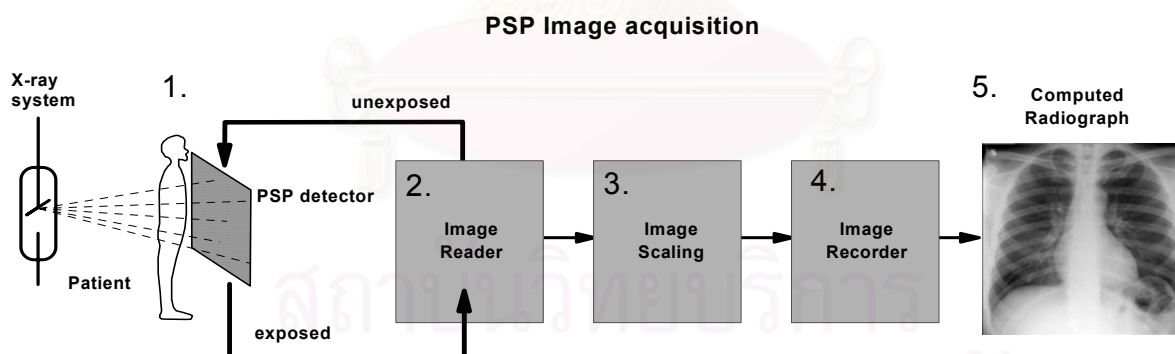


Figure 2. PSP image acquisition and processing.

2.3.1.1. Photostimulable phosphors

The PSP material is a barium-fluoro-bromide/iodide (BaFBr/I) compound doped with trace amounts of europium (Eu). In operation, the PSP material captures transmitted x-ray flux and creates a transient latent image by the trapping of electrons from the ground state into spatially localized higher-energy-level “F-center” traps. X-rays absorbed in the phosphor create a proportional number of trapped electrons. The spatial distribution of trapped electrons represents the unprocessed latent image. X-ray absorption efficiency is dependent on energy of the x-ray photon and the thickness of the PSP compound and sets

the upper limits of detective quantum efficiency (DQE) achievable with the CR imaging system. A relative comparison of BaFBr, Gd₂O₂S, and CsI is illustrated in figure 3 for typical “standard” thicknesses used in radiographic detectors.

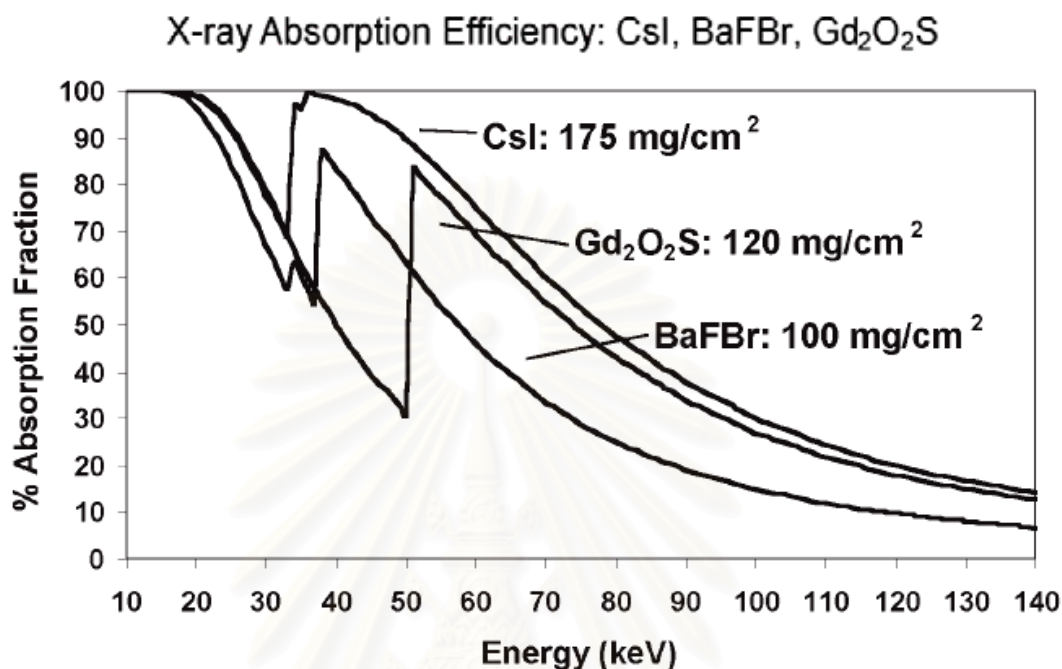


Figure 3. Absorption characteristics of BaFBr, CsI, and Gd₂O₂S phosphors of “typical” thickness for digital radiography. These characteristics are shown as a function of incident x-ray energy.

Extraction of the electron latent image requires a simulating light source, which is usually a diode laser (680 nm wavelength), that pumps the electrons out of the trap to a higher energy level within the compound and then immediately to the ground state with only a short lag. As the electrons drop to the valence shell, emission of a blue, ~415 nm photostimulated luminescence (PSL) photon emerges from the phosphor as the visible latent image signal. Because the PSL is of shorter wavelength than the stimulating source, optical filtering can separate these two “simultaneous” light sources. Collection and amplification of the signal with photosensitive electronic devices followed by digitization of the signal produces the equivalent digital signal. Spatial mapping of the output signals projected onto the detector is achieved by either point-scan methods using a small diameter laser beam (e.g., 100 μm effective diameter) or the recently introduced laser beam line-scan method.

2.3.1.1.1. Types of photostimulable phosphors.

The photostimulable phosphor first used for CR was BaFBr:Eu²⁺. Its crystal structure is non-cubic, i.e. a layered structure that gives rise to phosphor grains with a plate-like rather than the more desirable cubic morphology. BaFBr:Eu²⁺ is a good storage phosphor in that it can store a latent image for a long time, e.g. the latent image 8 h after irradiation will still be ~75% of its original size. The family of phosphors BaFX:Eu²⁺ where

X can be any of the halogens Cl, Br or I (or an arbitrary mixture of them) have been studied extensively. The decay time after photostimulation of all these phosphors is now known to be approximately the same ($\sim 0.7 \mu\text{s}$) and so they can all be used in CR. In earlier literature there was a long decay noted for BaFCl:Eu^{2+} which can now be eliminated. In recent years most manufacturers have used $\text{BaFBr}_{0.85}\text{I}_{0.15}:\text{Eu}^{2+}$ not for the marginal increase in x-ray absorption compared to BaFBr:Eu^{2+} , but rather for the better optical match of the wavelength of maximum stimulation of the phosphor to diode lasers. Recently Konica has utilized pure BaFI:Eu^{2+} in commercial systems where the change in absorption is significant.

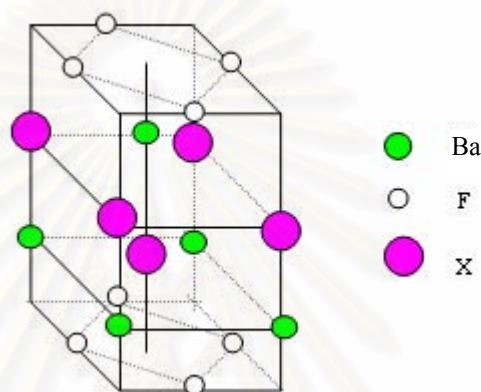
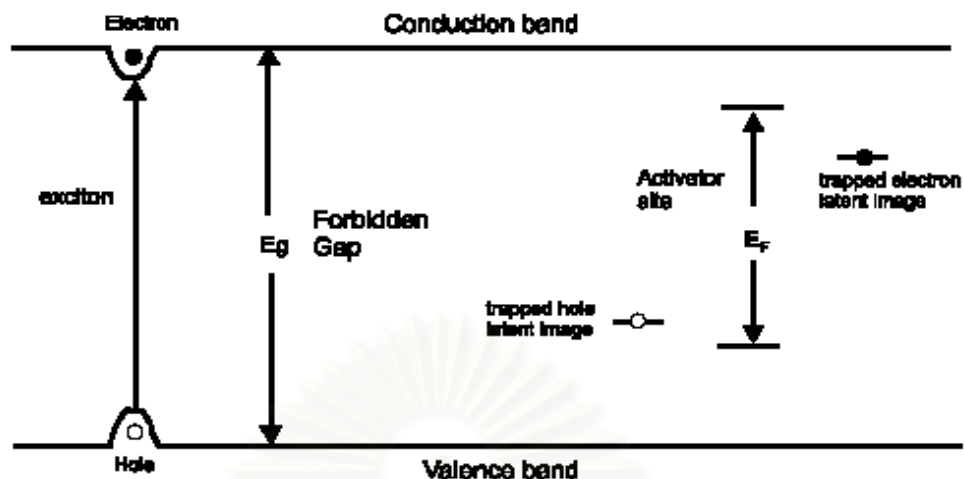


Figure 4. Crystal structure of BaFx ($X = \text{Cl, Br, I}$)

The spectrum of light emitted by an efficient phosphor is controlled by a dilute (< 1 atomic %) impurity called an *activator*. Such activated phosphors have a characteristic line spectrum caused by the isolated atom in the host or *matrix*. In BaFX phosphors used in CR the activator is Eu^{2+} , which substitutes for Ba in the crystal lattice. Additionally in a photostimulable phosphor there should be effective electron and hole traps at every activator site so that the maximum number of x-ray induced excitations can be trapped. The detailed mechanism of PSL is still controversial and probably differs between specific photostimulable phosphors.

2.3.1.1.2. PSP receptor characteristics. Many compounds possess the property of PSL. Few of these materials have characteristics desirable for radiography, i.e. a stimulation-absorption peak at a wavelength produced by common lasers, a stimulated emission peak readily absorbed by common photomultiplier tube input phosphors, and retention of the latent image without significant signal loss due to phosphorescence. The compounds that most closely meet these requirements are alkali-earth halides. $\text{BaFBr}_{0.85}\text{I}_{0.15}:\text{Eu}^{2+}$ the typical phosphor grain size is 4 or 5 μm a trend to yet smaller sizes as the ability to make smaller grains with good PSL properties improves, in an organic binder with a thickness between 25 and 150 μm deposited on a flexible polymer support film, typically the binder is nitrocellulose, polyester, acrylic or polyurethane and the backing material is also a polymer, e.g. polyethylene terephthalate (PET) film 200–400 μm thick.



(a) Band structure representation of exciton (b) Exciton trapped on PSL complex

Figure 5 shows energy levels expressing the PSL mechanism of the photostimulable phosphor. The europium ions in the crystal are ionized by the primary excitation (imaging) of the x-rays from bivalent to trivalent ions and electrons are released to the conduction band. The electrons thus released are captured in the vacancy of the halogen ions (previously formed) by Coulomb's force and a semi-stable F center state is produced. It is in this state that the x-ray image information is stored. If visible light (second stimulation light, reading light) is absorbed at the F center, it will be released again to the conduction band; they will be captured by the trivalent europium ions to generate excited bivalent ions, and energy will be discharged in the form of luminescence.

2.3.1.1.3. Mechanisms of trapping and photostimulation.

2.3.1.1.3.1. Doping. Trace amounts of impurities, such as the europium ion crystallized (Eu^{2+}), are added to the PSP to alter its structure and physical properties. The trace impurity is also called an *activator*. Eu^{2+} replaces the alkali earth in the crystal, forming a luminescence center.

2.3.1.1.3.2. Absorption Process. Ionization by absorption of x-rays (or ultraviolet radiation) forms electron hole pairs in the PSP crystal. An electron hole pair raises Eu^{2+} to an excited state, Eu^{3+} . Eu^{3+} produces visible light when it returns to the ground state, Eu^{2+} . Stored energy (in the form of trapped electrons) forms the latent image. There are currently two major theories for the PSP mechanism, a bimolecular recombination model, and a photostimulable luminescence complex (PSLC) model to explain the energy absorption process and subsequent formation of luminescence centers. Physical processes occurring in BaFBr:Eu^{2+} using the latter theory appear to closely approximate the experimental findings. In this model, the PSLC is a metastable complex at higher energy ("F-center" where an electron has been caught at the point where a specific atom forming the crystal has been removed, called the vacancy) in close proximity to a Eu^{3+} - Eu^{2+} recombination center. X-rays absorbed in the PSP induce the formation of "holes" and "electrons", which either activate an "inactive PSLC" by being captured by an F-center, or form an active PSLC via formation and recombination of "excitons" explained by "F-center physics". In either situation, the numbers of active PSLC's created (number of

electrons trapped in the metastable site) are proportional to the x-ray dose to the phosphor, critical to the success of the phosphor as an image receptor.

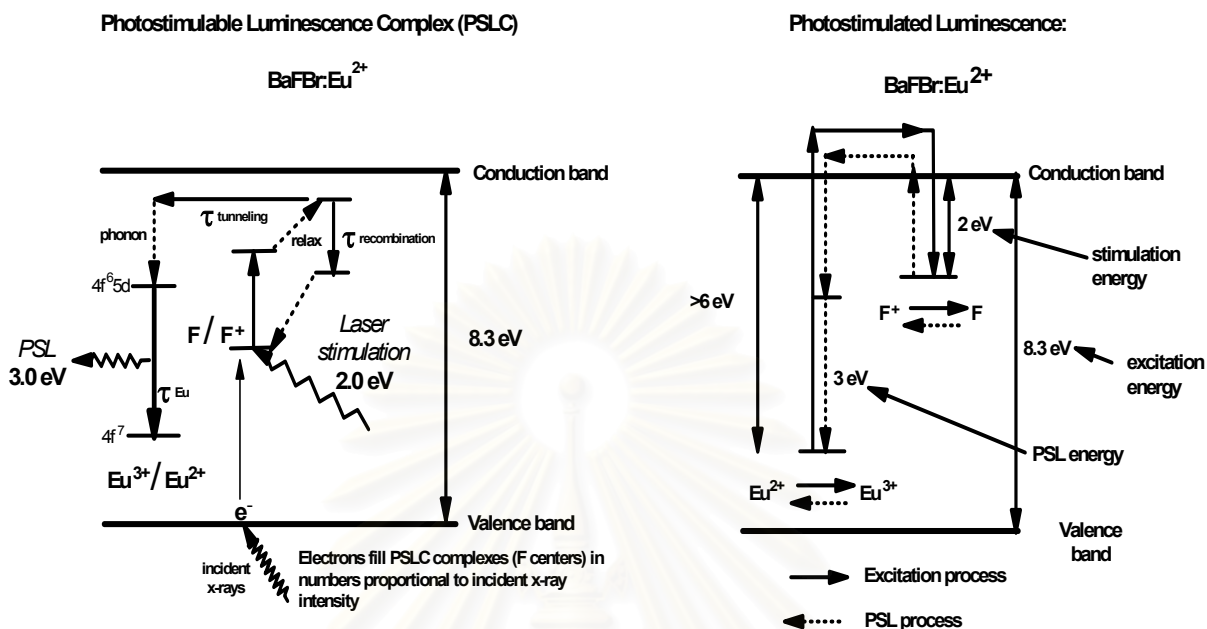


Figure 6. Energy diagram of the excitation and photo-stimulated luminescence processes in a BaFBr:Eu^{2+} phosphor [8, 9]. Incident x-rays form an “electron” latent image in a meta-stable “F” center site that can be processed with a low energy laser beam, producing the desired luminescent signals. τ is the decay constant of the indicated process above.

X-ray absorption efficiency of BaFBr:Eu^{2+} is compared to $\text{Gd}_2\text{O}_2\text{S:Tb}$ (rare-earth screens) for typical thicknesses of material encountered, as shown by attenuation curves illustrated in figure 6. Between ~ 35 to ~ 50 keV, the BaFBr phosphor is actually a better x-ray attenuator due to the lower k-edge absorption of barium; however, below and above this range, the gadolinium rare-earth phosphor is superior. A typical beam spectrum incident on the PSP phosphor often requires greater exposure to achieve similar quantum statistics compared to a 400 speed rare-earth receptor. In addition, high absorption probability of x-rays below the k-edge of the PSP receptor, where a significant fraction of lower energy scattered x-ray distribution occurs, causes a greater sensitivity to scatter.

In a storage phosphor, excitons can be trapped without the emission of light. It is believed that if photostimulation is to occur later, the trapping must occur on sites spatially correlated with the activator. This is called the PSL complex shown in figure 1(b). The energy levels in the crystal are critical to effective storage phosphor operation. The energy difference between the electron traps and the conduction band edge must be small enough to allow stimulation with laser light, yet sufficiently large to prevent significant random thermal release of the charge carriers from the traps. In BaFBr:Eu^{2+} the image storage is due to: (i) electron trapping at positive ion (Br or F) vacancies, forming an *F-centre*, or (ii) hole trapping at an unidentified site. An activated photostimulated luminescent site or *PSL centre* is therefore thought to be an arrangement of three spatially correlated components: an electron trap, a hole trap and the luminescent activation centre. The PSL emission spectrum has been correlated with an internal transition within the activator, Eu^{2+} . The

stimulation spectrum has been correlated with the absorption spectrum of the F-centre showing that the first step in the stimulation process is excitation of the trapped electron. However, it is believed that a great inefficiency arises because ~80% of the electrons are trapped at F sites and ~20% at Br sites but only the latter contribute to PSL. It was first thought that the hole was trapped on the activator site itself (Eu^{2+} thereby increasing the valency to Eu^{3+}). However as there is no change in the electron spin resonance spectrum following x-ray irradiation, this trapping mechanism cannot be operative. Thus the nature of the hole trap is in doubt and the details of the entire process are not fully understood.

2.3.1.1.3.3. Fading. Fading of the trapped signal will occur exponentially over time, through spontaneous *phosphorescence*. A typical imaging plate will lose about 25% of the stored signal between 10 minutes to 8 hours after an exposure, and more slowly afterwards. Fading introduces uncertainties in output signal that can be controlled by introducing a fixed delay between exposure and readout to allow decay of the “prompt” phosphorescence of the stored signal.

2.3.1.1.3.4. Stimulation and Emission. The “electronic” latent image imprinted on the exposed BaFBr:Eu^{2+} phosphor corresponds to the activated PLSC’s (F-centers), whose local population of electrons is directly proportional to the incident x-ray flux for a wide range of exposures, typically exceeding 10,000 to 1 (four orders of exposure magnitude). Stimulation of the Eu^{3+} - F-center complex and release of the stored electrons requires a minimum energy of ~2eV, most easily deposited by a highly focused laser light source of a given wavelength. Lasers produced by HeNe ($\lambda = 633 \text{ nm}$) and “diode” ($\lambda \cong 680 \text{ nm}$) sources are most often used. The incident laser energy excites

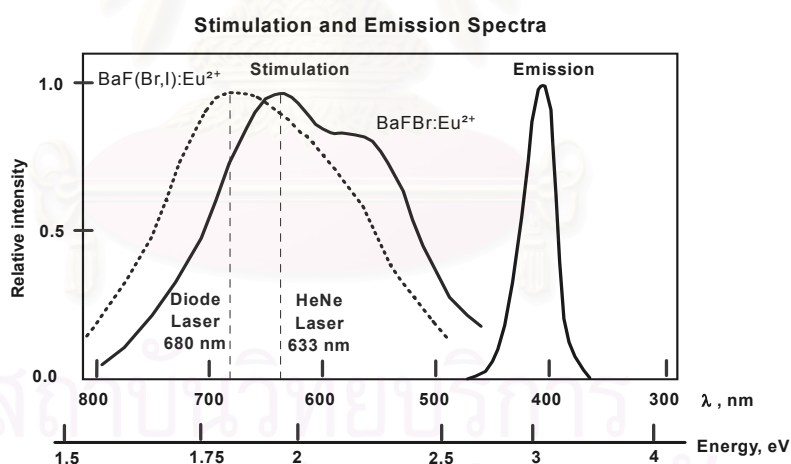


Figure 7. Stimulation and emission spectra for BaFBr:Eu^{2+} and $\text{BaFBr}_{0.85}\text{I}_{0.15}:\text{Eu}^{2+}$ storage phosphors demonstrate the energy sensitivity of different phosphor formulations and the energy separation of the excitation and emission events. Selective optical filtration isolates the light emission intensity from the incident laser intensity. In absolute terms, intensity of the emitted light is significantly lower.

electrons in the local F-center sites of the phosphor. A light photon of 3 eV energy immediately follows as the electron continues to drop through the electron orbital of the Eu^{3+} complex to the more stable Eu^{2+} energy level. Figure 7 shows a plot of the energy spectra of the laser induced electron stimulation and subsequent light emission. Note that

different phosphor formulations will impact the stimulation energies; thus it is important for optimal results that the PSP receptors be matched with the energy of the stimulating laser source.

2.3.1.2. X-ray properties of photostimulable phosphors

The number of x-rays used limits the image quality since x-ray image noise arises from the random interactions of x-rays with the detector. The square of signal-to-noise ratio (SNR) at the input of a detector, SNR_{in}^2 , defines the ultimate SNR which a perfect detector could achieve. It is equal to the number of x-rays incident on the detector N_{I} . At the output of the detector $\text{SNR}_{\text{out}}^2 = N_{\text{d}}$ (the number of x-rays detected) for a detector that *counts* x-rays. The ratio of detected to incident x-rays is called the quantum efficiency A_{Q} . Thus for a photon counting detector

$$\frac{\text{SNR}_{\text{out}}^2}{\text{SNR}_{\text{in}}^2} = \frac{N_{\text{d}}}{N_{\text{I}}} = A_{\text{Q}}. \quad (1)$$

From equation (2) it is evident that A_{Q} is the single most important determinant of the ultimate image quality possible from an x-ray detector.

2.3.1.3. CR imaging plates (IPs)

The design and physics of IPs are very similar in concept to conventional phosphor screens used with film. The phosphor grain size is a critical design parameter for several reasons. First, there are factors related to the intrinsic luminescence properties. If the grains are too small, then the defects created on the outside of the grain, e.g. non-photostimulable electron or hole traps, may dominate the bulk properties of the material. Secondly, there are factors related to the diffusion of light through the screen. If the grains are too large, then non-uniformity of light output or structural noise will be more pronounced. Thirdly, a larger scattering length will reduce the resolution of the screen. Thus screens designed for a low-resolution task, e.g. chest, can use larger phosphor grains than a high-resolution, e.g. mammography task. Screens are usually designed to be ~10–20 phosphor grains thick.

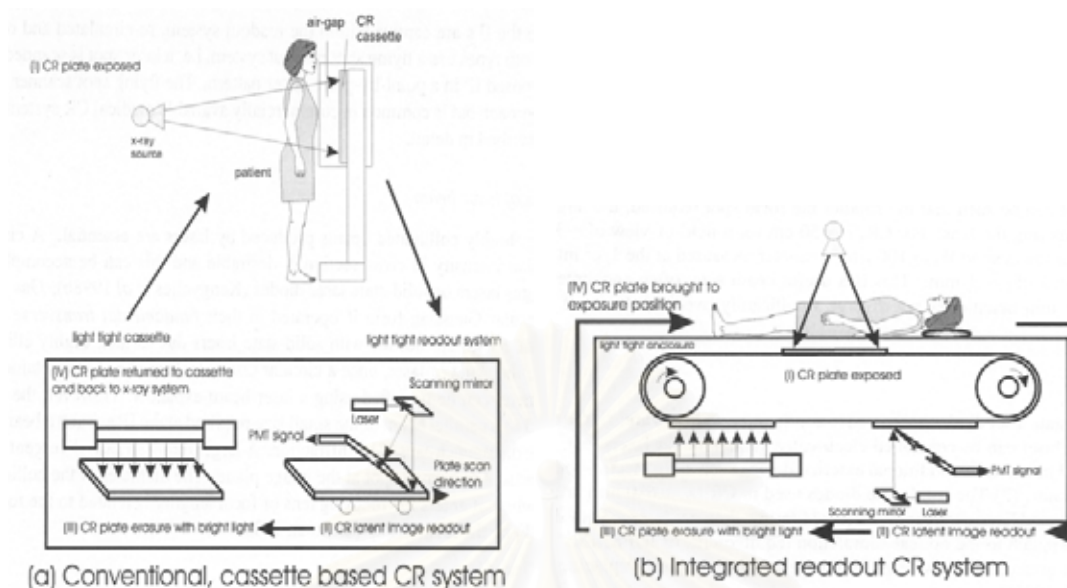
A recently introduced capability in the design of IPs is the possibility of having different optical boundary conditions for the laser (absorptive) and PSL light (reflective) by use of *anti-halation* backing layers. The exposed phosphor surface and the back of the screen have additional protective layers. The purpose of both these layers is to protect the optical surface of the phosphor layer because during stacking and transport within the reader, the bottom surface rubs against the top of other IPs.

2.3.2. Image processing

2.3.2.1. The CR reader

Present day CR systems are of two general types:

(i) *Cassette-based systems* as shown in figure 8(a) where the IP is enclosed in a light-tight cassette for the x-ray exposure, and subsequently moved by hand to the readout system.



(a) Conventional, cassette based CR system

(b) Integrated readout CR system

Figure 8. Overall concept of CR readout systems.

- (a) Cassette-based requiring carrying cassette back and forth between the x-ray and readout systems. (An important component in practical application not shown in the diagram is a stacker needed to buffer the demand on the system.)
- (b) Integrated readout systems requiring no operator intervention in the exposure readout cycle.

(ii) *Integrated readout systems*, shown in figure 8(b) where the IPs are captive within the readout system, re-circulated and reused without handling.

Both types use a flying spot readout system, i.e. a laser spot is scanned with a mirror over the exposed IP in a point-by-point raster pattern. The flying spot scanner is not the only possible approach but is common in commercially available medical CR systems.

2.3.2.1.1. Point-Scan CR Readers

The CR reader orchestrates the latent image extraction of the exposed IP and applies subsequent amplification and conversion to a digital signal. A typical reader is composed of an optical stage, scanning laser beam, IP translation mechanics, light pickup guide(s), photomultiplier tube (PMT), signal transformer/amplifier, and analog-to-digital converter (ADC). The exposed cassette is inserted into the reader, and the IP is extracted and translated through an optical stage by precisely controlled pinch rollers. As the plate is translated, the scanning laser beam sweeps across the plate row by row, with a speed that is adjusted according to the luminescent signal decay time constant ($\sim 0.8 \mu\text{s}$ for BaFBr:Eu^{2+}). The effective laser beam spot size is controlled by the laser optics and $f\text{-}\theta$ lens, and the speed of IP translation is set to ensure appropriate coverage by the laser beam as well as to achieve equal sampling in the row and column directions of the output digital image. The laser beam sweep is called the “scan” or “fast-scan” direction whereas the plate translation represents the “sub-scan” or “slow-scan” direction. This distinction is important

for analyzing spatial resolution characteristics of the CR system and tracking down possible problems. Characteristics of the plate readout geometry are shown in figure 11.

An illustration of the CR reader components is shown in figure 9. Readout of the detector typically requires from 45 to 90 seconds, depending on the specifications of the given CR reader (not including subsequent erasure of the residual signal so that the IP can be used again). Although the PSL is produced in all directions, only the light scattered backwards is collected. Recently introduced dual-side reading technology is now available, in which the phosphor material is layered on a transparent substrate and the forward directed PSL is captured by a second light guide on the other side of the IP, thus increasing the capture efficiency of PSL. A thicker phosphor layer is also used, which increases the detective quantum efficiency of the system by up to 50%.

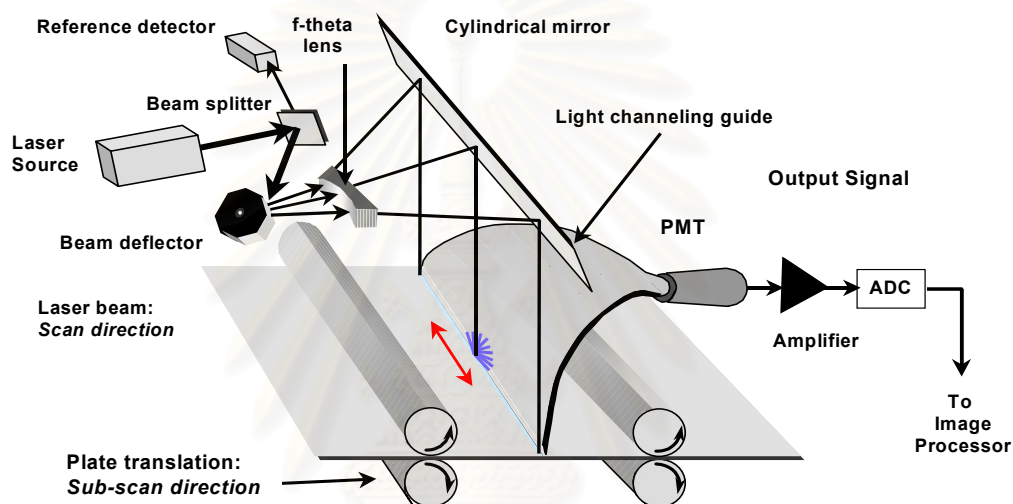


Figure 9. Major components of a PSP reader include the stimulating laser source, a beam splitter, oscillating beam deflector, f- θ lens, cylindrical reflecting mirror, light collection guide, and photomultiplier tube (PMT). The plate is translated in a continuous motion through the laser beam scan by pinch rollers. All component functions are orchestrated by digital computer. In dual-side readout systems, a second light guide positioned underneath the scanning IP collects the PSL transmitted through the transparent substrate. In some readers, multiple PMT's are used for capturing the signal.

Spatial resolution depends on the laser beam spot size, the decay lag of PSL during the readout, the speed of the laser beam sweep, the frequency of the electronic sampling, and the translation speed of the IP. Because at any instant in time only a single point irradiates the IP, the capture of the PSL within the light guide will generate a signal that corresponds to that point. The spread of PSL within the light guide will not adversely affect resolution. (This is not, however, true of line-scan systems, described in the next section, which require a linear lens array to ensure proper mapping of the PSL generated from the IP to the source.) Adjustments are made to ensure that the resolution is approximately equal in the scan and sub-scan directions. Typical "effective" resolution element size is 100, 150 and 200 μm , which correspond to 5.0 to 2.5 line pairs per millimeter (lp/mm)-certainly less than that achieved by a 400-speed screen-film system, which provides approximately 7.5 lp/mm.

Residual signals remain on the IP after readout; in fact, a given IP can be scanned several times and reveal a recognizable (albeit noisy) image. Thus, erasure is subsequently applied with the use of a high-intensity light source. In many systems, the length of erasure time is dependent on the x-ray exposure to the IP. Often, in severe overexposures (particularly for unattenuated beam areas), erasure can require several minutes to ensure adequate removal of the latent image and can be a potential bottle-neck in sequential, single-plate reader systems. Verification of adequate erasure after a severe overexposure is one test to be performed at acceptance. These and other validations of performance are described in Seibert (2004) in this monograph. Another consideration is IP mechanical wear and tear, which can ultimately limit the lifetime of the detector. Systems that mechanically bend the IP during the readout will likely have a shorter lifetime and require earlier replacement than straight-through or solid plate IPs. A guarantee from the vendor on the number of cycle times is important for budgetary purposes because the combined IP and cassette costs are fairly substantial, which significantly adds to the initial and ongoing upkeep/maintenance costs.

The PSL captured by the light guide(s) is optically filtered and channeled to the photocathode of the PMT(s), causing emission of electrons and subsequent acceleration and amplification through a series of dynodes. Overall gain of the PMT is controlled by the adjustment of the voltage placed on the dynodes, which is usually set at a fixed value that corresponds to the expected exposure levels for clinical diagnostic procedures. High gain and extremely large dynamic range of the PMT produces light intensity variations from the phosphor that span a range of 10,000, or “four orders of magnitude.” In older CR readers, a low-energy laser pre-scan was used to determine the range of x-ray exposures on the plate (and thus light emission) in order to adjust the gain of the PMT. Current readers use a preset PMT gain that achieves good linearity over clinical exposure ranges of usually 0.1 mR to 100 mR or 0.01 to 10 mR (determined by the preset gain of the PMT) to allow optimal digitization of the PSL signal intensities. Prior to conversion of the PMT signal to a digital value, most CR systems apply a non-linear transformation with a logarithmic or square-root amplifier. Logarithmic conversion provides a linear relationship of incident exposure to output signal amplitude; square-root amplification provides a linear relationship, with the noise associated with the exposure. In either case, the total dynamic range of signal is compressed so that digitization accuracy can be preserved over a limited number of discrete gray levels.

2.3.2.1.2. Line-Scan CR Readers

Fast, parallel CR line-scan systems are now available for clinical use; they are based on the simultaneous stimulation of the PSP one line at a time and the acquisition of the PSL with a charge-coupled-device (CCD) linear array photodetector. A scanning module contains several linear laser units, optical light collection lenses along the length of the scan unit, and an inline high-sensitivity CCD photosensitive array to capture the resultant PSL signal simultaneously, one row at a time (figure 10). Unlike the point-scan system, which does not require focusing, the line-scan system has a lens array to focus the light along each point of the stimulated IP to a corresponding point on the CCD array. The module scans above the stationary IP of 43 cm x 43 cm in less than 7 seconds with a compact laser-lens-CCD module.

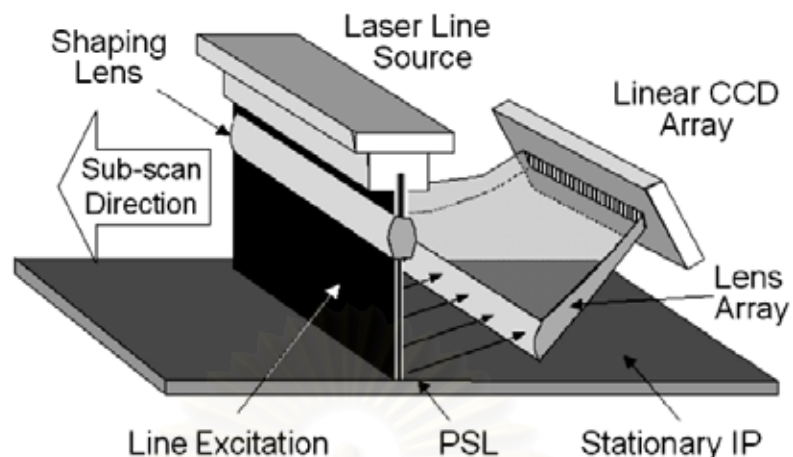


Figure 10. Component-level illustration of a line-scan CR detector. The laser source, shaping lens, PSL lens array, and CCD camera assembly move as a unit over the stationary imaging plate. Note that the lens array focuses the light emerging from the IP onto the corresponding detector elements of the CCD array. Not illustrated are individual lenses and color filters (to eliminate the stimulating laser signal) along the excitation array.

Another CR vendor is working on a similar system that uses an interesting “structured storage phosphor” that will purportedly combine good detection efficiency with good spatial resolution (characteristics that are usually trade-offs with unstructured phosphor materials). Even though information and details of these systems are somewhat sketchy, preliminary indications portend competitive capabilities and the use of CR technology and PSP detection/PSL conversion as viable alternatives to direct radiographic devices using 2-D CCD or flat-panel technology. Because of the compact size of the laser/detector module, the overall size of the detector has a similar form factor to that of a thin-film transistor direct radiography device, but currently at a much lower cost than a corresponding DR detector.

2.3.2.1.3. Laser types

The advantages of solid-state laser diodes compared to continuous gas lasers are:

- (i) the output intensity of a solid-state laser can be controlled electrically; Note that gas lasers, e.g. HeNe with wavelength $\lambda = 633 \text{ nm}$, need an additional external device such as an electro-optical or electro-acoustical modulator;
- (ii) The solid-state diodes used in CR ($\lambda = 680 \text{ nm}$) are more compact, energy efficient, and have a longer operational lifetime than gas lasers. They do not, however, have as good a match to the optical stimulation requirements of BaFBr:Eu^{2+} . This necessitated using both a greater laser power and a redesign of the phosphor (replacing Br by $\text{Br}_{0.85}\text{I}_{0.15}$).

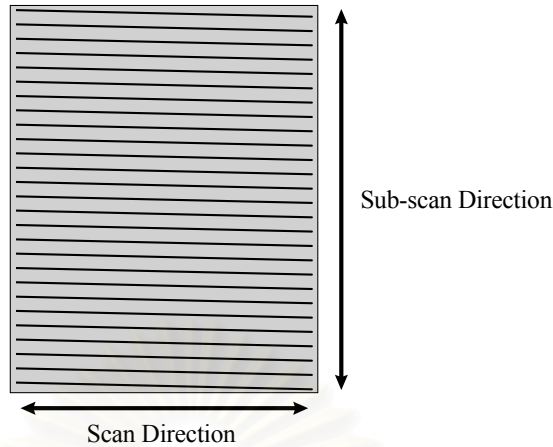


Figure 11. A diagram of the raster-scan of the phosphor detector indicates the fast scan (laser scan) direction and the sub-scan (plate scan) direction. Note the slightly skewed angle of the readout lines relative to the edge of the phosphor plate, due to the simultaneous laser beam scanning and linear plate translation.

2.3.2.1.4. Readout rate limits

In designing a readout system one must know the required readout rate. The plate throughput of medical scanners is ~30–110 plates per hour, which is adequate for the workload of a typical clinic. The engineering limit on the transport and stacking of IPs is a component of the total readout time.

2.3.2.1.5. Beam scanning

The diode laser beam is sent through several subsystems before reaching the CR plate as shown in figure 12(a). The laser beam is divided (not necessarily equally) into two with a beam splitter such as a partially silvered mirror. The main beam passes to the scanning system; the side beam is sent to a photodiode used to monitor, and with feedback, stabilizes the laser output intensity. The laser focusing lens is generally of the $f-\theta$ design. It has three further functions:

- (i) to make the focal plane flat so that focus is uniform across the IP,
- (ii) to convert the constant angular motion of the scan mirror into a constant linear speed at the image plane so that the pixel spacing is constant and
- (iii) to move the entrance aperture of the lens, i.e. locus defining region where any ray within the angle of acceptance will be imaged by the lens, significantly out from the body of the lens so that the rapidly scanning mirror has space to operate. Either a rotating polygonal mirror driven by a synchronous motor or an oscillating flat mirror driven by a galvanometer can perform the scanning function. The advantage of the rotating polygon mirror is that the transition from one facet to the next performs the flyback, i.e. retrace which occurs at the end of one line as the beam rapidly returns to the start of the next line. This maintains a high laser duty cycle, i.e. the fraction of the time the laser is actually reading out the IP. In contrast, a galvanometer has to be driven in an oscillatory manner by a saw tooth signal and after fly-back takes a fixed time to return to stable operation.

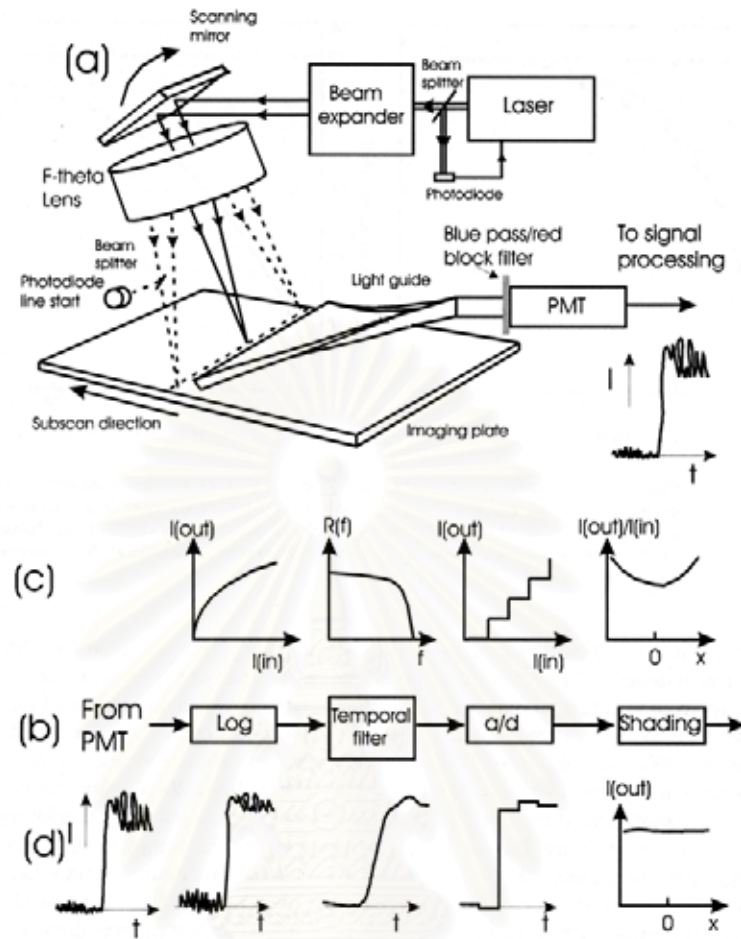


Figure 12. Flying spot CR readout scanner. (a) Scanner components also showing the graph of direct output of PMT response to a step in intensity on the IP, (b) processing stages, (c) response curves of processing stages and (d) typical form of output signal as it passes through the processing stages.

Thus the polygon is used for faster scanning speeds but it has two disadvantages which lead to periodic errors that appear as banding artifacts in the sub-scan direction.

- (i) The reflective properties of its facets may each differ slightly, which requires a further correction to the laser output.
- (ii) Unintentional scanning of the beam perpendicular to the scan direction results in an effect called *cross-scan error*, caused by slight angular shifts between facets. This can be corrected passively using a pair of cylindrical optics. CR, as in any destructive readout, is very sensitive to cross-scan error. If the beam moves one way, there will be reduced signal as it rereads already partially discharged regions of the IP and in the other way, it will steal signal from the next line. Control of cross-scan error to $<1 \mu\text{m}$ is required. Any uncorrected periodic error leads to banding with a period equal to the number of facets on the polygon.

The scan mirror repetitively scans a line and retraces the laser beam thus defining the scan direction. During retrace the laser beam is turned off and restarted just before it is expected to reach the active area of the IP. The laser beam positioning with respect to the

previously read out pixels is accomplished with a *line start detector*, i.e. a photodiode near to the starting point of the scanning. The linear motion of the plate in the sub-scan direction combined with the laser scan creates a raster pattern that is read out progressively.

2.3.2.1.6. Collection of PSL—light guide

The light guide is located as close as feasible to the IP to efficiently collect the blue PSL as shown in figure 12. Using the physical process of total internal reflection, the light guide transfers the PSL to the photomultiplier (PMT). To be efficient, careful design of the light guide is needed. Any light reaching the guide entrance must be accepted at an angle appropriate for total internal reflection within the guide. Made of a transparent plastic such as acrylic, the conditions for total internal reflection only occur if the guide is bent gently, i.e. on a large radius. It cannot perform demagnification, as light would escape from the sides. The light guide shape changes from a line to match the laser scan line at the IP, to an annulus to match the circular shape of the input window of the PMT. A more compact system using laser cuts to the acrylic has also been shown. Care has to be exercised to prevent laser light scattering or reflecting from the light guide onto the IP where it would discharge another part of the image creating flare (figure 12(c)). A related effect can occur in the top layer of the IP where unwanted reflections can produce *halation* (figure 12(d)). Thus the top layer thickness has been reduced to $\sim 3\ \mu\text{m}$. A conductive layer is also incorporated in the IP structure to prevent build up of static electricity.

2.3.2.1.7. Signal processing

The processing of the stimulated PSL signal from the IP is shown in figure 12. In figure 12(b) are the processing modules, in (c) their function and in (d) examples of the waveform at corresponding points in the processing cycle.

The first processing step is logarithmic amplification, which reduces the dynamic range prior to digitization and prepares the data for better visualization on a monitor.

The second processing step is to temporally filter the signal. This has several important functions: to correlate the signal prior to digitization so as to optimally match the analogue signal to the digitization sample rate f_d . This also prevents aliasing of noise and reduces or eliminates fixed pattern noise of an x-ray grid oriented with the grid lines perpendicular to the scan direction.

The third processing step is digitization. The digitization rate is relatively slow, e.g. $4\ \mu\text{s}$ per pixel, therefore an a/d (analogue to digital converter) operating at a frequency $f_d = 250,000$ samples per second is required.

2.3.2.1.8. Isolation of PSL from laser light

To permit the PSL signal to be isolated from the laser light, the phosphors chosen for CR can be stimulated with laser light with a different wavelength from the PSL light.

Laser power used in CR is $\sim 30\ \text{mW}$ or $\sim 2 \times 10^{17}$ red light photons/s (assume $2\ \text{eV}$ per red light photon). At this power and the $4\ \mu\text{s}$ dwell time per pixel derived earlier, there are $\sim 8 \times 10^{11}$ red light photons incident on each pixel. The first approach used to separate these light photons depends on the PMT. A typical transparent bi-alkali photocathode has a quantum efficiency of $\sim 25\%$ in the blue and $\sim 0.1\%$ in the red. The second approach is the filter, which still needs to selectively remove five orders of magnitude brighter light in the red while efficiently passing light in the blue if interference with the output of the PMT from the laser light is to be avoided.

2.3.2.1.9. Quantum accounting diagram

The maximum signal to noise ratio (SNR) of any imaging system occurs where the x-rays are absorbed. If the SNR of the imaging system is essentially determined here, the system is said to be *x-ray quantum noise limited* in its performance. Inevitably the SNR is reduced as the signal passes through the system. It is possible to make high image quality x-ray detectors because of the large intrinsic conversion gain as the x-ray energy. It is important that the detector maintains a large number of quanta representing each x-ray if *secondary quantum noise* is to be minimized. A quantum accounting diagram aids in locating the *secondary quantum sink*.

2.3.2.1.10. Readout linearity

Figure 13 shows the native characteristic curve response of a typical PSP receptor to a 400-speed screen-film system, i.e. a plot of PMT signal output before logarithmic compression, of a CR reader. A linear, wide latitude response to variations in incident exposure is characteristic of the phosphor plate, while film is optimally sensitive to a restricted range of exposures. For screen-film detectors, which serve as both the acquisition and display medium, it is necessary to tune the detector (film) contrast and radiographic speed to a narrow exposure range to achieve images with optimal contrast and minimal noise characteristics. PSP receptors are not constrained by the same requirements because the acquisition and display events occur separately so that compensation for under- and over-exposures is possible by the algorithms applied to the digital data. However, identification of useful signal range must be accomplished prior to the autoranging and contrast enhancement of the output image. In addition, since under or over exposed images can be “masked” by the system, a method to track exposures on an image by image basis is necessary to recognize those situations that exceed the “proper” exposure range so that appropriate action can be taken to resolve any problems.

Characteristic curve response

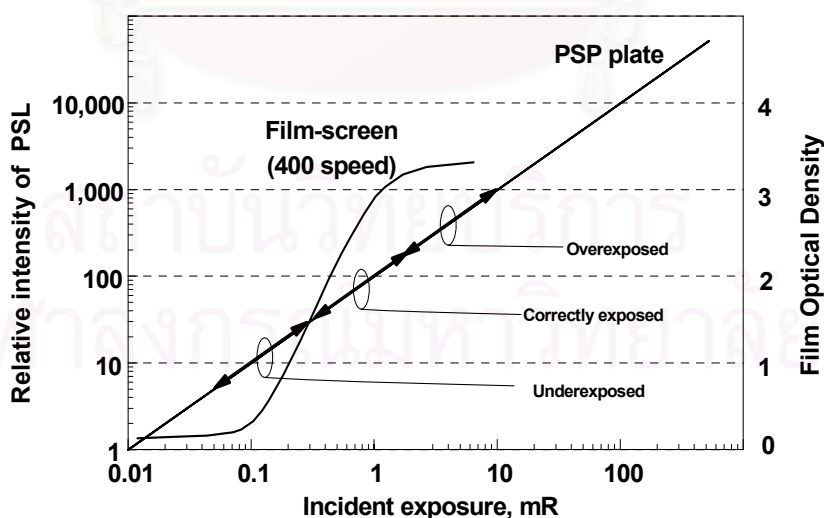


Figure 13. The characteristic curve of rare-earth screen-film (400 speed) and the PSP receptor are compared. Exposure ranges superimposed on the PSP curve roughly indicate the exposure range for screen film response of a 200 speed system [7].

2.3.2.1.11. Plate reconditioning

A residual latent charge image remains on the CR plate after readout. Erasure of the image using a high intensity light source must be performed before the plate is reused. This is accomplished using a high-pressure sodium or fluorescent lamp. The erasure time depends on the brightness of the lamp and the level of erasure required. The level of erasure achieved also depends on the prior x-ray exposure. The erasure rate is enhanced if the initial erasure is performed with a light spectrum including ultraviolet followed by a spectrum with the UV filtered. This is probably due to the creation of trapped charge by UV irradiation. Erasure times are 10–20 seconds for the Fuji AC-3 and ~ 50 s for the Lumisys ACR-2000 readers. In practice, unless exposed to an excessive x-ray irradiation (such as during a quality control procedure), the previous latent image is effectively removed during a single erase cycle. It is possible to accumulate an image on the CR plate due to natural radioactivity and cosmic radiation. Therefore, before clinical use the IPs should pass through a further erasure cycle if they have been in storage for more than a day. A summary of the PSP receptor cycle is illustrated in figure 14.

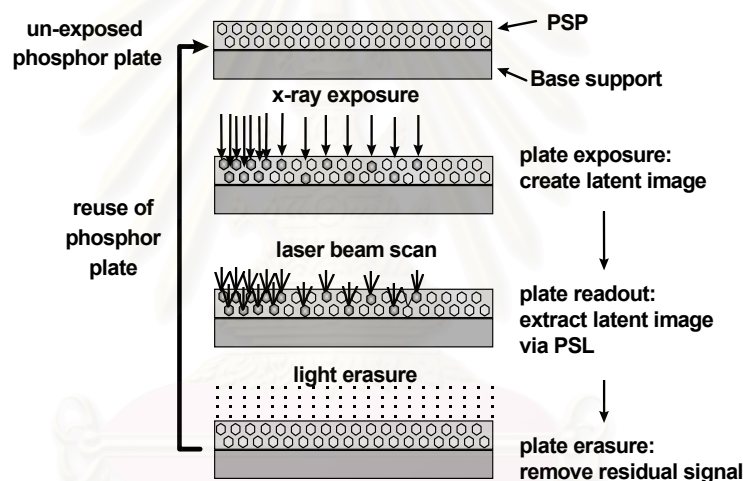


Figure 14. The phosphor plate cycle is depicted above. An unexposed plate is comprised of the PSP material layered on a base support and protected by a thin, transparent coating. Exposure to x-rays creates latent image centers of electrons semi-stable energy traps in the crystal structure. Latent image processing is accomplished with a raster-scanned low power laser beam (e.g., 20-milliwatt HeNe laser at 633 nm). Trapped electrons are released from the luminescent centers and produced light that is collected by a light guide assembly and directed to a photomultiplier tube. Residual trapped electrons are removed with a high intensity light source, and the plate is returned to the inventory for reuse.

2.3.2.2. Image Data Pre-Processing

In the earliest commercial CR readers an 8-bit a/d was used. Two methods were required for the large raw dynamic range to be adequately digitized. The first used a pre-read cycle to scan the laser across the image at a greatly reduced power. This allowed a determination of the actual image content and the PMT gain was adjusted to match that content. The second method added a logarithmic converter to process the signal from the

PMT before it entered the a/d as shown in figure 12. This further reduced the effective dynamic range of the signal and the number of bits required. Currently, analogue logarithmic processing or square root processing is used to reduce the dynamic range of the signal before digitization by a 12-bit a/d. Alternatively if logarithmic processing is performed digitally, i.e. after the a/d, using look-up tables, then a 16-bit a/d will be necessary. The prescan approach has been eliminated due to the ready availability of high bit depth converters and the ability of handling large amounts of digital data, which was far from trivial in the early eighties when CR systems were introduced. Finally a *shading* correction is applied to allow for the varying light collection efficiency of the light guide as a function of the laser position along the line. This is a one-dimensional correction as every line is the same.

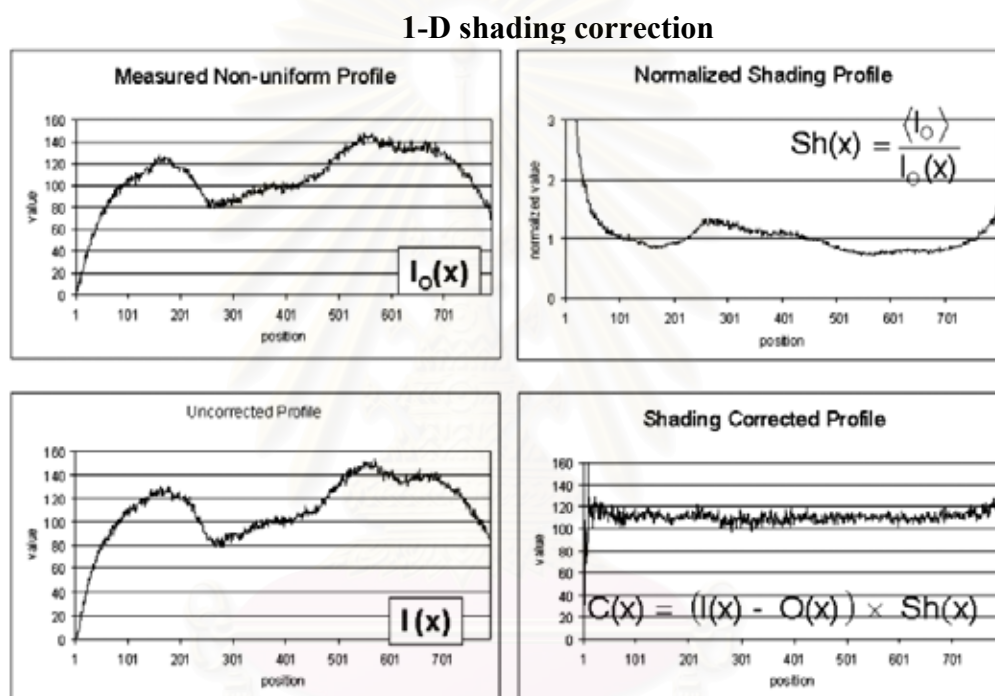


Figure 15. One-dimensional flat field methods correct for “shading” variations caused by the repetitive variations in laser-beam output and light-guide pickup characteristics. This is not—and should not be—dependent on the emission characteristics of the IP and, in fact, requires an IP of uniform light output. Reprinted from Seibert (2003) with permission from Radiological Society of North America (RSNA).

2.3.2.2.1. Shading Corrections

The “raw” data streaming from the CR reader requires shading corrections to compensate for variations in the light-guide response for a uniform exposure to the plate. For instance, equivalent PSL intensity captured at the edge of the light guide will have a lower response than if captured at the center of the light guide. Variations in the transmission efficiency will introduce static noise patterns that are reproduced at every scan. Over time, subtle deposits of material on the light guide produce fixed variations in light intensity. Adjustments to achieve uniformity are known as “shading corrections” applied to the raw data during acquisition. In the calibration mode, a uniformly irradiated IP of high-incident exposure (the latter to reduce quantum noise) is the source that measures the

intensity gain response, G , at each position x along the scan, $G(x)$, averaged over n independent lines. The dark-level offset variations, O , are also measured at the same positions (x) along the scan, $O(x)$, and averaged over m independent lines, $O_m(x)$. The shading-normalized and averaged correction, $S(x)$, is calculated as:

$$S(x) = \frac{M}{G_n(x) O_m(x)} \quad (2)$$

where; M is the global mean value of the evaluated profiles (the mean value of the denominator). Typically, $S(x)$ remains stable for a significant period (e.g., 6 months). As raw data are acquired, the dark current offset is subtracted from the incoming data at each scan position, x , and multiplied by the normalized shading correction array, producing the corrected data point, $I_c(x)$, as

$$I_c(x) = (I_{uc}(x) - O_m(x)) \times S_n(x) \quad (3)$$

For all x positions along the fast-scan direction. These steps are illustrated for shading correction CR image in figure 15. Because these are linear operations, this correction is performed prior to logarithmic or square-root transformation.

Newer line-scan systems can benefit from two-dimensional flat field processing, which provides a more robust correction because of the reproducible scanning of the fixed detector. Two-dimensional corrections can improve the elimination of stationary noise patterns along the sub-scan direction not possible with point-scan systems that use imaging plates of different size and number.

2.3.2.2.2. Identification and Scaling of “Pertinent” Data

The raw digital image data must be properly identified prior to subsequent post-processing for specific anatomical display. This typically involves finding collimator

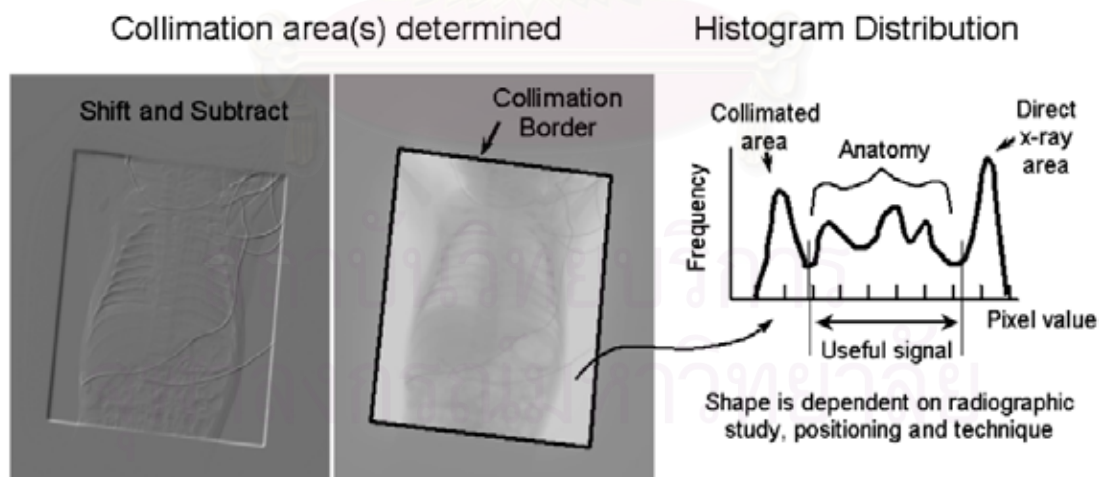


Figure 16. Shift and subtract reveals collimation borders and image area (left). Histogram analysis identifies minimum and maximum useful values within the defined collimation area to digitize over the range based upon the anatomy-specific shape (right). Incorrect histogram identification is often caused by positioning errors, collimator shadows off of the IP, or incorrect exam selection, among several causes.

processing for specific anatomical display. This typically involves finding collimator borders for one or more exposures on the plate, specifically identifying the areas, and then producing a histogram from which the examination-specific distribution is used for determination of the minimum and maximum useful signals. Manufacturers employ different methods. A particularly straightforward and useful algorithm is a “shift and subtract”: the image is subtracted from an identical copy of itself and then shifted in the horizontal and vertical directions by two or more pixels. This produces differential signals at locations of rapid change (e.g., collimator shadows) and identifies the area of interest. Algorithms to identify the resultant histogram shape—based upon the selected examination—are applied. Because the histogram distribution is strongly affected by anatomical variability, errors in shape identification occur as a result of collimator borders not correctly found, wrong examination, poor patient positioning, excessive scatter, highly attenuating objects such as prostheses, extreme under or overexposure, and inappropriate kV_p , among other causes. Failures were frequent with earlier systems. Although the potential problem list is long, advances in technology and algorithm improvements have reduced these errors to a small fraction. Figure 16 illustrates the data “finding” and “scaling” steps. The result of histogram analysis allows the normalization of raw image data for standard conditions of speed, contrast, and latitude determined by the digital number analysis. Rescaling and contrast enhancements are optimized for the specific patient examination to render the appropriate grayscale characteristics of the final output image.

2.3.2.3. Image data post-processing

CR data represents the baseline from which nonlinear contrast enhancement is applied. There are many contrast enhancement and spatial frequency algorithms, all of which strive to render the image with the anatomically best grayscale and detail. Image processing done poorly or inappropriately makes the image clinically inadequate. By the same token, excellent image processing cannot produce a clinically adequate image from poor pre-processing. Fortunately, reprocessing pre-scaled data and applying proper transformations can provide image quality good enough to reduce retakes to a minimum. Nevertheless, optimization of the processing algorithms according to radiologists preference during installation and at yearly intervals is extremely important.

2.3.2.3.1. Contrast Enhancement

The most simplistic contrast enhancement relies on non-linear transformation curves that mimic the response of a screen-film receptor. A variety of curves applied to the raw data provide wide latitude, high contrast, contrast inversion, etc. More sophisticated enhancement methods use a “harmonization” method, whereby a strongly blurred version of the image is weighted over a specific range of image values and subtracted from the original image. This approach will increase the apparent transmission under the diaphragm in a chest image by selectively reducing the slowly varying signal without affecting the detail and by reducing the dynamic range of the image. The overall contrast of the image can be increased simultaneously without saturation or threshold of portions of the image. Dynamic Range Control is a common name for this particular type of image processing.

2.3.2.3.2. Spatial Frequency Enhancement

In addition to contrast enhancement, spatial frequency processing is also important in providing edge details for evaluation of bone trabeculae, pneumothorax, and other high-detail characteristics that are otherwise difficult to appreciate, particularly given the lower spatial frequency of CR compared to the conventional 400-speed screen-film combination. Spatial frequency enhancement can be applied in different ways as well. An easy method is the short-range blurring of an image—such as can be done with a 3 x 3 (or specifically designed) pixel “kernel” averaging of the original image— creating the blurred version from the central pixel values and taking the difference image. This results in a bandpass image that is scaled (depending on the degree of enhancement desired) and added back to the original image. The outcome is an edge-enhanced composite image, as shown in figure 17.

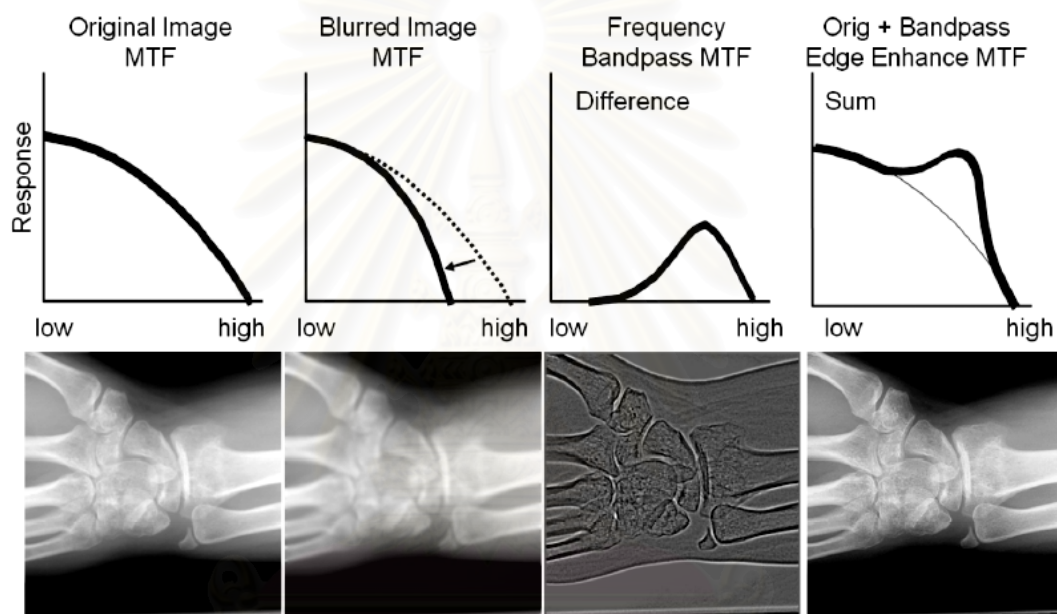


Figure 17. Simplified edge-enhancement example using a single bandpass frequency kernel is implemented by obtaining a blurred version of the image and subtracting from the original, giving a bandpass image with the bandpass frequency determined by the blurring kernel. A sum of the original image with the bandpass image results in the frequency-“boosted” image [6].

2.3.2.3.3. Multi-Scale, Multi-Frequency Enhancement

More sophisticated image processing methods use a “multi-scale” approach, whereby multiple scales (different bandpass ranges) of the same image are created by harmonization methods, from very low to very high frequency. Selective linear or non-linear amplification of each frequency band allows manipulation of the output image in terms of contrast enhancement, dynamic range control, and spatial frequency enhancement across all scales when combined to form the output image. Vendors have characteristic names for this type of image processing, including Multi-Scale Image Contrast Amplification (MUSICA) by Agfa, Multi-objective Frequency Processing (MFP) by Fuji, and Enhanced Visualization Processing (EVP) by Kodak. This type of processing is now becoming the standard mode of processing, chiefly because of the flexibility of the

algorithm over multiple frequency ranges with the ability to achieve simultaneous increased contrast and selectable edge enhancement over all areas of the image. Figure 8 shows a simplified methodology of the multi-scale approach.

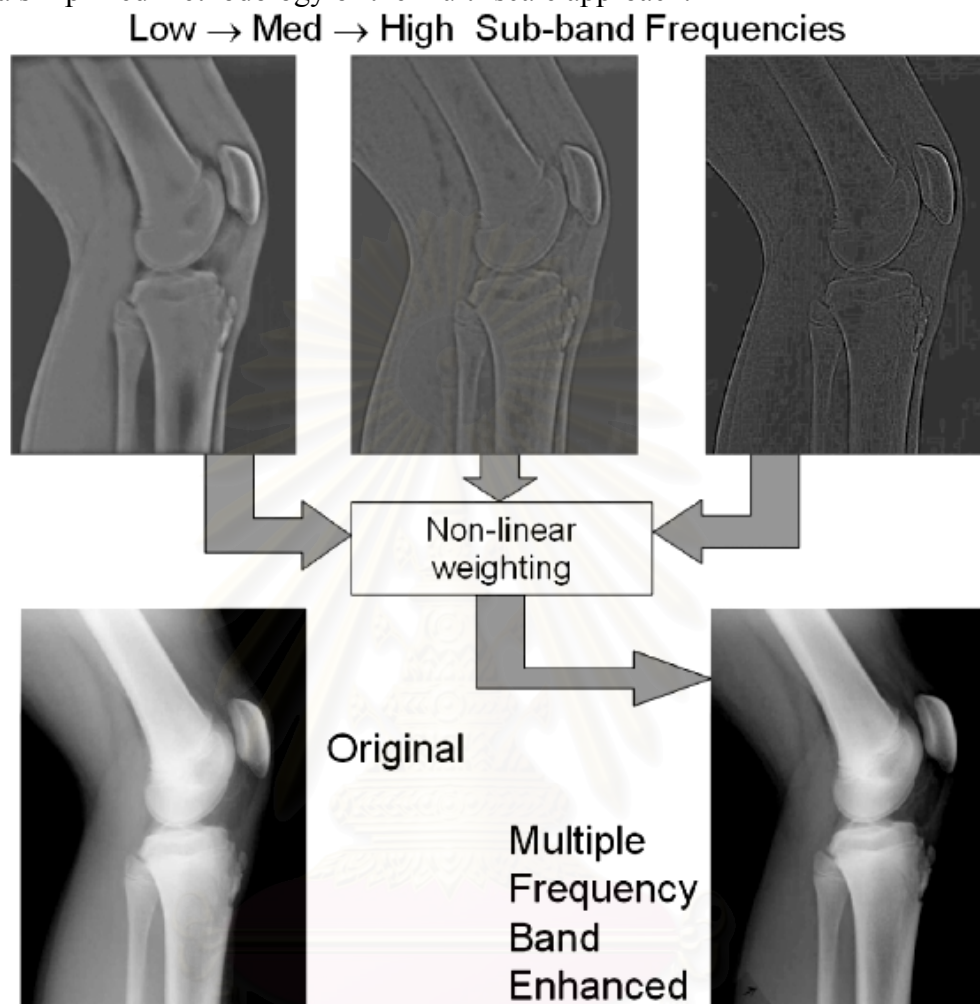


Figure 18. Multi-scale, multi-frequency approach for simultaneous contrast and frequency enhancement of images across all frequency ranges of the image. Typically, multiple frequency bands of eight or more are used; three are shown here. In this example, note the ability to enhance the soft tissue and bone contrast simultaneously compared to the original image.

2.3.2.3.4. Disease-Specific and Dual-Energy Processing with CR Imaging

Other advanced image processing techniques have “disease-specific” algorithms that emphasize characteristics that improve the detection of particular characteristics of the image based on the indication for the study or the suspected pathology, such as subtle linear structures to detect a pneumothorax. Dual-energy radiography—made possible by the large dynamic range characteristics of CR detectors and the simultaneous acquisition of low- and high-energy images obtained with a copper filter sheet sandwiched between two IPs—provides the ability to generate tissue-selective images (bone and soft tissue-only renditions). Electronic imaging infrastructure combined with computer-aided diagnosis

processing can bring sophisticated detection capabilities to the general radiologist in the evaluation of pulmonary lesions and the ability to distinguish benign from malignant lesions.

2.3.2.4. Exposure Indicators

The PSP system can provide proper optical density or image luminance for under or over exposures because of a wide latitude response and ability to scale the signal. Potential problems with inappropriate techniques can therefore be masked. As a result, it is important to have an indicator of the average incident exposure on the imaging plate to verify proper radiological techniques. Each PSP manufacturer has a specific method for providing this information. In the case of Fuji, a *sensitivity* number is provided, which is an indication of the amount of amplification necessary to adjust the image information to the correct digital range, and is inversely related to the incident exposure. In the case of Kodak, an *Exposure Indicator* provides a value directly proportional to an average exposure, while Agfa provides a relative exposure value, *lgm*, based upon a history of previous exposures. A calibration of the system is necessary for reporting accurate results, and is described in the acceptance testing procedures.

Fuji PSP systems utilize a *sensitivity number* to provide an *estimate* of the incident exposure on the plate transmitted through the object (if any) for the automatic and semi-automatic modes of operation. Under normal processing conditions for the standard resolution (ST) plates, the system sensitivity number for an unattenuated 80 kVp beam is given as:

$$S \cong \frac{200}{\text{exposure (mR)}} \quad (4)$$

A low incident exposure on the phosphor receptor creates fewer activated luminescence centers, and results in a lower PSL signal. Amplification of the signal is required to obtain the optimal analog signal range for digitization. The amount of amplification (or de-amplification when an overexposure occurs) is indicated by the system sensitivity value. As opposed to screen-film systems, PSP systems offer flexibility in exposure level choices. When the system sensitivity number is equal to 200 with the “semi-automatic” or “automatic” mode, an average photostimulated luminescence within the area sensed by the reader is *estimated* as 1 mR (80 kV_p, no object, no added x-ray tube filtration other than inherent). This corresponds to a digital value of 511 (the central value of the 10 bit grayscale range), and to roughly the speed of a 200 speed screen-film combination. (A 400-speed screen/film combination requires approximately half of the incident exposure). For the *fixed* sensitivity mode available with the Fuji PSP system, the sensitivity number is set by the user, making the system perform similar to a screen-film detector. Calibration of the system sensitivity response is part of the acceptance test procedures. Since the energy of the x-ray beam determines the relative absorption by the PSP receptor, the system sensitivity response varies with kVp and beam filtration. Fuji does not harden the x-ray beam used to “calibrate” the system, which limits the usefulness of “S” as an estimate of the incident exposure on the detector for clinical applications.

2.3.2.5. CR Exposure Recommendations

Whichever exposure indicator method is used, the output values are sensitive to segmentation algorithms, effective energy of the beam (kVp, filtration), delay between exposure and readout, positioning of the patient relative to the phosphor, and the source-image distance, among other causes. Nevertheless, the exposure indicator number is important to quality assurance, patient exposure, and technologist training issues. In general, the optimal exposure required to provide good image quality at the lowest possible dose to the patient for CR systems corresponds to an ~200 speed screen-film detector system, based upon the noise limitations of the image acquisition process. To use the CR system optimally, however, the incident exposures must be tuned to the specific examination. For example, tube placement exams that are frequently acquired to verify location can use significantly reduced exposures because of the relatively high signal of the tube. Likewise, for pediatric scoliosis exams, after the first “standard-dose” exam, repeat exams can be acquired at one-fourth the dose when the features of the vertebral column for measurement are needed. On the other hand, extremity exams requiring low noise and high detail should be acquired with a correspondingly higher dose. The bottom line is the need to tune the CR system exposure techniques to a level appropriate for each exam at acceptance testing and to continuously strive to ensure that these levels are consistently maintained through feedback and continuous training. Exposure indicators for CR should be audited at least quarterly and more frequently when first installing a unit. Guidelines for quality control of the exposure indicator are listed as a part of continuous quality control procedures in this monograph.

Table 1. Recommended “S” number limits for general “adult” imaging procedures. Values are based on a Fuji 5000 CR reader and “ST – V” imaging plates. Note: This does not apply to pediatric or extremity imaging, which will have slightly higher and slightly lower equivalent speed points, respectively. Assumed is proper positioning and exam processing algorithms matched to the anatomy imaged.

| CR “S” number | Detector exposure(mR) | QC action to be taken |
|---------------|-----------------------|-----------------------------------|
| > 1000 | < 0.2 | Underexposed: REPEAT |
| 600 – 1000 | 0.3 – 0.2 | Underexposed: QC exception |
| 300 – 600 | 1.0 – 0.3 | Underexposed: QC review |
| 150 – 300 | 1.3 – 1.0 | Acceptable range |
| 75 – 150 | 1.3 – 2.7 | Overexposed: QC review |
| 50 – 74 | 4.0 – 2.7 | Overexposed: QC exception |
| < 50 | > 4.0 | Overexposed: REPEAT |

With too low an incident exposure, the image is dominated by quantum statistics, the corresponding SNR is very poor, and the ability to detect subtle differences in x-ray attenuation is compromised. With too high an incident exposure, on the other hand, highly penetrated areas in the image will suffer from saturation effects and loss of contrast that cannot be adjusted. These recommendations depend on several issues, including the type of

CR reader (newer systems, such as the dual-light collection systems, have a higher DQE and will consequently have a lower exposure recommendation for all indications), type of imaging plate (later-generation IPs have better exposure performance), quality of the CR reader and IP, and tolerance of the radiologist to image noise, among other considerations. Continuous analysis and feedback are required to get the optimal range of exposures and indications for a given examination at a given site.

2.3.2.6. PSP image characteristics

2.3.2.6.1. Spatial Resolution

High-contrast spatial resolution is determined by several factors that contribute to the modulation and loss of the signal, including (1) composition and thickness of the phosphor plate, (2) the size of the laser spot, (3) light scattering within the phosphor, and (4) PSL signal lag. Large x-ray absorption and high spatial resolution are usually not simultaneously achievable for producing the optimal image with CR (although some future photostimulable “structured” phosphors have been touted as being able to overcome this limitation). Typical CR phosphor thickness is on the order of 100 mg/cm^2 for BaFBr. A thicker phosphor layer absorbs more x-ray photons and produces more trapped electrons in the matrix; however, PSL from the laser spot spreads out with depth, contributing to image blur. Digital image pixel size, usually between 100 and 200 μm , and determines the maximum *spatial resolution* of the system, up to physical limits imposed by the composition of the imaging plate and the size of the laser spot. Digital sampling confines the maximum spatial frequencies contained in the output image to a maximum determined by the Nyquist frequency, equal to the inverse of twice the pixel dimension, $(2\Delta x)^{-1}$ that can be accurately transferred through the system. Higher spatial frequencies contained in the spectrum beyond the Nyquist frequency will reflect back into the lower spatial frequencies and contaminate the image with “aliasing” artifacts such as moiré patterns. Unlike conventional screen-film detectors, smaller IPs will often provide better limiting resolution because the “effective” sampling pitch/aperture is determined by IP size (the number of samples is kept roughly constant, independent of the field of view). Spatial resolution is increased with a thinner phosphor layer, but the trade-off is lower detection efficiency and higher radiation dose. A majority of CR systems now use “standard” resolution IPs in lieu of the less dose-efficient “high-resolution” IPs. Phosphorescence lag and signal carry-over to adjacent pixels in the fast-scan direction cause the spatial resolution to be reduced near the Nyquist frequency.

2.3.2.6.2. Contrast Resolution

Contrast resolution depends upon several variables as well. The most important is the subject contrast generated by energy absorption differences of the tissues. In a digitally sampled system, the minimum difference between “noiseless” signals depends on the total number of possible digital values (quantization levels) as well as the target signal amplitude relative to the background. In most CR systems, digital values change with the logarithm or square root of the photostimulable luminescence, or equally with the logarithm radiation dose to the plate, so the numerical difference between digital values is the contrast. Contrast sensitivity of CR depends on the number of bits representing each pixel, on the gain of the system (e.g., number of electrons per x-ray photon or number of x-ray photons per analog-to-digital unit), and on overall noise amplitude relative to the contrast. The

ability to differentiate a signal in the image of an object is strongly dependent on the inherent subject contrast (kVp and scatter acceptance), amount of noise (x-ray, luminance, electronic, and fixed pattern noise sources), image viewing conditions, and the observer's ability to discern regions of low contrast with respect to size. Digital post-processing can enhance contrast to a level limited only by the noise in the image. Noise sources contributing to the output image include the limited number of x-rays absorbed in the IP (quantum mottle), the stimulated luminance variations during the readout process, quantization noise added by the analog-to-digital signal conversion (dependent upon the bit depth of the ADC, which is typically 10 to 12 bits in current systems), and electronic noise sources added during processing of the electronic latent image signals.

2.3.2.6.3. Detective Quantum Efficiency

Detective Quantum Efficiency (DQE) is a measure of the signal transfer efficiency for a given incident exposure as a function of spatial frequency. DQE is determined on a system with a linear or linearizable system with respect to exposure variations. The characteristic curve response is used to linearize the system, and the presampled MTF (f) and two-dimensional NPS(f) values are measured to calculate the DQE as:

$$DQE(f) = \frac{SNR_{out}^2}{SNR_{in}^2} = \frac{\langle PV \rangle^2 \times MTF(f)^2}{NPS(f)\phi} = \frac{NEQ(f)}{\phi} \quad (5)$$

In this equation, the SNR_{in}^2 is equal to the incident fluence (number of x-ray photons per unit area on the detector), and the SNR_{out}^2 is the square of the measured SNR of the output signal at a specific spatial frequency, f . This is determined by the measurement of the average global pixel value ($\langle PV \rangle$), the $MTF(f)$, and $NPS(f)$, as defined by specific methodologies (IEC 2003; AAPM 2004). NEQ is a measure of the “effective” noise characteristics of the detector as a function of spatial frequency. The DQE(f) is measured over a range of incident exposures to determine incident exposure dependencies (if any) of the detector. Ideally, the DQE is 100% at all useful spatial frequencies, but in reality it is typically less than 30% for conventional CR detectors, mainly limited by the absorption efficiency of the phosphor. The DQE drops rapidly with spatial frequency because of a loss of signal modulation and a greater fraction of additive noise sources. As the incident exposure increases, a loss of DQE occurs at all spatial frequencies from an increase in noise contributions because of blemishes and thickness variations in the phosphor that are otherwise “hidden” by quantum noise at low incident exposures. DQE values indicate incident exposure requirements for a given SNR in the output image.

2.3.3. Image presentation

PSP images are matrices of digital pixel values that are readily manipulated to produce alternative image presentations. Three broad categories of processing include image contrast variation, spatial frequency content modification, or special image algorithm implementation.

PSP systems manufacturers provide sophisticated computer hardware and software to process images. Some vendors provide similar functionality for remote processing of image data. No comprehensive source of information about manufacture specific algorithms and implementation exists. This is due in part to the immature nature of the PSP

marketplace and digital image processing in the practice of radiology. Significant misunderstanding exists, both inside and outside the manufacturer community, about the proper use of image processing software. Selection and optimization of processing parameters is a non-trivial task that potentially requires “many thousands of man-hours by highly skilled staff”. A common problem is that the range of processing parameters far exceeds clinically useful values and leads to gross over-processing artifacts. Modification of processing parameters should not be undertaken lightly.

2.3.3.1. Laser Film Printers convert the digital images to film images to mimic the conventional screen-film radiography paradigm, where the film is trans-illuminated for viewing. With some PSP systems, the image size must be reduced (de-magnified) by a variable amount, depending upon the phosphor plate size and output film format. Hard copy presentation of the PSP image commits the user to a single rendering, obviating a major advantage of convenient display processing. In order to provide two different grayscale/edge enhancement renderings, the image size may be further reduced to accommodate two images on a single film. This two-on-one format requires a reduction to 50% of the 35×43 cm (14×17 inch) field of view on small format PSP films ($\sim 26 \times 36$ cm). Size reductions complicate direct measurements, comparison to historical studies on film/screen, and inter-comparison of views where the size reduction may be different. Full field of view printing is available on 35×43 cm format film, with large sampling matrices up to approximately 4000×4000 pixels ($\sim 3500 \times 4300$ by one manufacturer) to provide high spatial resolution on the order of 5 lp/mm over the full field of view.

2.3.3.2. CRT and LCD Monitors are used for “soft-copy” display. Digital images from the PSP reader are displayed on CRT or LCD monitors for a variety of purposes, including verification of correct patient positioning, Quality Control review and image modification, primary diagnosis, and clinical reference. The capabilities of the monitors, the image processing toolkits available in their associated workstations, and the criticality of their display properties vary according to their function. CRT monitors provide for simultaneous viewing of images throughout the hospital and for real-time modification of image appearance by the observer. CRT monitors share a number of characteristics, including lower luminance levels than a standard light-box or film alternator, an image produced by fluorescence emission rather than by trans-illumination, an inherently nonlinear display transfer function, potential for fading, geometric distortion, and defocusing. If the monitor is linked to production of hard copy images, matching the appearance of the image on the monitor with the film is an important consideration. The adverse effect of high ambient light levels on the appearance of the image is more problematic with a CRT than with a trans-illuminator because of the lower CRT luminance. In addition, CRT phosphors produce different colors and have difference phosphorescence lag when changing images. An increased emphasis on the acceptance testing and quality control of display monitors and viewing conditions is necessary to ensure optimal image rendition.

2.3.4. Image data managing

Interface of the PSP system(s) to Radiology and Hospital information computers is necessary. Specific details regarding the in-house RIS/HIS vendor must be explained. In return, the PSP vendor should be expected to provide a standard interface (e.g., Health Level-7 (HL-7)) or other non-standard interfaces along with specific demographic

information to be transferred. Automatic downloading and uploading of patient demographics, examination type, and scheduling times should be requested. A DICOM-3 conformance statement for interface to existing or future picture archiving and communications system (PACS) infrastructure is also essential. Interfaces to existing dedicated and network-based laser printers should be included in the bid. Ask the vendor to describe the interfaces (e.g., are the interfaces implemented in the system design, or is extra peripheral hardware required in close proximity to the PSP reader?). As there are several capable third-party vendors that provide interfacing functionality of the types described above, request the vendor to indicate an “approved” third-party vendor list, and consider these alternatives. The assistance of knowledgeable experts is helpful for these complicated issues.

2.3.4.1. System configurations and digital soft copy interfaces

The diagnostic radiological physicist is likely to encounter PSP devices manufactured by any of several vendors. These devices often represent different generations of technology and exist in different functional configurations. The specific system configuration significantly affects how the physicist conducts acceptance tests. The display media, display processing and content of the digital image data file varies depending on system configuration.

Many PSP devices operate as general-purpose devices inside or outside the radiology department. In this application, an imaging plate is inserted into the device and a dedicated laser camera produces a film. Other PSP devices are dedicated to acquisition of upright examinations of the thorax and may be integrated into the x-ray generator. Some PSP devices are constructed into a radiographic table. In some hospitals, PSP devices are operated independently with dedicated laser printer. In other hospitals, PSP devices are used to acquire digital data for a sophisticated image and information management system (IMACS).

Two decades of research and development, combined with advances in computer technology, have resulted in major improvements in PSP devices. The integration of PSP devices and the development of commercial PSP devices have followed a parallel path. A PSP device is a system that must provide the user with several functions to be clinically useful. In addition to acquiring digital data representing the projected x-ray beam, the integrated system must provide a facility to process, store and render the resulting image data for display.

Independent PSP Reader with Quality Control (QC) Workstation. The data available through the FDLR-DASM, however, was not fully processed by the PSP device, and required additional image processing to match the appearance of the film output. Early use of these interfaces was largely limited to academic institutions. Fuji subsequently introduced the HIC-654 computer workstation to interface to the AC-1+ and AC-2 via the proprietary DMS interface. The HIC-654 provided the capability to temporarily store data onto a local disk drive, reprocess image data stored on disk, print the reprocessed data and provided processed through a FDLR-DASM.

Networked PSP reader with Networked QC Workstation and Networked Laser Printer. All manufacturers have the capability to transfer data processed data to attached

laser cameras and to remote computer systems and laser printers via networks using the DICOM3 communications protocol. At this writing, Agfa is the only PSP manufacturer whose PSP reader communicates directly to the network according to DICOM3 conventions.

Acquisition and Association of Patient Demographic and Exam Information. Early PSP devices required the operator to manually enter patient demographic and exam information associated with each PSP image. As PSP devices became integrated into radiology operations, more efficient methods were developed to acquire this data including creation of magnetic cards, bar codes, and ultimately, functional interfaces with the Radiology Information System (RIS). In order to perform acceptance tests on integrated PSP systems, the physicist may have to create phantom patients in the RIS corresponding to the planned test exposures.

2.4. Clinical application of complete CR systems

The first issue in establishing a new imaging system is how it compares to previous system. For x-ray systems, the important measurements are image quality and patient dose, the former being highly dependent on the latter. Computed radiography has been compared to the digitized film from a film–screen combination. Image quality is very difficult to compare across imaging systems because of their inherently different properties. An interesting technical concept is to expose the CR IP in the same cassette with a conventional screen–film system, thus obtaining a perfectly matched CR and screen–film image in the same exposure and without additional radiation. Recent studies have used more conventional approaches and comparisons of CR against DR systems. There is little agreement as to whether the image quality of CR is better, worse or the same as screen–film.

In a digital system the exposure can be varied over a large range yet still deliver an optimally bright image with a correct mean intensity and tone scale. In practice, there is a very narrow margin where the image is subjectively equivalent to screen–film. This is the basis for the statement that twice the exposure is necessary for standard CR plates to achieve the image noise perception characteristic of commonly used 400 speed screen–film, i.e. $\sim 2.5 \mu\text{Gy}$ mean exposure to obtain an optical density of 1 above base plus fog, since standard CR plates are considered to be ~ 200 speed ($5 \mu\text{Gy}$ mean exposure).

New systems mean new artifacts. The form of these artifacts and the diseases they may camouflage or imitate are well documented. A primary criterion used by radiologists in comparing image quality in films is the appearance of x-ray noise in the image or *quantum mottle*. Any visual signs of mottle make an image unacceptable. The blurring in CR, by reducing the x-ray bandwidth, effectively reduces the appearance of noise. The control of latitude is important and the digital nature of CR makes quantification of images possible. The specific clinical applications of CR will be reviewed by the followings;

2.4.1. Portable

Photostimulable phosphor systems are widely used for emergency and bedside radiography where the variable readout sensitivity allows for compensation for under- and overexposure problems. Portable chest radiography presents particular problems especially in intensive care situations. In bedside applications accurate lining up a grid is impractical and thus scatter [10] is difficult to control.

2.4.2. General radiography

For chest radiography, comparative studies of the threshold perception of CR compared to screen–film, indirect conversion flat-panel imagers, and selenium-based systems have been performed. Radiation dose requirements for adults and pediatrics have been investigated [11, 12]. A one-shot dual energy CR procedure has been investigated for the detection of pulmonary nodules and has been compared with asymmetrical screen–film. Further studies with variation of dose have been performed. For both adult and children musculoskeletal, extremities, hand, cervical spine and scoliosis have been identified as useful applications of CR. The combination of equalization with CR has also been investigated.

The application of CR to radiographic magnification is obvious, since magnification requires increasing the distance between the detector and patient; and hence the IP from the x-ray source. Using screen–film with a fixed radiographic speed requires additional radiation to the patient to obtain an adequately exposed image. CR works well at reduced dose so that the exposure can be based on the radiation requirement of the imaging task and not simply the technology. A similar argument can be used for the application of CR to phase contrast imaging where the need for very large patient–imager distances combined with as small a magnification as possible (to avoid focal spot blurring) gives an additional freedom for optimization not available with screen–film.

2.4.3. Mammography

Early CR mammography used a 100 μm pixel and conventional high resolution IP with a mixed reception. Using a contrast–detail phantom specially designed for mammography, study of the visibility of micro-calcifications and linear analysis demonstrated comparable performance to screen–film despite a poorer limiting resolution. These results were confirmed using a clinical ROC study. However, the introductions of flat-panel DR systems with improved dose efficiency and MTF have raised expectations. CR readers with 50 μm pixel size and a two-sided readout mammographic system have shown improved results and clinical trials of these systems have begun.

2.5 Quality assurance (QA) and quality control (QC) for computed radiography system:

2.5.1. Adjustment of the hardcopy recording device

As most primary diagnosis is currently made with hard-copy laser films generated from the acquired digital data, the following steps must be checked to ensure proper operation.

- (1) The film image is properly positioned on the film.
- (2) Shading variations caused by non-uniformities in the laser-light intensity across the film are minimal.
- (3) Processor chemistry is maintained at an optimal level.
- (4) Internal laser calibration is within tolerance limits specified by the vendor.

There will typically be system-generated test scans available to assist in the verification of these parameters.

2.5.2. Film Processor and Laser Printer Tests

A film processor audit requires the verification of proper chemistry activity, replenishment levels, developer temperature, and lack of processor generated artifacts. The film processor should be evaluated according to the manufacturer's quality assurance recommendations as well as methods outlined in the literature. The film processor chemistry and the developer

temperature influence the optical density values of the printed films. It is advisable to independently test processor performance with sensitometric strip methods on a daily to weekly basis, depending on system use. This will allow any potential problems with the film processor to be uniquely identified and separated from those caused by the PSP system hardware and calibration mis-adjustment.

2.5.3. Laser printer calibration/Sensitometry

Laser-generated sensitometric strips should be printed to determine the proper laser performance and function, and to calibrate the printer when out of tolerance. Each test point of the laser-generated pattern is measured with a calibrated densitometer. The optical density values should fall within the tolerance limits indicated by the vendor documentation. Should the values fall outside the recommended density range, a correction (calibration) algorithm should be invoked (often under the guidance of the service engineer) and the test repeated. For a second failure, a request for repair should be initiated prior to doing other acceptance tests. In certain situations, the PSP system laser writer can compensate for variations of film processor chemistry or malfunction that can ultimately lead to a catastrophic failure. It is important, therefore, to understand and determine the degree of compensation effected by the laser subsystem.

2.5.4. Image workstation display monitor calibration/resolution tests

In a soft-copy environment, display workstations are a critical link in the overall image quality verification of a PSP system. A short list of items that should be evaluated initially and frequently via quality control tests are:

- Adjustment of brightness/contrast via SMPTE test pattern or equivalent.
- Determination of high contrast spatial resolution, both centrally and peripherally
- Determination of geometric distortion, particularly in the periphery of the image
- Evaluation of luminance output with a luminance meter
- Evaluation of room lighting conditions with luminance meter

Hardware and software tools to perform these tests should be specified in the original purchase agreement to be delivered with the system. This is an area critically important to image display and evaluation of the PSP system, where further work is necessary to describe and implement acceptance tests and quality control procedures.

2.5.5. Calibration and Characterization of the X-ray Beam

X-ray beam characterization of a calibrated x-ray system is important for achieving reproducibility in PSP system tests of sensitivity, linearity, and uniformity. A beam produced by a high frequency generator system that is likely to be available to the physicist for future QC testing is preferred. For general-purpose PSP systems, a standard 80 kVp beam with 3.0 to 3.5 mm aluminum equivalent HVL should be characterized. An identical beam, or nearly identical beam, should be used in subsequent QC testing and performance monitoring of the PSP system. Also, at the time of acceptance testing, identification of several image receptors to be set aside and safeguarded for the physicist's sole use in subsequent QC testing is highly recommended. For specialty PSP systems, more appropriate beams should be characterized and used (e.g., 120 kV_p for a dedicated chest PSP system).

Sensitivity and linearity tests should challenge PSP system response under conditions representative of the clinical environment. To ensure reproducibility of results, a simple phantom of 1 mm copper and 1 mm aluminum is recommended. The phantom should be

placed at the collimator with the copper side facing the x-ray tube. Uniformity tests may be conducted with or without the phantom.

2.5.6. Specific Testing Procedures

Once familiarized with the system parameters of the particular PSP system to be tested, proper function and adherence to specifications can be determined with the tests recommended in this section. Assessment of initial operating characteristics and measurements of all testable components is essential to determine baseline performance, and to ensure continued optimal functionality and image quality throughout the system's lifetime during periodic quality control testing and preventative maintenance service.

2.5.7. The Physicist's Role in CR Implementation

The physicist should be the technical expert and liaison between the radiology and hospital administrators, the radiologists, technologists, and IT/PACS staff. Knowledge of the CR system characteristics (resolution, detection efficiency, radiographic technique charts, sensitivity of the CR plate to scattered radiation and requirements for grids, compensation for under- and overexposure, decreased kV dependence, image processing, system specifications, etc.) is the key to being a successful arbitrator in a sometimes difficult—but necessary—transition from screen-film to CR/DR imaging. One critical role is the establishment of a training program that describes the changes in operation with CR. These changes include: exposure sensitivity of CR relative to that of 400-speed screen-film cassettes; the role of image processing in contrast optimization and noise suppression of the output radiograph (particularly for pediatric imaging); and how to implement and maintain ALARA (As Low As Reasonably Achievable) concepts using CR for this very radiosensitive population. Issues related to clinical considerations and details regarding exposure indicators as well as signal-to-noise ratio (SNR) and DQE details are described below. Acceptance testing and quality control tests are certainly part of the physicist's domain; these issues are covered in a separate article in these summer school proceedings.

2.6. Dose Reference Level (DRL)

Diagnostic reference levels are used to help manage the radiation dose to patients so that the dose is commensurate with the clinical purpose. The existing ICRP guidance Publication 60 [13] provided the recommendation on optimization of protection in medical exposure in paragraph (S34): "Consideration should be given to the use of dose constraints, or investigation levels, selected by the appropriate professional or regulatory agency, for application in some common diagnostic procedures. They should be applied with flexibility to allow higher doses where indicated by sound clinical judgment." ICRP Publication 73 [14] explained its place in the broader ICRP concept of reference levels, and expanded the ICRP Publication 60 recommendation in (S34) in more detail (paragraphs (99) through (106) of ICRP Publication 73). The objective of a Diagnostic Reference Level is to help avoid radiation dose to the patient that does not contribute to the clinical purpose of a medical imaging task. DRL can be used:

(a) To improve a regional, national or local distribution of observed results for a **general medical imaging task**, by reducing the frequency of unjustified high or low values: for a general medical imaging task which is applied to this study used Entrance surface air kerma (in air, no backscatter) or entrance surface dose (in a specified material, with backscatter) in mGy, for a given radiographic projection (e.g. PA chest).

(b) to promote attainment of a narrower range of values that represent good practice for a *more specific medical imaging task*; or

(c) To promote attainment of an optimum range of values for a *specified medical imaging protocol*, e.g. a protocol for a PA chest radiograph that specifies the clinical purpose, the technical conduct of the procedure, the image quality criteria, any unique patient characteristics, and other appropriate factors.

A reference group of patients is usually defined within a certain range of physical parameters (e.g. height, weight). If an unselected sample of patients were used as a reference group, it would be difficult to interpret whether the observed value for the sample is higher or lower than the diagnostic reference level. A diagnostic reference level is not applied to individual patients. The array of considerations and approaches to reference levels, whose features are displayed in Table 31 and Table 32 (Appendix C).

International Basic Safety Standards Protection against Ionizing Radiation and for the Safety of Radiation Sources, Safety Series No. 115, IAEA[15] had measured dose quantity for the radiographs as ESD in mGy (for film-screen combinations with relative speed 200; reduce by factor of 2 to 3 for film speed 400-600) and derived from wide-scale surveys for typical adults corrective actions if doses fall substantially below levels with no useful information or medical benefit or if doses exceed levels.

REVIEW OF RELATED LITERATURES

The radiation dose reduction and the diagnostic information are the output of quality control tests to assess the efficiency of computed radiographic system [16]. QA represents a comprehensive, ongoing program to evaluate all aspects of medical imaging. The ultimate goal of a QA program is to optimize image quality and patient safety. QC typically refers to the performance of periodic monitoring of imaging performance. Some authors [17] showed that the reduced retake rate due to exposure factors by using CR led to a reduction in the overall retake rate. Despite 50% dosage reduction, films were of better or equal quality when compare to conventional radiography. Several authors [18, 19, 20, 21] suggested that dose reduction can be achieved by means of a reduction in the number of examinations that must be repeated owing to incorrect exposure factors. In addition, it is often suggested that computed radiography could be used with lower radiation doses than conventional screen-film systems and thus reduce patient doses [22]. Though the artifacts on radiographic images are distracting and may compromise accurate diagnosis, users' understanding the potential sources of CR artifacts will aid in identifying and resolving problems quickly and help prevent future occurrences [23]. The goal of computed radiography (CR) acceptance testing is to establish the storage phosphor reader and phosphor screen baseline performance. Quality control testing then detects changes in the CR system that could affect radiographic image quality. In this project, two main parameters are identified as influencing diagnostic reference levels (DRL) and entrance skin dose (ESD).

CHAPTER III

CONCEPTUAL FRAMEWORK, RESEARCH QUESTIONS AND RESEARCH OBJECTIVES

In this study, two parameters are identified as influencing the patient radiation dose in term of entrance skin dose (ESD). They are the quality of radiation that represents by quality control of x-ray unit and the quality of images that represent by meaning of quality control of the CR unit.

3.1. Conceptual Framework

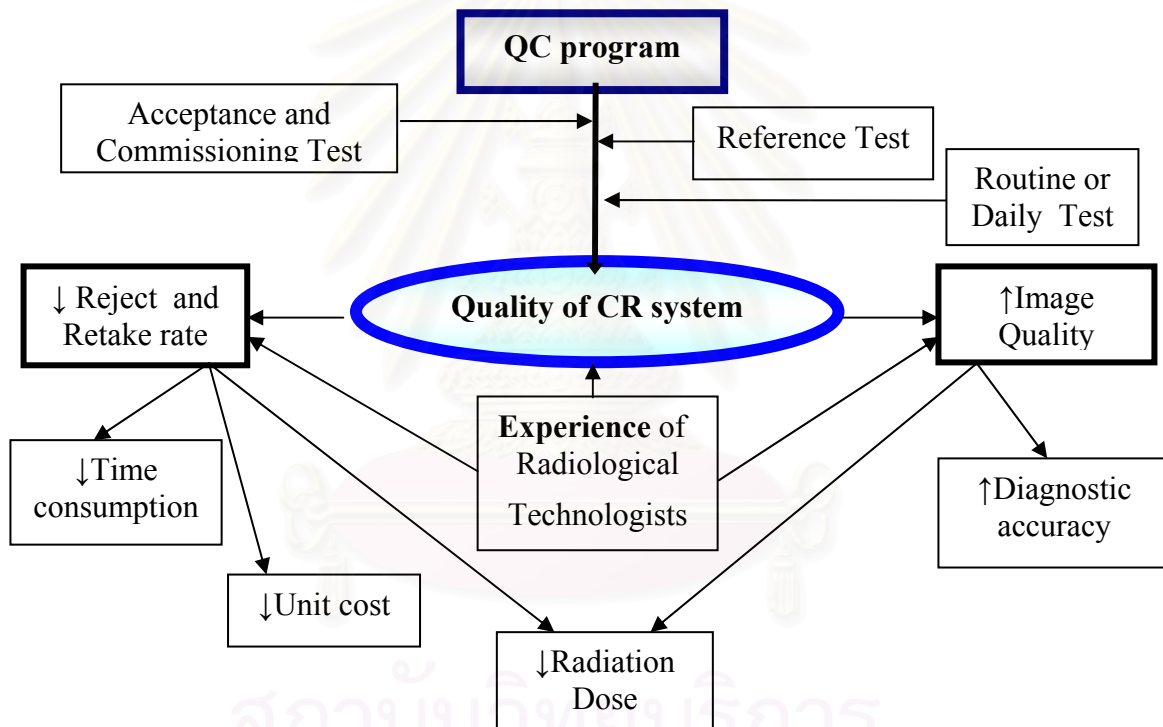


Figure 19. Conceptual Framework of research

3.2 Research Questions:

Primary Research Question

- Is the patient dose reduced after the implementation of QC protocol?

Secondary Research Questions

- Is the image quality improved after the implementation of QC protocol?
- How is the relationship between the image quality, the patient doses and other parameters such as body weight, kV_p , mAs and etc.?

3.3 Research Objectives

General Objectives

- 3.3.1 To set up a quality control program for the computed radiography system, that could affect radiographic image quality at this center, according to well accepted standards such as AAPM or IEC.
- 3.3.2 To implement the QC program for the CR system.
- 3.3.3 To record the changes in image quality and the reject-retake rate.

Specific Objectives

To relate the patient radiation dose and image quality after implementing the standard QC program for the computed radiography system at the Department of Radiology of King Chulalongkorn Memorial Hospital, Thai Red Cross Society.

3.4 Hypothesis

Implementation of a QC program for the CR system results in the reduction of the reject-retake rate (and thus, radiation dose to the patient), and improve image quality.



สถาบันวิทยบริการ
จุฬาลงกรณ์มหาวิทยาลัย

CHAPTER IV

RESEARCH METHODOLOGY

4.1 Research Design

This work has been designed as a prospective experimental study comparing dose to the patient and image quality before (controls) and after (experimental group) implementation of QC of the CR system. All data was collected under the criteria developed by the senior technologist. The entrance skin dose (ESD) was calculated and matched for before and after image quality evaluated by two radiologists. All data was analyzed by using SPSS version 11.5 for window to test the hypothesis.

4.1.1 Research Design Model

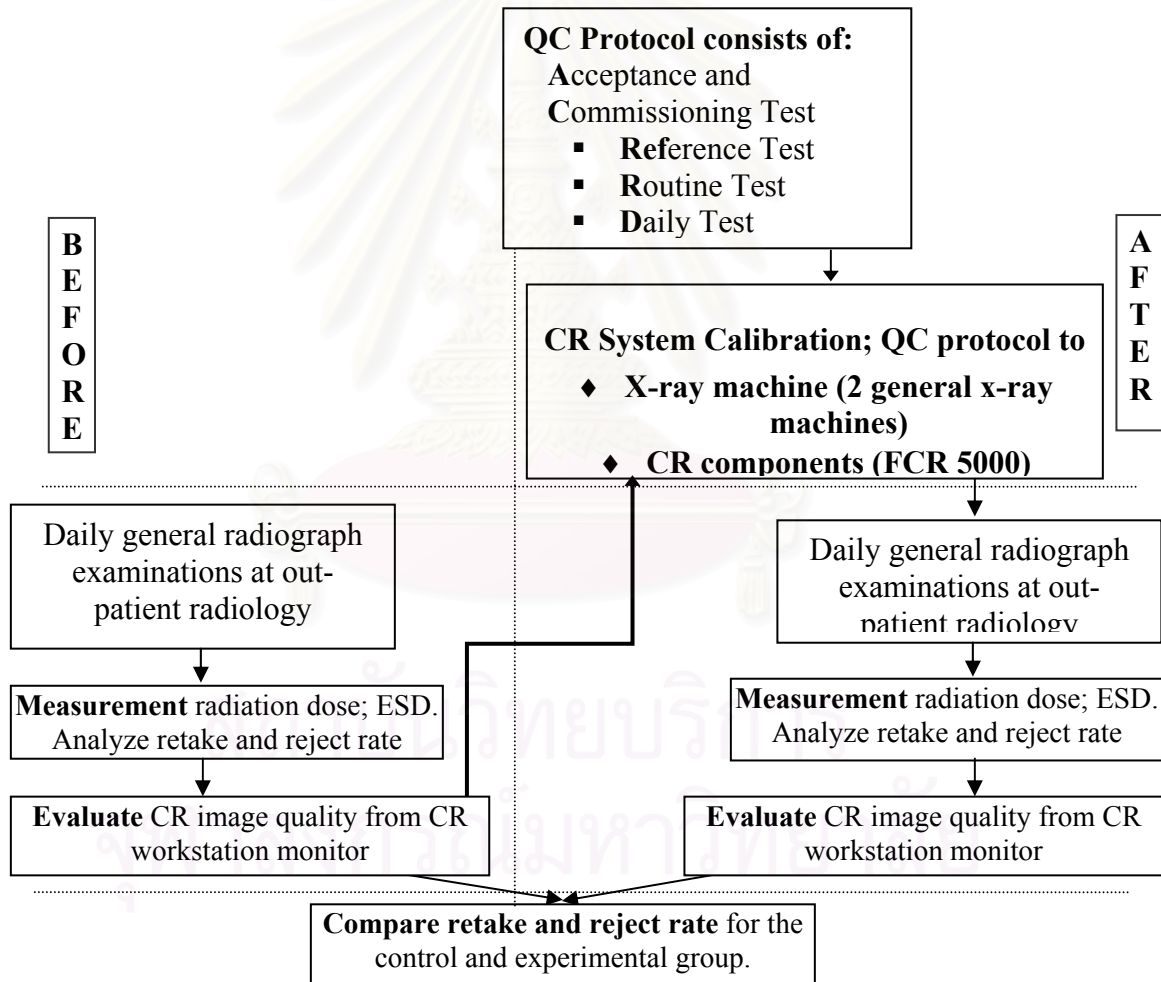


Figure 20. Research Design Model

4.2 The Sample

4.2.1 Target Population: All patients who were requested for general radiography and processed by CR. The period of collection was 3 months (2 groups).

4.2.2 Sample Population: All patients who were requested for general radiography and processed by CR (the number of patients in each examination, follow sample size estimation table 2) which meet the following eligible criteria.

4.2.3 Eligible criteria:

4.2.3.1 Inclusion criteria for patients

1. The patients undergoing one or more of the following 8 examinations:
 - Skull PA from paranasal sinuses series
 - Lateral cephalometry
 - Cervical spine AP
 - Chest PA
 - Abdomen AP
 - Lumbo-sacral spine AP
 - Lumbo-sacral spine lateral and
 - Pelvis AP
2. The patient must be conscious and able to control movement
3. The age of the patient was between 16 to 75 years with body weight was between 35 to 114 kilogram.
4. Patient data recorded:-
 - 4.1 Hospital number
 - 4.2 Date of examination
 - 4.3 Age (years)
 - 4.4 Body weight (kg), height (cm) and the patient thickness at part of exposed (cm).
 - 4.5 Part of examination (8 given radiographic projections).
 - 4.6 Exposure factors (kV_p , mAs and FFD)
 - 4.7 Causes of reject-retake images (position, motion, technical error, selected menu, high "S" value, low "S" value, artifacts)
5. The repeated images of the same patients must be included.

4.2.3.2 Exclusion criteria

1. Emergency or acute disease patients who can not co-operate the examination.
2. Incomplete image data.
3. Missing data transferred to the optical disk filing (Fuji: ODF-624).

4.2.4 Sample Size Estimation:

Since the primary outcome is the radiation dose that will be normalized by applying each group of radiograph's ESD value to the proportion of reject and retake data, then, comparing to overall examinations in the period of collecting data time. The sample size for each group is determined by the cluster sampling method under these conditions;

1. The data is the dichotomous data.
2. The primary outcome is the reject and retake percentage.

3. The sample population is independence, prospective data.
4. The Chi-square will be used to calculate data.

$$\text{By formula; } n / \text{group} = \frac{\{ Z_{\alpha} \sqrt{2\bar{P}(1-\bar{P})} + Z_{\beta} \sqrt{P_1(1+P_1) + P_2(1-P_2)} \}^2}{(P_1 - P_2)^2} \quad (6)$$

$$\bar{P} = (P_1 - P_2) / 2 ; (P_1 = 9\%, P_2 = 5\%)$$

$$\text{CI} = 95\%, \text{ Power} = 90\% = 1 - \beta, \quad Z_{\alpha} = 1.64, \quad Z_{\beta} = 1.28 \text{ (see } Z_{\beta} \text{ table)}$$

$$\text{Size of Population (N) for each group} = \mathbf{4,697} \text{ examinations}$$

$$\text{Derived; } n / \text{group} = \frac{\{ 1.64 \sqrt{2 \times 0.07(1-0.07)} + 1.28 \sqrt{0.09(1+0.09) + 0.05(1-0.05)} \}^2}{(0.09 - 0.05)^2}$$

$$\text{Sample Size (n) for 95\% confidence interval} = \mathbf{692} \text{ examinations / group}$$

$$\text{Total sample size for control and experimental groups} = \mathbf{1,384} \text{ examinations}$$

4.3. Experimental Maneuver

Patient data were collected at the general x-ray room (Room number 4 and 5) of outpatient building (Por Por Ror 4th floor), Department of Radiology, King Chulalongkorn Memorial Hospital, Bangkok. Two sets of single-phase x-ray machine (Hitachi DR-155HM, Hitachi, Japan, 1989) with bucky table, non-AEC (automatic exposure control) were used. One set of the CR system was a Fuji computed radiography (Fuji, FCR 5000, Fuji Photo Film Co. Ltd., Tokyo, Japan, 2000) containing a helium neon laser (633 nm). Imaging phosphors were of Europium doped barium fluoro-bromide. Storage phosphor plate size for skull PA from paranasal sinuses series, lateral cephalometry, and cervical spine AP was 24 x 30 cm, and 35 x 43 cm for chest PA, abdomen AP, lumbo-sacral spine AP, lumbo-sacral spine lateral and pelvis AP. Soft copies were observed on Fuji CR Workstation model HI-C 655 by using Totoku high resolution monochrome LCD display model ME 201L. Hard copies were made on Fuji computed radiography film type 780-H (25.7 x 36.4 cm) and type LI-LM (35 x 43 cm) by using Fuji wet laser imager model FL-IM D with developer (RD-20) and Fixer (RF-15). 2 sets of x-ray machines (Hitachi DR-155 HM, Hitachi, Japan) were used.

4.3.1. Study Methodology

Sample random technique: The procedures in this study are:

1. The selected randomly of the target patients had been done by the preliminary survey of 8 given radiographic projections and 4 age groups for 33 working days. Table 2 showed to arrange the specification of each age range.
2. Select the cases of "Before QC program" (control group) by using table 2 and meet the criteria; collect and complete the patient data to table 6 table 20 to 27 in appendix A for the period of 1.5 months.
3. Analyze the data for Before QC program period.
4. Calibrate the x-ray and the CR systems using the following procedures:
 - 4.1 Calibrate the X-ray machines, Room 4 and Room 5 (Hitachi DR-155HM, Hitachi, Japan) using AAPM protocol [24] and record in data sheet table 28-29 (Appendix B).

4.2 Calibrate the FCR 5000 system [25] (CR Reader, HIC-655 workstation monitor, Wet laser printer (FL – IM D) and Photo- stimulable phosphor imaging plate standard type (ST - V_N)) using protocol for the QA of Computed Radiography Systems Routine QA Tests and Acceptance Testing and Draft Document: AAPM Task Group No.10 and input all calibrated data to datasheet in table 33-36 (Appendix B).

5. Repeat step 2 - 3 for “After QC program” (experimental group).

Table 2. The total sample size and total number of each examination group used to collect the patient data.

| Part of examination | Age (y) | Population (N) | Sample size (n) | |
|--------------------------------------|---------|------------------|-----------------|------------|
| | | | Total | Each range |
| 1. Skull PA for paranasal sinuses | 16 – 30 | 87 | 13 | 2 |
| | 31 – 45 | | | 4 |
| | 46 – 60 | | | 6 |
| | 61 – 75 | | | 1 |
| 2. Cephalometry lateral | 16 – 30 | 17 | 3 | 0 |
| | 31 – 45 | | | 2 |
| | 46 – 60 | | | 0 |
| | 61 – 75 | | | 1 |
| 3. C spine AP | 16 – 30 | 143 | 21 | 2 |
| | 31 – 45 | | | 3 |
| | 46 – 60 | | | 9 |
| | 61 – 75 | | | 7 |
| 4. Chest PA | 16 – 30 | 3,210 | 473 | 111 |
| | 31 – 45 | | | 145 |
| | 46 – 60 | | | 135 |
| | 61 – 75 | | | 82 |
| 5. Abdomen AP | 16 – 30 | 347 | 51 | 7 |
| | 31 – 45 | | | 12 |
| | 46 – 60 | | | 20 |
| | 61 – 75 | | | 14 |
| 6. L-S spine AP | 16 – 30 | 373 | 55 | 5 |
| | 31 – 45 | | | 16 |
| | 46 – 60 | | | 20 |
| | 61 – 75 | | | 24 |
| 7. L-S spine lateral | 16 – 30 | 407 | 60 | 4 |
| | 31 – 45 | | | 14 |
| | 46 – 60 | | | 29 |
| | 61 – 75 | | | 13 |
| 8. Pelvis AP | 16 – 30 | 107 | 16 | 2 |
| | 31 – 45 | | | 2 |
| | 46 – 60 | | | 6 |
| | 61 – 75 | | | 6 |
| Total | | N = 4,697 | n = 692 | |

6. Calculate ESD for each examination by the following formula;

$$\text{ESD} = \frac{\text{mAs} \times \text{ESD}_M \times \text{FSD}^2}{100^2} \quad (7)$$

Where; mAs = setting milli-ampere-second for each examination

ESD_M = ESD modified at 100 cm in $\mu\text{Gy/mAs}$ unit

FSD = FFD minus to Skin-to-film distance

7. Obtain the radiation dose and image quality of the control group and the experimental group.

Image quality grading technique: The procedures in this study are:

1. Matching cases for image quality grading had been done by using the similarity of body part thickness and BMI in each group of the same examination type.

2. Retrieving the selected cases from ODF-624 and transferring to HI C-655.

3. Scoring the image quality by two of equivalent experience radiologists using the European Commissioning (EC) image quality criteria guideline as shown in table 39 in Appendix D.

Grading positioning and image quality in detail use scale 0, 0.5 and 1;

0 - Not fulfill

0.5 - Partial fulfill

1 - Fulfill

P - Pathology / Excluded

4. Average the scores in 3 parts, the first was total scores of positioning and image quality, the second was the image noise scores and the overall image quality scores for the third.

4.3.2. Materials

4.3.2.1. X-ray machine:

Use AAPM task group No.4 protocol for quality control of the x-ray machine to evaluate the status of x-ray machine and components in table 28-29 (Appendix B).

Table 3. The items of x-ray machine QC and list of test tools to be used.

| Items of x-ray machine QC | List of test tools |
|--|--|
| 1. General mechanical conditions | 1. Ionization chamber (Victoreen 4000M) |
| 2. All indicator lamps and "beam ON indicator" | 2. Pure Aluminum plates (0.1, 0.5 and 1.0 mm in thickness) |
| 3. Dead man switch | 3. Beam alignment test tool |
| 4. Source image distance (SID)indicator | 4. Collimator test tool |
| 5. Mechanical motion test | 5. Sensitometer |
| 6. Field size indication | 6. Densitometer |
| 7. Light VS radiation congruence | 7. Tape measure |
| 8. Cross-hair centering | |
| 9. Automatic collimation or Positive beam limit (PBL) | |
| 10. Photo timer reproducibility and density compensation | |
| 11. Exposure reproducibility | |
| 12. Linearity of exposure with mR/mAs | |
| 13. Timer accuracy | |
| 14. (HVL)Beam quality | |
| 15. kVp accuracy | |
| 16. Entrance skin exposure (ESE) | |

4.3.2.2. CR system:

“Acceptance Testing and Quality Control of Photo Stimulable Phosphor Imaging Systems Report of **Task Group No.10** American Association of Physicists in Medicine” and “Protocol for the QA of Computed Radiography System Commissioning and Annual QA Tests, **KCARE CR QA Protocol Draft 4.0** by Kings College Hospital” to evaluate the status of CR system and components in the following items:

Table 4. The items of CR machine QC and list of test tools to be used for Commissioning Tests.

| Items of CR machine QC | List of test tools |
|---|--|
| 1. Monitor & laser printer | 1. TO20 threshold contrast test object or equivalent |
| 2. Dark Noise | 2. Small lead or Copper block (~5 x 5 cm) |
| 3. Erasure cycle efficiency | 3. 1.5 mm Copper filtration (>10 x 10 cm) |
| 4. Sensitivity Index calibration | 4. Farmer Ionization chamber 0.6 cc. |
| 5. Sensitivity Index consistency | 5. Huttner test object or equivalent |
| 6. Uniformity | 6. M1 geometry test object or lead ruler |
| 7. Scaling errors | 7. Contact mesh |
| 8. Blurring | 8. Steel ruler |
| 9. Limiting Spatial Resolution | 9. Adhesive tape |
| 10. Threshold Contrast Detail Detectability (TCDD) | 10. Tape measure |
| 11. Laser beam function | |
| 12. Moiré Patterns | |
| In all tests, the unique CR imaging plate identification code should be recorded. | |

4.3.3. Computed Radiography System Quality Control Method

1. Monitor & laser printer set-up

Purpose: To test that devices used to view the image data are of sufficient quality to maximize the information available to the observer.

- View an image of the SMPTE test pattern on each of the monitors used for reporting clinical images or for the QA tests.
- Decide whether the 5% on 0% and 95% on 100% details are visible.
- Score the resolution bars at centre and corners of the image.

If images are viewed from hard copies then the laser printer should also be assessed.

Tolerances: The 5% on 0% and 95% on 100% details should be clearly visible. The horizontal and vertical resolutions should not differ by greater than 20%.

2. Dark Noise

Purpose: To assess the level inherent noise of the system

- Erase an image plate without making an exposure, and read it using the following parameters:

| |
|---|
| Fuji: Readout mode – ‘Fixed’ (S = 10000. I = 1) |
|---|

- Examine the images visually for uniformity and record the sensitivity index value (Fuji- Sensitivity S, Latitude L).

- c) Record a mean pixel value using region of interest analysis (for Fuji systems details measure a mean pixel value).

Reduce the window width to 1, so that the image has only pixels appear as either one of just two levels, black or white. Adjust the level until approximately half the pixels are black and half are white. This level value is the mean pixel value of the image.

- d) If possible either archive or print the image for future reference.

For Fuji systems a uniform artifact free image should be expected. This results in series of bands appearing across the image.

3. Erasure cycle efficiency

Purpose: To test that minimal residual signal (ghosting) remains on a plate after readout and erasure.

- Position a plate on the table at ~1.5 m. Set a 10 cm x 10 cm field and position a piece of attenuating material (e.g. copper or lead) at the centre of the CR plate. Expose at 80 kV_p, 25 mAs with no filtration.
- Read the plate (the readout parameters are not important).
- Re-expose the plate with a 9 cm x 9 cm field center on the same point on the plate with no attenuating material in place, using 80 kV_p, 0.5 mAs and no filtration.
- Read the plate using the following parameters;

Fuji: Readout mode – ‘Semi Auto’ L = 1 or 2

- Visually inspect the resultant image for any remnant of the previous image, using region of interest analysis if available.

Tolerance: There should be less than 1 percent (remedial) difference between the pixel values in the ghosted region and the surrounding areas. A suspension level of <5% is set.

4. Sensitivity Index calibration

Purpose: To assess the accuracy of the plate exposure values calculated using exposure indicators.

- Position an ion chamber at ~1.2 m from the focus (see figure 21) and at least 30 cm above the table (record the actual distances). Collimate to the ion chamber.
- Expose the chamber such that the inverse square law corrected dose to the table level is approximately 10μGy, using the following beam qualities;

| | | |
|-------------------|--------------------|------------------------------------|
| Fuji CR system | none Filtration | Tube Voltage 80 kV _p |
|-------------------|--------------------|------------------------------------|

- Record the measured dose and repeat twice.
- Remove the chamber and place a 24 x 30 cm cassette on the table. Set the field to just cover the cassette. Mark the corners of the cassette on the table with transpore, so that the cassette can be easily repositioned.

N.B. An alternative dosimetry set up can be used: Position the chamber on a 20 cm foam pad to determine the mAs required to deliver the required plate dose. Then position the plate on the foam pad. This negates the need for an inverse square law correction.

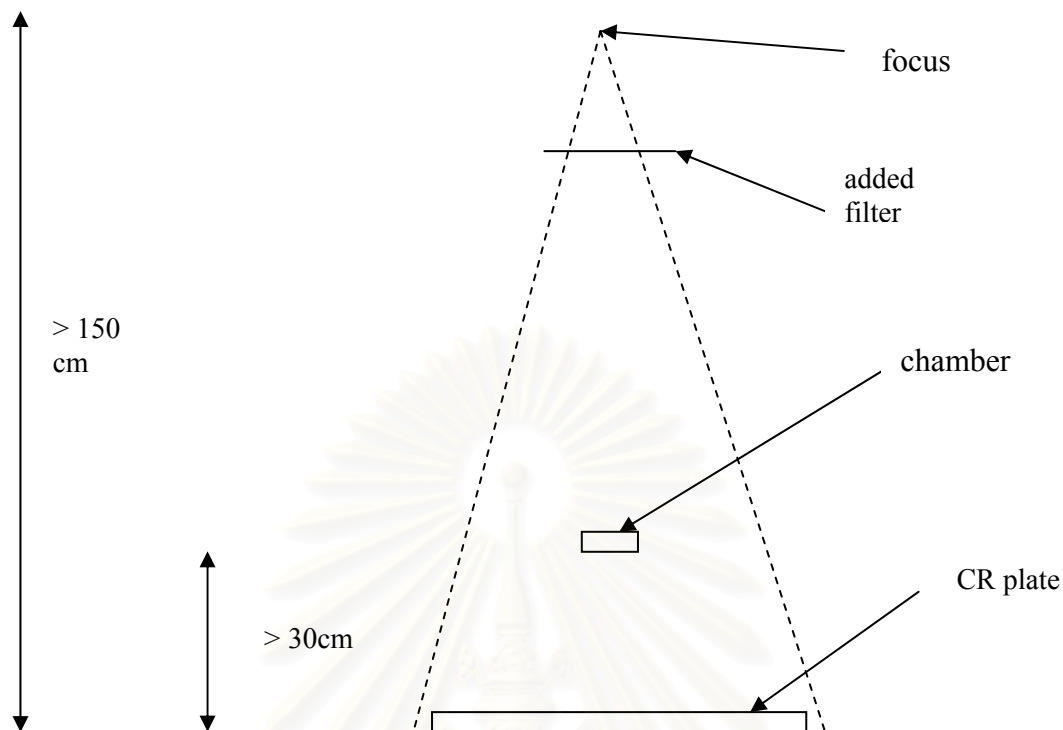


Figure 21: Set-up for exposure index calibration

- e) Expose the plate to a known dose of $\sim 10 \mu\text{Gy}$ as above.
- f) Read the plate out as described below

Fuji: A 10 minute delay between exposure and readout, readout using semi-auto, L=1 or 2

- g) Record the sensitivity index, and calculate the indicated exposure using the following equations.

For Fuji systems the indicated exposure, E_{fuji} , in μGy , is given by

$$E_{fuji} = \frac{1740}{S} \quad (8)$$

- h) Repeat twice and take a mean value of the indicated exposures.

Tolerance: The indicated exposure should agree with the measured exposure within 20%.

5. Sensitivity Index consistency

Purpose: To assess the variation of sensitivity between plates, and set a baseline for monitoring system sensitivity for future QA testing.

- a) Place a 24 x 30 cm CR cassette on the couch and set up as described for test 4 (see figure 21).
- b) Expose the plate using the beam qualities described in test 4, to a known dose of $\sim 10 \mu\text{Gy}$. The dose to the plate calculated from inverse square law corrected ion chamber measurements should be recorded.
- c) Read the plate as described for test 4, but with minimal delay (or short fixed- e.g. 5 mins.) between exposure and readout for Fuji system.
- d) Record the sensitivity index, and calculate the indicated exposure using equations 8. Repeat three times for the same plate.
- e) Repeat this test for all plates if time allows (making only one exposure to each plate).

Tolerance: The variation in the calculated indicated exposures should not differ by greater than 20% between plates. The measurements repeated on the same plate should be used to lay down a baseline for future QA tests.

6 Uniformity

Purpose: To assess the uniformity of the recorded signal from a uniformly exposed plate. A non-uniform response could affect clinical image quality.

- a) Expose a plate as described for test 5 but with half the mAs.
- b) Rotate the plate through 180° about the vertical axis and re-expose using the same parameters (this should largely cancel out the non uniformities due to the anode heel effect).
- c) Read the plate as described for test 5 with no delay between exposure and read out.

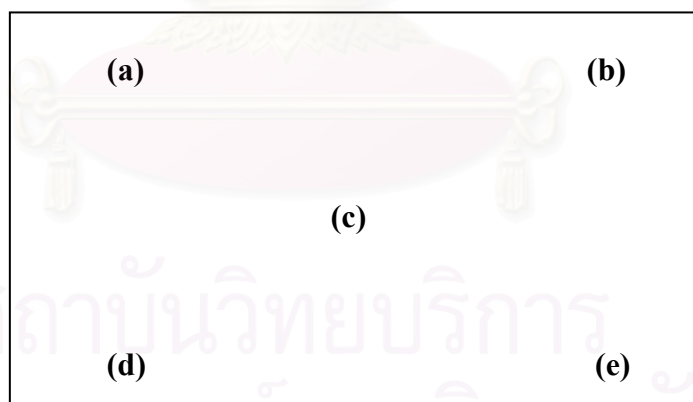


Figure 22: Positions of the ROI's for uniformity tests

- d) Visually inspect all images obtained in test 5 for uniformity and artifacts. Likely artifacts include dust on the plate or readout optics, and scratches on plates.
- e) The uniformity of the image obtained in 6b should be assessed using region of interest analysis if available, to measure the mean pixel values in positions a-e, as indicated in figure 22. For Fuji systems where ROI analysis is not available, read uniformly

exposed plates using the FIX mode with S-200 and L=2. Print the images onto laser films and measure the optical densities in the positions indicated in figure 22.

Tolerance: The images should not have obvious artifacts. If measuring uniformity from film the maximum variation in optical densities should be less than 10%. Using region of interest analysis, values should be within a range of 10% of each other.

7. Scaling errors

Purpose: To assess the accuracy of software distance indicators and check for distortion.

- Position the M1 test object directly on the centre of a CR cassette at > 150 FDD.
- Expose at 50-60 kV_p with no filtration and 10 mAs.

N.B. A lead ruler could be used in place of the M1 test object. If so 2 exposures should be made with the ruler placed in first the scan direction then the subscan direction.

- Read out plate using processing as for test 4 but without delays between exposure and readout.
- If digital calipers are available in the software, check that the pixel size is correctly calibrated for the particular image receptor size.
- Using the distance measuring software tools measure the dimensions (x and y) of five central squares in both fast and slow scan directions. Calculate the aspect ratio x/y.
- Reposition the test object over the edge of the plate as indicated in figure 23 and repeat steps b to d.
- Along the edge of the plate measure the horizontal (x1) and vertical (y1) sizes of two squares as indicated in figure 24. Calculate the aspect ratio x1/y1.

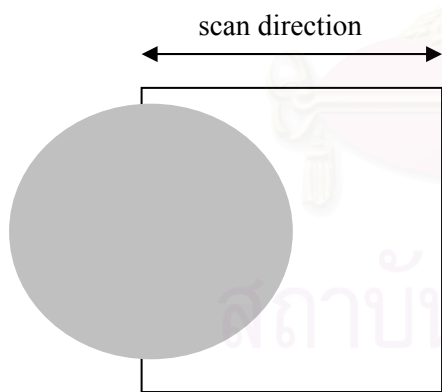


Figure 23: Scaling assessment.

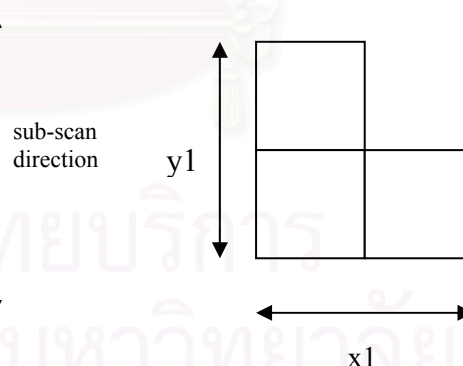


Figure 24. Calculated the aspect ratio $x1/y1$.

Tolerance: The measured distances x and y should agree within 3% of the actual distances. All calculated aspect ratios should be within 1.00 ± 0.03 .

8. Blurring

Purpose: To test for any localized distortion or blurring of the image.

- With the contact mesh in place expose and read a plate as described for test 7.

- b) Visually inspect the image for distortions. If distortion occurs clean the plate and repeat.
- c) Repeat for at least two other plates.
- d) Repeat with a fine mesh if available.

Tolerance: No blurring should be present. If blurring is present on all plates this suggests the reader is at fault, whilst imperfections in individual plates may also lead to blurring. If blurring remains on a region of a plate after cleaning it should not be used clinically.

9. Limiting Spatial Resolution

Purpose: To test the high contrast limit of the systems ability to resolve details.

- a) Place a general purpose cassette on the couch with the Huttner test object positioned at its centre aligned at 45° to its edges.
- b) Set 50 kV_p expose the cassette to ~10 mAs.
- c) Readout the plate using the following parameters;

Fuji: Readout mode – ‘fix’ with L=2 and S=200

- d) Adjust the window level and magnification to optimize the resolution. Score the number of resolvable groups of lines from the screen. Look up the corresponding resolution.
- e) Repeat the measurement twice with the resolution test object placed at a slight angle to the first the lateral or then the longitudinal axis.
- f) Repeat this process for all available image plate resolutions.
- g) If possible either archive or print the image for future reference.

Tolerance: For the 45° angled test object the resolved line pairs per mm should be $>1.2/2p$ where p is the pixel dimension in mm. In the scan and subscan directions the limiting resolution should be $>0.85/2p$. These measurements should be used to set a baseline for future QA tests.

N.B. A Huttner test object with line spacings up to 8 lp.mm^{-1} may be required.

10. Threshold Contrast Detail Detectability

Purpose: To monitor image quality by assessing the visibility of low contrast details.

- a) With the tube, plate, and copper in the same positions as for the sensitivity tests, place the TO20 (or equivalent) test object on the plate. Collimate down to the size of the test object.
- b) Set 75 kV_p and an mAs to deliver $\sim 4 \mu\text{Gy}$. Read the plate using the following parameters.

Fuji: Readout mode – ‘semi-auto’ with test/sensitivity GA=1

- c) Ascertain whether clinical images are most commonly viewed soft or hard copy. If they view hardcopy, adjust the window to optimize the visibility of the details, ensuring that background noise is perceptible, and print the image out on the largest film size. View the image on a masked light box, and score each detail size using

fixed distance viewing (<1m). If images are viewed softcopy, score them on a reporting workstation optimizing window and level settings for each detail size.

- d) Calculate an image quality factor, IQF,

$$IQF = \frac{1}{n} \sum_{i=1}^n \frac{H_T(A_i)}{H_T^{ref}(A_i)} \left[\frac{D_{ref}}{D} \right]^{0.5} \quad (9)$$

where;

$H_T(A)$ = threshold contrast detail index values calculated from the image,

$H_T^{ref}(A)$ = threshold contrast detail index values calculated from a reference image of a system known to be in good adjustment,

D = the dose to the image plate,

D_{ref} = the dose to the image plate for the reference image,

n = the number of details in the test object.

- e) Repeat this test for two other imaging plates and also for a single plate at exposures of ~1 μ Gy and ~12 μ Gy.
- f) If possible either archive or print the images for future reference.

Tolerance: The results of this test are used to set a baseline for future QA tests. Results could be compared to those from other similar systems if available

11. Laser beam function

Purpose: To assess laser beam scanline integrity and jitter.

- Place a steel ruler slightly angled to the subscan direction on a large cassette.
- Expose at ~80 kV_p, 150 cm FSD and an mAs to deliver an incident exposure of ~50 μ Gy.
- Using the software magnify the image x10. Select a narrow window width such that the image appears largely polarized to black or white. This should allow the edge to be easily differentiated from the background. Laser beam jitter can be evaluated by examining the edge of the ruler on the image.

Tolerance: The edge should be continuous across the full length of the image. Stair step characteristics should be uniform across the length of the image. Regions of over or undershoot of the scan lines indicate a timer or laser beam modulation problem.

12. Moiré Patterns

Purpose: To test for the presence of Moiré pattern artifacts caused by grids.

- Place a CR cassette in the bucky such that the scan lines are vertical to the gridlines. The cassette should be 1.5 m from the focus, and the collimation should cover the whole plate.
- Expose at 70 kV_p using the AEC with 1.5 mm of copper in the beam, and the grid in place.
- Read the plate as described for test 4 but with minimal delay, with the highest possible sampling rate.

- d) Visually inspect the image for Moiré line pattern artifacts.
- e) Repeat with the CR cassette positioned in the bucky such that the scan lines are horizontal to the grid lines.
- f) Repeat for all buckies and grids that may be used with the CR system, including any grids used in mobile radiography.

Tolerance: No Moiré patterns should be visible. If Moiré patterns are visible with a particular grid, it should not be used with the CR plates. The cause of Moiré patterns may be the failure of the motion of moving grids or insufficient grid density.

4.4. Measurement

Variables: Independent Variable = Quality control program for the x-ray machine and the CR system.

: Dependent Variable = Radiation dose, reject and retake rate and image quality before and after QC program.

4.4.1. Instruments and Evaluator

Patient radiation dose was assessed by the number of reject radiographs caused by the CR equipment calculated with the total examined samples and represented in term of reject and retake rate. The major advantage of reject and retake rate is to review the causes of the repeated images from the backup data on the workstation viewer monitor. Entrance skin dose (mGy) is obtained by the calculation [26] the entrance surface air kerma, backscatter factor of each x-ray machine at each voltage, mAs, focus-to-film distance (FFD) and focus-to-skin distance (FSD).

4.4.2. Outcome

Main outcome: The primary outcome is radiation dose, measured in the entrance skin dose (ESD), by calculation. The measurements were performed on each general radiograph, the calculation of average radiation dose of patient was based on reject and retake rate and used in the statistical analysis.

Secondary outcome: Quality of diagnostic information of CR images was determined in terms of the visualization score which should be evaluated on CR workstation monitor after image reconstruction in each scanning. Quality criteria had been used to score each radiograph which had been correlated to patient dose.

4.5. Data Collection

Data collection had been performed in two rooms dedicated to general radiography. Number and causes for retake were recorded as well as image quality graded for two periods of 1½ months before and after introduction of QC respectively.

The preliminary patient and other relevant data had been filled in the form by the radiological technologists (RTs); such as the examination type, H.N., age, sex, weight, height, body mass index (BMI), body part thickness, x-ray room number, exposure factors, S-value (sensitivity), L-value (latitude), the image quality satisfaction grading and causes of reject or retake images, etc. Every patient must sign in the consent form and receive the patient information before examination. These two forms were transferred and managed on a personal computer using Access for Windows 2000. Calculation of the BMI and the

entrance skin dose (ESD) were done in this process. 692 samples of the before QC group were completely collected at the beginning of July 2004. These processes had been repeated after the QC of CR system and the exposure chart finished.

The quality control of the computed radiography system including two x-ray machines in room number 4 and number 5 were performed and the results recorded after completing measurements before implementation of QC. The system performance was recorded in Excel data sheets and evaluated for compliance with the tolerance level results.

The exposure chart for 8 examinations were set in order to keep the optimal exposure dose for each patient by using the exposure index (S-sensitivity value) base line from the before QC sample group. As optimized dose setting exposure factors yielding a sensitivity close to 200 were targeted for standard IP (Fuji ST-V_N). (Finally, the exposure factors for each sample were set, based on each patient BMI and body part thickness; such as kVp, mA, time (second) and focus- film-distance (FFD)).

The image quality assessment was done by two senior radiologists after matching the data from both groups based on the equity or similarity between the body part thickness and the body mass index of the sample in the same examination. 4 types of examinations were chosen for evaluation: 35 pairs of chest PA, 20 pairs of abdomen AP, 15 pairs of lumbo-sacral spine AP and 15 pairs of lumbo-sacral spine lateral view. Image viewing order was randomized. Each image quality scoring represents an exposure over 2 radiologists' grading and correlated to dose and group (i.e. before or after implementation of QC) was averaged from the total scores from each radiologist and matched back to compare the radiation dose and the effectiveness of QC intervention.

4.6. Data Analysis

4.6.1. Summarization of Data

The data was analyzed by using the SPSS version 11.5 for Windows software package to test for statistical significance before and after introduction of the QC program. The analysis was performed first according to the actual modality that was used for each examination. This was of interest because, if the patient underwent imaging with the different modality; the quantity of the entrance surface air kerma (ESAK), the back scatter and the entrance skin dose (ESD in unit mGy per 1 mAs) would be different.

4.6.2. Data Presentation

The comparison of patient characteristics was shown in table 6. Reject and retake data for the groups before and after implementation of QC were analyzed as shown in table 7-8 as below, table 20-27, Appendix A and in figure 25-26, the comparison of exposure factors in table 9-11 and in figure 27, the comparison of entrance skin dose in table 12 and in figure 28, the comparison of image quality in table 13 and the relationship between the thickness (cm) to the entrance skin dose (mGy) and to the image quality data in the period of before and after QC is shown in table 14. Table 15-16 were shown the QC of x-ray machines and table 17 for the QC of CR system.

4.6.3. Hypothesis Testing

This study was to compare the percentage difference of independent variables. The primary outcome is the reject-retake proportion. Two independent-sample cases, one-tailed

test with significant level (α) .05 and power (1- β) 90% will be used to test the hypothesis [27];

$$H_0 : P_1 \geq P_2 (0.04) \text{ versus } H_a : P_1 < P_2 (0.04)$$

The final primary effectiveness end point was radiation dose. The primary effectiveness analysis was based on a protocol of QC program to intervene to the CR system. A secondary analysis had been performed using diagnostic quality of CR images.

Chi-square Test, T-Test and Mann-Whitney Test, SPSS 11.5 for windows was used for statistical analysis.

4.6.4. Problem from Protocol Deviation

From all patients informed consent, body dimensions and body weight had to be obtained. In some cases measuring patient dimensions may be compromised by considerable uncertainties, especially in chest PA of female patients.

Also, when deciding a retake, the criteria applied may differ slightly for individual RTs.

4.7. Ethical Consideration

This study was performed on the routine clinical examination that the intervention will not directly be operated to the patient during examination. However, the ethical approval by the Ethics Committee of Faculty of Medicine, Chulalongkorn University had been determined the patient information and inform consent had to be processed.

4.8. Limitations

The period is short took about 4 months (1½months for the control group data collection , 1 month for data analysis and another of 1½ months for the experimental group data collection) then, total population for each period is about 5,000 examinations (150 exams per day multiply to 33 working days).

4.9. Benefit of the Study

4.9.1. A QC program for the CR system is established. The data is used to compare to the result of further test.

4.9.2. Patient dose for various examination is obtained confirm the safety standards and to meet hospital accreditation (HA).

4.10. Administration and Time Schedule

Table 5. Time table for the study.

| Month – Year Procedure process | 2004 - 2005 | | | | | | | | | | |
|--|-------------|-----|------|------|--------|-----------|---------|----------|----------|---------|----------|
| | APRIL | MAY | JUNE | JULY | AUGUST | SEPTEMBER | OCTOBER | NOVEMBER | DECEMBER | JANUARY | FEBRUARY |
| • Preparation selected randomize case study method | ←→ | | | | | | | | | | |
| • Data collection for BEFORE QC program | | ←→ | | | | | | | | | |
| • X-ray units and CR system Calibration | | | | ←→ | | | | → | | | |
| • Data collection for AFTER QC program | | | | | | | | | ←→ | → | |
| • Data Analysis | | | | | | | | | | ←→ | |
| • Thesis Writing | | | | | | | | | ←→ | → | |
| • Presentation | | | | | | | | | | | * |

สถาบันวิทยบริการ
จุฬาลงกรณ์มหาวิทยาลัย

CHAPTER V

RESULTS

5.1. Analysis results

Three major studies were performed, the first was the patient data collection, the second was the study of control performance of the equipment to evaluate the computed radiography system, and the third was the assessment of image quality and radiation dose before and after QC implementation in term of the percentage reject and retake radiographs.

5.1.1. Patient Data

The 1,384 examinations were exactly met the criteria and included in the study. Two groups of study were well matched for number, age, sex, body weight and body height as shown in table 6 and table 20-27 in appendix A. Retaken after the quality control program had been done as shown in table 7-8 and figure 25-26.

Table 6. Comparison of the reject and retake rate data in the period of before and after QC program of 8 examinations.

| Part of examination | Before group | | After group | | Total | |
|-------------------------|--------------|-------|--------------|-------|--------------|--------------|
| | No. of exam. | % | No. of exam. | % | No. of exam. | Percentage % |
| All examinations | | | | | | |
| Age (y) | | | | | | |
| 16 – 30 y | 130 | 18.79 | 130 | 18.79 | 260 | 18.79 |
| 31 – 45 y | 204 | 29.48 | 204 | 29.48 | 408 | 29.48 |
| 46 – 60 y | 219 | 31.65 | 219 | 31.65 | 438 | 31.65 |
| 61 – 75 y | 139 | 20.09 | 139 | 20.09 | 278 | 20.09 |
| Gender | | | | | | |
| Male | 267 | 38.58 | 288 | 41.62 | 555 | 40.10 |
| Female | 425 | 61.42 | 404 | 58.38 | 829 | 59.90 |
| Weight (kg) | | | | | | |
| 35 – 54 kg | 260 | 37.57 | 242 | 34.97 | 502 | 36.27 |
| 55 – 74 kg | 363 | 52.46 | 372 | 53.76 | 735 | 53.111 |
| 75 – 94 kg | 62 | 8.96 | 75 | 10.84 | 137 | 9.90 |
| 95 – 114 kg | 7 | 1.01 | 3 | 0.43 | 10 | 0.72 |
| Height (cm) | | | | | | |
| 140-159 cm | 326 | 47.11 | 304 | 43.93 | 630 | 45.52 |
| 160-179 cm | 355 | 51.30 | 379 | 54.77 | 734 | 53.03 |
| ≥ 180 cm | 11 | 1.59 | 9 | 1.30 | 20 | 1.45 |

The difference of reject –retake rate before, 22 from 692 examinations and after, 10 from 692 examinations, is statistically significant (*Pearson Chi-square Test*, $P < 0.05$).

Table 7. Shown the percentage of the reject and retake by causes.

| Types of reject and retake examination | Before group | | After group | | Total | | <i>P value</i> |
|--|--------------|-------------|-------------|-------------|------------|-------------|----------------|
| | Retake No. | % | Retake No. | % | Retake No. | % | |
| Position | 8 | 1.16 | 6 | 0.87 | 14 | 1.01 | 0.591 |
| Motion | 2 | 0.29 | 0 | 0.00 | 2 | 0.14 | 0.157 |
| Technical error | 2 | 0.29 | 1 | 0.14 | 3 | 0.22 | 0.350 |
| Selected menu | 0 | 0.00 | 0 | 0.00 | 0 | 0.00 | 1.000 |
| High “S” value | 7 | 1.01 | 0 | 0.00 | 7 | 0.51 | 0.008 |
| Low “S” value | 0 | 0.00 | 0 | 0.00 | 0 | 0.00 | 1.000 |
| Artifacts | 3 | 0.43 | 3 | 0.43 | 6 | 0.43 | 1.000 |
| Total | 22 | 3.18 | 10 | 1.45 | 32 | 2.31 | 0.032 |

Pearson Chi-square Test (χ^2) for association

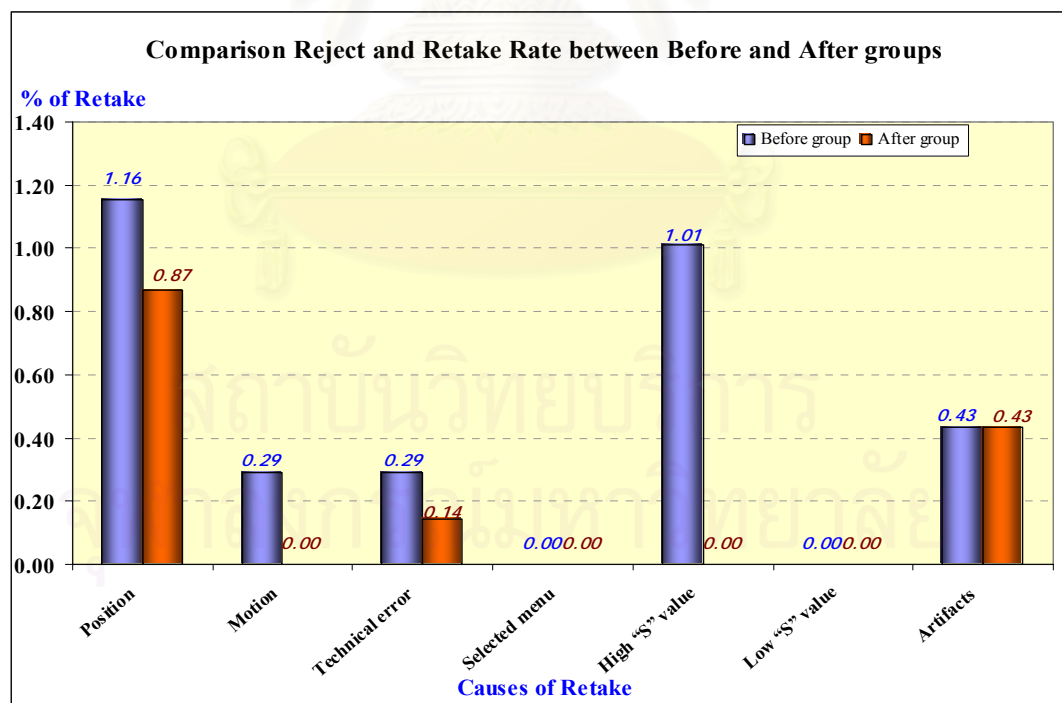
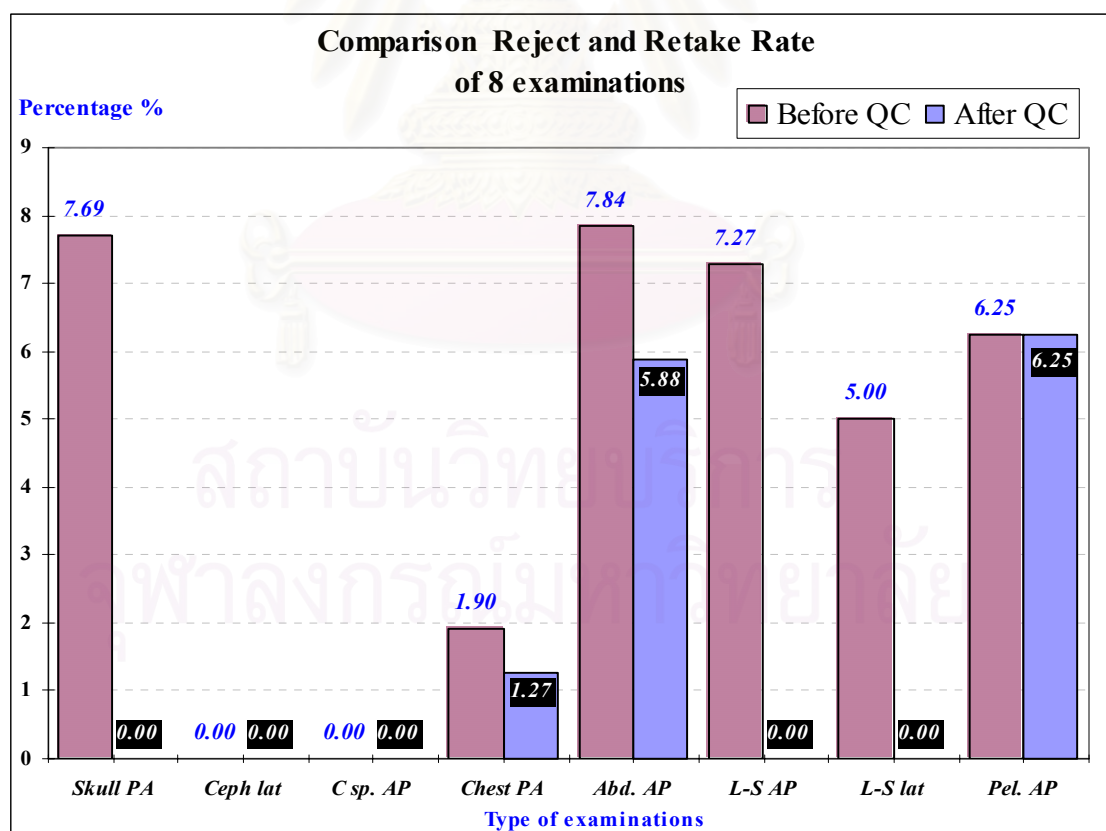


Figure 25. Bar graph was shown the reject and retake rate by causes.

Table 8. Shown the percentage of reject and retake by the types of examination.

| Types of exam. | Total exam. in each group | Before QC | | After QC | | Total | | |
|----------------|---------------------------|------------|------|------------|------|-------------|------------|-------------|
| | | Retake No. | % | Retake No. | % | Total exam. | Retake No. | Retake Rate |
| PNS PA | 13 | 1 | 7.69 | 0 | 0.00 | 26 | 1 | 3.85 |
| Ceph lat | 3 | 0 | 0.00 | 0 | 0.00 | 6 | 0 | 0.00 |
| C sp. AP | 21 | 0 | 0.00 | 0 | 0.00 | 42 | 0 | 0.00 |
| Chest PA | 473 | 9 | 1.90 | 6 | 1.27 | 946 | 15 | 1.59 |
| Abd. AP | 51 | 4 | 7.84 | 3 | 5.88 | 102 | 7 | 6.86 |
| L-S AP | 55 | 4 | 7.27 | 0 | 0.00 | 110 | 4 | 3.64 |
| L-S lat | 60 | 3 | 5.00 | 0 | 0.00 | 120 | 3 | 2.50 |
| Pel. AP | 16 | 1 | 6.25 | 1 | 6.25 | 32 | 2 | 6.25 |

**Figure 26.** Bar graph was shown the reject and retake rate by types of examination.

5.1.2. Exposure Conditions

The body part thickness (cm) and BMI of the patients that effected to the patient entrance skin doses had been compared as shown in table 9 – 10. The exposure factors (kV_p and mAs) used had been compared as shown in table 11.

Table 9. Comparison of affect exposure factors data in the period of before and after QC program by body part thickness.

| Types of exam. | Thickness | | | | P value* |
|---|-----------------|----------------|----------------|----------------|--------------|
| | Before QC group | | After QC group | | |
| | Mean | SD (min-max) | Mean | SD (min-max) | |
| PNS PA | 18.46 | 1.13 (17 – 20) | 17.00 | 1.29 (15 – 20) | 0.005 |
| Ceph. lat | 15.33 | 2.52 (13 – 18) | 14.00 | 1.73 (12 – 15) | 0.492 |
| C sp. AP | 11.52 | 2.20 (8 – 18) | 10.71 | 3.81 (8 – 26) | 0.404 |
| Chest PA | 20.61 | 2.99 (14 – 30) | 20.29 | 2.81 (14 – 29) | 0.093 |
| Abd. AP | 23.71 | 4.05 (16 – 37) | 22.27 | 3.66 (15 – 32) | 0.064 |
| L-S AP | 21.67 | 3.84 (14 – 31) | 20.62 | 3.19 (14 – 31) | 0.065 |
| L-S lat | 27.72 | 3.85 (20 – 36) | 26.78 | 3.15 (18 – 36) | 0.087 |
| Pel. AP | 22.06 | 4.14 (17 – 30) | 21.81 | 3.4 (16 – 29) | 0.862 |
| * T- Test, 2-tailed independent. | | | | | |

Table 10. Comparison of affect exposure factors data in the period of before and after QC program by body mass index (BMI).

| Types of exam. | BMI | | | | P value** |
|---|-----------------|----------------------|----------------|----------------------|--------------|
| | Before QC group | | After QC group | | |
| | Mean | SD (min-max) | Mean | SD (min-max) | |
| PNS PA | 23.23 | 3.98 (17.24 - 30.12) | 21.79 | 3.08 (17.60 - 27.34) | 0.313 |
| Ceph. lat | 24.53 | 5.59 (18.90 - 30.07) | 23.42 | 2.36 (20.77 - 25.32) | 0.767 |
| C sp. AP | 22.85 | 2.75 (28.52 - 28.52) | 22.74 | 2.71(18.73 - 28.98) | 0.902 |
| Chest PA | 22.9 | 4.07 (12.25 - 38.00) | 22.84 | 3.48 (16.22 - 38.22) | 0.822 |
| Abd. AP | 24.66 | 3.98 (18.75 - 42.22) | 24 | 3.43 (17.96 - 33.70) | 0.367 |
| L-S AP | 22.37 | 3.28 (15.56 - 30.92) | 23.11 | 3.34 (15.63 - 30.36) | 0.243 |
| L-S lat | 23.74 | 4.41 (15.43 - 35.65) | 23.51 | 3.66 (15.63 - 31.21) | 0.751 |
| Pel. AP | 20.37 | 3.03 (15.56 - 25.95) | 22.68 | 3.62 (15.94 - 31.25) | 0.060 |
| * T- Test, 2-tailed independent. | | | | | |

Table 11. Comparison of exposure factor data in the period of before and after QC program of 8 examinations.

| Types of exam. | Before QC group | | | | After QC group | | | |
|-------------------|-----------------|-----------------|--------|-------------------|-----------------|-----------------|--------|-------------------|
| | kV _p | | mAs | | kV _p | | mAs | |
| | Mean | SD (min-max) | Mean | SD (min-max) | Mean | SD (min-max) | Mean | SD (min-max) |
| PNS PA | 69.77 | 2.20 (65-75) | 42.38 | 4.54 (40-51) | 70.77 | 1.88 (70-75) | 34.62 | 5.50 (32-50) |
| Ceph. lat | 77.00 | 1.73 (75-78) | 21.67 | 5.77 (15-25) | 75.33 | 2.31 (74-78) | 8.00 | 2.00 (6-10) |
| C sp. AP | 69.00 | 5.06 (58-79) | 16.90 | 6.86 (8-40) | 67.67 | 4.14 (66-85) | 16.52 | 19.20 (7-100) |
| Chest PA | 73.65 | 3.51 (66-85) | 13.13 | 2.71 (6-20) | 71.22 | 2.71 (63-80) | 11.11 | 2.25 (5-16) |
| Abd. AP | 76.43 | 1.97 (75-82) | 59.49 | 12.20 (50-100) | 75.45 | 1.99 (70-80) | 55.82 | 10.50 (40-100) |
| L-S AP | 76.91 | 2.89 (70-82) | 61.73 | 15.21 (40-104) | 75.42 | 1.66 (70-80) | 53.00 | 12.25 (40-100) |
| L-S lat | 82.70 | 2.77 (77-89) | 112.40 | 19.12 (80-165) | 85.65 | 3.18 (80-93) | 104.38 | 19.01 (64-158) |
| Pel. AP | 74.81 | 4.79 (70-85) | 45.88 | 7.54 (32-64) | 72.47 | 2.90 (67-75) | 45.80 | 5.02 (40-52) |

The entrance surface air kerma (ESAK) and backscatter factor of each x-ray machine that effected to the patient entrance skin doses had been compared in term of room using as shown in figure 27.

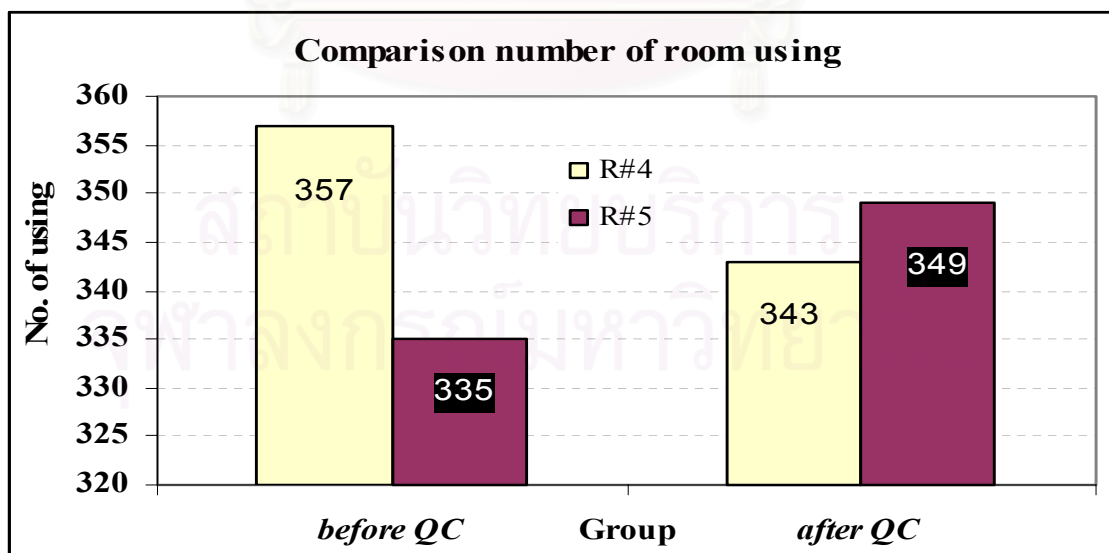


Figure 27. Bar graphs of the number of room using were compared between before and after QC group.

5.1.3. Patient doses and image quality

Most of the entrance skin dose (ESD) between two groups of the study were higher in the before QC group (compared median) as shown in table 12 and figure 28.

Table 12. Comparison of the entrance skin dose (mGy) data in the period of before and after QC program of 8 examinations.

| Types of exam. | ESD (IAEA) | ESD Before QC group | | | ESD After QC group | | | P *** |
|----------------|------------|---------------------|--------|-----------------------|--------------------|--------|----------------------|-------|
| | | Mean | Median | SD (min-max) | Mean | Median | SD (min-max) | |
| PNS PA | 5 | 1.90 | 2.00 | 0.21 (1.62 - 2.27) | 1.46 | 1.29 | 0.38 (1.23-2.44) | 0.001 |
| Ceph. lat | 0.25 | 0.29 | 0.34 | 0.10 (0.18 - 0.35) | 0.15 | 0.17 | 0.03 (0.11-0.17) | - |
| C sp. AP | 1.25 | 0.18 | 0.17 | 0.09 (0.08 - 0.53) | 0.12 | 0.11 | 0.03 (0.06-0.20) | 0.000 |
| Chest PA | 0.4 | 0.17 | 0.18 | 0.04 (0.06 - 0.37) | 0.14 | 0.12 | 0.09 (0.06-1.84) | 0.000 |
| Abd. AP | 10 | 4.39 | 4.02 | 1.42 (2.67 - 8.91) | 3.82 | 3.48 | 1.23 (2.02-8.81) | 0.010 |
| L-S AP | 10 | 4.37 | 3.9 | 1.66 (1.86-10.41) | 3.49 | 3.21 | 1.26 (2.08-7.91) | 0.001 |
| L-S lat | 30 | 11.09 | 10.39 | 3.59 (5.47-24.39) | 11.15 | 10.39 | 3.68 (5.02-22.64) | 0.485 |
| Pel. AP | 10 | 3.12 | 2.4 | 1.37 (1.86 - 6.44) | 2.90 | 3.06 | 0.84 (1.8 - 4.14) | 0.326 |

*** *Mann-Whitney Test (1-tailed)*

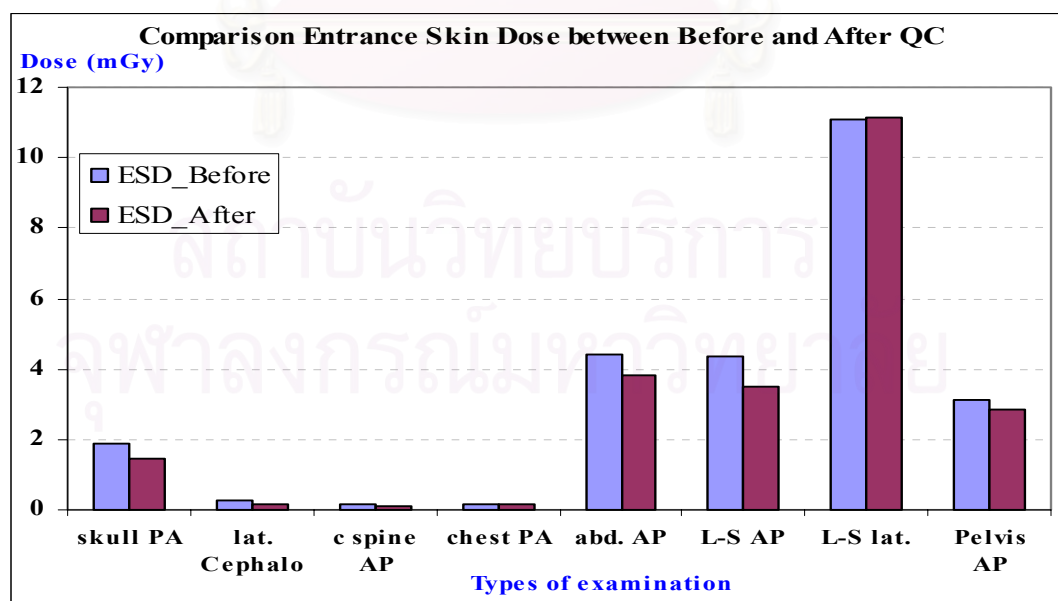


Figure 28. Bar graphs of the average entrance skin dose (mGy) were compared between before and after QC group.

Statistical significant of the 4 main examinations (chest PA, abdomen AP, lumbo-sacral spine AP and lateral view) were compared mean of image quality between two groups was shown in table 13.

Table 13. Comparison of the image quality data in the period of before and after QC program of 4 examinations.

| Types of exam. | Total scores | Before QC group | | | After QC group | | | <i>P-value</i> |
|-------------------------------------|--------------|-----------------|--------|------------------------|----------------|--------|------------------------|----------------|
| | | Mean | Median | SD (min-max) | Mean | Median | SD (min-max) | |
| Chest PA | 12 | 9.81 | 10.00 | 1.19 (7.25 - 11.75) | 9.74 | 10.00 | 1.21 (7.00 - 11.50) | 0.976 |
| Abd. AP | 14 | 11.84 | 12.25 | 1.46 (8.50 - 13.50) | 11.34 | 11.75 | 1.35 (9.00 - 13.75) | 0.197 |
| L-S AP | 8 | 5.75 | 6.125 | 1.64 (3.00 - 7.75) | 5.34 | 5.125 | 1.73 (3.00 - 7.50) | 0.710 |
| L-S lat. | 7 | 4.93 | 5.125 | 0.87 (3.50 - 6.25) | 5.00 | 5.25 | 0.97 (3.50 - 6.50) | 0.790 |
| Mann-Whitney Test (2-tailed) | | | | | | | | |

Matching the major parameters of the 4 main examinations that effect to the null and alternative hypotheses which chest PA, abdomen AP and lumbo-sacral spine AP are accepted null hypotheses except lumbo-sacral spine lateral is rejected null hypotheses is shown in table 14.

Table 14. Relationship between the body part thickness (cm) and BMI to the entrance skin dose (mGy) and the image quality of 4 main examinations in both groups were matched by using P value presentation.

| Type of examinations | <i>P value</i> | | | |
|----------------------|----------------|-------|-----------|---------------|
| | Thickness (cm) | BMI | ESD (mGy) | Image Quality |
| Chest PA | 0.093 | 0.822 | 0.000 | 0.976 |
| Abd. AP | 0.064 | 0.367 | 0.010 | 0.197 |
| L-S AP | 0.065 | 0.243 | 0.001 | 0.710 |
| L-S lat | 0.087 | 0.751 | 0.485 | 0.790 |

The Computed Radiography System Quality control

Both of the x-ray machine and the computed radiography performances were in the acceptable range except the specification of some accessories could not be change in this time. The QC results were shown in table 15-17 and the details were shown in table 28-29 and 34-36 in appendix B.

Table 15. Main report of x-ray machine performance room number 4

| | |
|----------------------|---|
| LOCATION: | BBR 4F King Chulalongkorn Memorial Hospital |
| DATE: | 9/10/2004 |
| ROOM NUMBER: | 4 |
| MANUFACTURE: | Hitachi, Japan; April 1989 |
| MODEL NUMBER | DR-155HM (Tube unit; U-6GE-55T) |
| SERIAL NUMBER | KC12808904 (beam limiting device KC 12003803) |

| | |
|------------|---|
| P | General mechanical conditions |
| P | All indication lamps and "Beam on indicator" |
| P | Dead man switch |
| F | Source image distance indicator (SID) |
| P | Mechanical motion test |
| P | Field size indication |
| P | Light VS Radiation congruence |
| P | Cross hair centering |
| N/A | Automatic collimation (PBL) |
| N/A | Photo timer reproducibility and density compensation |
| P | Exposure reproducibility |
| P | Linearity of exposure with mR/mAs |
| P | Timer accuracy |
| P | Beam quality (HVL) |
| P | kV_p accuracy |
| P | Entrance skin exposure (ESE) |

P PASS

F FAIL

N/A NOT APPLICABLE

N/P NOT PERFORMED

NOTE RECOMMENDATION SUGGESTED

Table 16. Main report of x-ray machine performance room number 5

| | |
|----------------------|---|
| LOCATION: | BBR 4F King Chulalongkorn Memorial Hospital |
| DATE: | 15/10/2004 |
| ROOM NUMBER: | 5 |
| MANUFACTURE: | Hitachi, Japan; April 1989 |
| MODEL NUMBER | DR-155HM April 1989 (Tube unit; U-6GE-55T) |
| SERIAL NUMBER | KC 17714403 JUNE 1994 (from Beam limiting device) |

| | |
|------------|---|
| P | General mechanical conditions |
| P | All indication lamps and "Beam on indicator" |
| P | Dead man switch |
| N/A | Source image distance indicator (SID) |
| P | Mechanical motion test |
| P | Field size indication |
| P | Light VS Radiation congruence |
| P | Cross hair centering |
| N/A | Automatic collimation (PBL) |
| N/A | Photo timer reproducibility and density compensation |
| P | Exposure reproducibility |
| P | Linearity of exposure with mR/mAs |
| P | Timer accuracy |
| P | Beam quality (HVL) |
| P | kV_p accuracy |
| P | Entrance skin exposure (ESE) |

P **PASS**
F **FAIL**
N/A **NOT APPLICABLE**
N/P **NOT PERFORMED**
NOTE **RECOMMENDATION SUGGESTED**

Table 17. Main report of CR system performance

| CR system Calibration Test | Tolerance -The Established Criteria | Result |
|---|---|----------|
| 1. Monitor & laser printer set-up | The 5% on 0% and 95% on 100% details was clearly visible. The horizontal and vertical resolutions differ by lesser than 20%. | P |
| 2. Dark Noise | Many artifacts were found on the images of 4 years IP used but were not on the new ones. | P |
| 3. Erasure cycle efficiency | Absence of a ghost image of the lead block from the first exposure in the re-exposed image. | P |
| 4. Sensitivity Index calibration | The indicated exposure should agree with the measured exposure within 20%. | P |
| 5. Sensitivity Index consistency | The variation in the calculated indicated exposures should not differ by greater than 20% between plates. | P |
| 6. Uniformity | The images do not have obvious artifacts. The maximum variations in pixel values were within a range of 10% of each other. | P |
| 7. Scaling errors | The measured distances x and y should agree within 3% of the actual distances. All calculated aspect ratios were within 1.00 ± 0.03 . | P |
| 8. Blurring | No blurring was present. | P |
| 9. Limiting Spatial Resolution | For the 45° angled test object the resolved line pairs per mm should be $>1.2/2p$ where p is the pixel dimension in mm. In the scan and subscan directions the limiting resolution should be $>0.85/2p$. | P |
| 10. Threshold Contrast Detail Detectability (TCDD) | The results of this test are used to set a baseline for future QA tests. Results could be compared to those from other similar systems if available. | P |
| 11. Laser beam function | Ruler edges were straight and continuous without any under- or overshoot of the scan lines in light to dark transitions. | P |
| 12. Moiré Patterns | Moiré patterns had been visible with the routine stationary grid using. | F |
| Result: P = Pass, F = Fail, N/A = Not Applicable , N/P = Not Performed | | |

5.2. Result Comparison

There was a statistically significant decrease in the entrance skin dose (Mann-Whitney, $P < 0.05$) when the exposure chart was followed in the routine work.

There was a significant difference between two groups ($P < 0.05$) in the number of repeat exposures. The majority—more than 95% -- of examinations for both groups did not need to be repeated, but there were fewer repeat studies in the after QC group (10 of 692 examinations) than in the before QC group (22 of 692 examinations).

Median ESD of the group data collected after implementation of QC were significant lower than the Dose Reference Level (DRL) by IAEA and NPRB (in table 38 in appendix C). Median ESDs of the group after implementation of QC are statistically significant lower than for the data before QC except L-S spine lateral and pelvis AP view (not significant) and cephalometry lateral view (data not consistent due to use of different technique).

ESD of room number 4 (35.9 $\mu\text{Gy/mAs}$) is lower than room number 5 (41.2 $\mu\text{Gy/mAs}$) at 80 kV_p, large focus, at 100 cm FSD for the same exposure factors and the same condition (in table 31-32 in appendix B).

There was no significant difference between two groups ($P > 0.05$) in the image quality by the meaning of the effort to reduce the ESD.

5.3. Analysis result factor

Performance of both x-ray machines was in acceptable range. Both generators do not provide AEC, so exposure factors were set manually.



CHAPTER VI

CONCLUSION, DISCUSSION AND RECOMMENDATION

6.1. Conclusion

The patients in the two groups of the study were well matched. Fewer examinations were retaken when the quality control of the computed radiography system was initiated and the reject and retake rate was reduced from 3.18% to 1.45% (differentiate reduction 54.55%, $P < 0.05$). The entrance skin doses is reduced to 17.69 % in chest PA view (mean, 0.17 mGy for before QC group and 0.14 mGy for after QC group) and 16.22 % for lumbo-sacral spine AP (mean, 4.37 mGy for before QC group and 3.49 mGy for after QC group) while maintaining optimum image quality. The exposure chart is implemented and applied for every examination in case of manual setting of the x-ray system. The performance of the x-ray system shows lower ESD from the system of room number 4 than the system of room number 5 for the same exposure factors and the same condition. The quality control program is used to inspect the system performance to keep it in optimal condition.

6.2. Discussion

The quality control program is effective to assess the quality of the machine and predict the image quality. In order to practice the QC procedures, the phantom, the testing device, and operators are most important.

Both of the x-ray machine performances were the manual exposure factor setting that still in the acceptable range. Room number 4 x-ray machine had given the lower the entrance surface air kerma (ESAK) which correlated to the ESD than room number 5.

The computed radiography system performance was also quite good condition. The only one item that must be improve is the Moire' pattern testing because the recommended grid ratio for bucky grid or the stationary grid should be 12:1 with lead strips at least 103 lines per inches.

6.3. Recommendation

In order to establish the first computed radiography system, the test device must be provided for the quality control program. X-ray machines with automatic exposure control (AEC) are strongly recommended to optimize radiation dose to the patient. For the manual setting x-ray machine, the detailed exposure factor chart must be strictly used in order to keep the ALARA (As Low As Reasonably Achievable) rule. Continuous training is scheduled for the quality improvement for the new technology in order to improve and increase the competence of RTs working with the digital modalities.

REFERENCES

1. Willis, C.E. 10 Fallacies about CR. Journal of Imaging Technology Management (December 2002): 1-6.
2. Reiner, B., and Siegel, E. Putting the quality back into QA without the headaches. insights & images (2003):5-8.
3. Committee 3 of the International Commission on Radiological Protection. Diagnostic reference levels in medical imaging web base.doc-Microsoft Word): ICRP, 2001.
4. Montagne, J.Ph., and Ducou Le Pointe, H. Digital Radiology. Service d'Imagerie Médicale Hôpital d'Enfants Armand-Trousseau. (2000).
5. Rowlands, J.A. The physics of computed radiography. Physics Medical Biology 47 (2002):123-166.
6. Seibert, J.A. Computed radiography technology 2004. MMP AAPM (2004):153-175.
7. Seibert, J.A., et al. Acceptance Testing and Quality Control of Photo Stimulable Phosphor Imaging Systems Report of Task Group 10 American Association of Physicists in Medicine. AAPM Task Group 10 version 3.1 (October 1997): 1-56.
8. von Seggern, H., Voigt, T., Knupfer, W. and Lange, G. Physical model of photostimulated luminescence of x-ray irradiated BaFBr:Eu²⁺. Journal of Application Physics 64 (1988)1405–12.
9. Takahashi, K., Kohda, K., Miyahara, J., Kanemitsu, Y., Amitani, K. and Shionoya, S. Mechanism of photostimulated luminescence in BaFX:Eu²⁺ (X = Cl, Br) Phosphors. Journal of Luminescence 31–32 (1984) 266–8.
10. Floyd, C.E. Jr., Baker, J.A., Lo, J.Y. and Ravin, C.E. Measurement of scatter fractions in clinical bedside radiology. Radiology 183 (1992):857–61.
11. Oda, N., Nakata, H., Murakami, S., Terada, K., Nakamura, K. and Yoshida, A. Optimal beam quality for chest computed radiography. Invest. Radiology 31 (1996)126–31.
12. Lo, J.Y., Floyd, C. E. Jr., Baker, J.A. and Ravin, C.E. Scatter compensation in digital chest radiography using the posterior beam stop technique. Medical Physics 21 (1994) 435–43.
13. Clark, R.H., et al. Annual of the ICRP publication 60. 2nd ed. Oxford:Pergamon Press, 1991.
14. ICRP Publication 73 Radiological Protection and Safety in Medicine. 26 Oxford: Pergamon Press 1996.
15. International Basic Safety Standards for Protection against Ionizing Radiation and for the Safety of Radiation Sources, IAEA Safety Series No 115. Oxford: Pergamon Press 1995.

REFERENCES (continued)

16. Williams, J.R., and Catling, M.K. Short communication, An Investigation of x-ray equipment factors influencing patient dose in radiography. British Journal of Radiology 71 (1998):1192-1198.
17. Polunin, N., Lim, T.A., and Tan, K.P. Reduction in retake rate and radiation dosage through computed radiography. Annual Academy of Medicine 27; 6 (November 1998): 805-7.
18. Artz, D.S. Computed radiography for radiological technologists. Semin Roentgenol 32 (1997):12-24.
19. Weatherburn, G.C., Bryan, S, and West, M. A comparison of image reject rates when using film, hard copy computed radiography and soft copy imaged on picture archiving and communication systems (PACS) workstations. British Journal of Radiology 72 (1999): 653-660.
20. Murphet, MD, Quale, J.L., Martin, N.L., Bramble, J.M., Cook, L.T., and Dwyer, S.J. Computed radiography in musculoskeletal imaging. American Journal of Roentgenol 158 (1992): 19-27.
21. Bowman, J.E. The future is now: digital radiography. Bytes Imaging's Future 30 (1998):12-15.
22. Weatherburn, G.C., Bryan, S., and Davies, J.G. Comparison of doses for bedside examinations of the chest with conventional screen-film and computed radiography: results of a randomized controlled trial. Radiology 217 (2000): 707-712.
23. Cesar, L.J., Schueler, B.A., Zink, F.E., Daly, T.R., Taubel, J.P., and Jorgenson, L.L. Artifacts found in computed radiography. British Journal of Radiology 74 (2001): 195-202.
24. Pasad, G. Report of Radiographic System Performance. ENH, (2000).
25. Kings College Hospital. KCARE CR QA Protocol Draft 4.0. Protocol for the QA of Computed Radiography System Commissioning and Annual QA Tests, 2003.
26. Petoussi-Hens, N., Zankl, M., Drexler, G., Panzer, W., and Regulla, D. Calculation of backscatter factors for diagnostic radiology using Monte Carlo methods. Physics Medical Biology 43 (1998): 2237-2250.
27. Bernard, R. Fundamentals of Biostatistics. 4th ed. ISBN 0-534-20940-8. USA:Wadsworth Publishing Company, 1995.



APPENDICES

สถาบันวิทยบริการ
จุฬาลงกรณ์มหาวิทยาลัย

APPENDIX A

Patient Characteristic

Table 18. Patient characteristic details collected by technologists for each examination.

| Variable | Description | Method* |
|--|--|---|
| Data group | Before or after QC group | Obtained from collected data period |
| Patient identification | Hospital number, patient name, age, sex and date of examination | Notes from patient identification and measure. |
| Exposure conditions: | | |
| Examination type | 1.skull PA from paranasal sinuses series 2.lateral cephalometry 3.cervical spine AP 4.chest PA 5.abdomen AP 6.lumbo-sacral spine AP 7.lumbo-sacral spine lateral 8. pelvis AP | Examination and position during exposure |
| Wt, Ht | body weight and height | Measured by technologist |
| BMI | Body mass index for each patient | Calculate by formula; $BMI = \frac{Weight(kg)}{Height(m)^2}$ |
| Thickness | body part of examination thickness (cm) in the central field | Measured by technologist |
| kVp | Kilovoltage across x-ray tube | Noted from control panel |
| mAs | Milliamperere second product | Noted from control panel |
| FFD | | Measured by technologist |
| Room ID | No. 4 or No. 5 | X-ray machine (Hitachi DR-155HM) was used during exposure |
| S-value | Sensitivity value of each image | Noted from CR reader panel |
| L-value | Latitude value of each image | Noted from CR reader panel |
| ESD (mGy) | Entrance Skin Dose in milli-Gray unit | Calculate by formula; $ESD = mAs \times ESD(\mu Gy/mAs)$ ESD(uGy/mAs) was shown in Table 37-38 in Appendix C. |
| Image Quality | Image quality grading for chest PA, abdomen AP L-S spine AP and lateral view | Grading by senior radiologists in European guideline forms |
| Repeat image required | Yes or No | Mark by qualified image technologist |
| Causes of reject or retake image | 1. position 2. motion 3. technical error 4. selected menu 5. high "S" value 6. low "S" value 7. artifacts | Mark by qualified image technologist |
| Note. Some data are missing in subsequence tables of the results for one of the three reasons: The technologist forgot to record them, they were unavailable, or the data could not be matched with patient. | | |

Table 19. CASE RECORD FORM

| | | | | | |
|------------------|---------------------------|-----------------|-------------------------------------|---------------------|---------------------|
| Study ID | Exam | HN | Exam Date | Before/After | |
| 1590 | Chest PA | 99928/47 | 28/1/48 | After QC | |
| Age | Gender | Wt(kg) | Ht(cm) | BMI | Thickness cm |
| 40 | Male | 61 | 167 | 21.87 | 23.00 |
| KVp | mAs | FFD | Img Quality Y/N | | |
| 73 | 13 | 180 | <input checked="" type="checkbox"/> | | |
| Room ID | Retake Information | RTs Name | | | |
| | | Indra | | | |
| Sv value: | Lv value: | ESTm Gy: | COMPLETE DATA | | |
| 325 | 1.45 | 0.1913 | <input checked="" type="checkbox"/> | | |

| | | | | | |
|------------------|---------------------------|-----------------|-------------------------------------|---------------------|---------------------|
| Study ID | Exam | HN | Exam Date | Before/After | |
| 1543 | Chest PA | 94267/47 | 28/1/48 | After QC | |
| Age | Gender | Wt(kg) | Ht(cm) | BMI | Thickness cm |
| 54 | Female | 45 | 154 | 18.98 | 18.00 |
| KVp | mAs | FFD | Img Quality Y/N | | |
| 70 | 10 | 180 | <input checked="" type="checkbox"/> | | |
| Room ID | Retake Information | RTs Name | | | |
| | | Clara | | | |
| Sv value: | Lv value: | ESTm Gy: | COMPLETE DATA | | |
| 277 | 1.40 | 0.0944 | <input checked="" type="checkbox"/> | | |

Table 20. Comparison of the Reject and Retake rate data in the period of Before and After QC program intervention for **Skull PA view (from paranasal sinuses series)**.

| Part of examination | Before group | | After group | |
|--|--------------|------------|--------------|------------|
| | No. of exam. | Percentage | No. of exam. | Percentage |
| 1. Skull PA (PNS) | | | | |
| Age (y) | | | | |
| 16 – 30 y | 2 | 14.29 | 2 | 11.11 |
| 31 – 45 y | 5 | 35.71 | 9 | 50.00 |
| 46 – 60 y | 6 | 42.86 | 6 | 33.33 |
| 61 – 75 y | 1 | 7.14 | 1 | 5.56 |
| Gender | | | | |
| Male | 5 | 38.46 | 2 | 15.38 |
| Female | 8 | 61.54 | 11 | 84.62 |
| Weight (kg) | | | | |
| 35 – 54 kg | 6 | 46.15 | 7 | 53.85 |
| 55 – 74 kg | 5 | 38.46 | 6 | 46.15 |
| 75 – 94 kg | 2 | 15.38 | 0 | 0.00 |
| 95 – 114 kg | 0 | 0.00 | 0 | 0.00 |
| Height (cm) | | | | |
| 140-159 cm | 8 | 61.54 | 9 | 69.23 |
| 160-179 cm | 5 | 38.46 | 4 | 30.77 |
| ≥ 180 cm | 0 | 0.00 | 0 | 0.00 |
| Types of reject and retake examination | | | | |
| Position | 1 | 100.00 | 0 | 0.00 |
| Motion | 0 | 0.00 | 0 | 0.00 |
| Technical error | 0 | 0.00 | 0 | 0.00 |
| Selected menu | 0 | 0.00 | 0 | 0.00 |
| High “S” value | 0 | 0.00 | 0 | 0.00 |
| Low “S” value | 0 | 0.00 | 0 | 0.00 |
| Artifacts | 0 | 0.00 | 0 | 0.00 |
| Others | 0 | 0.00 | 0 | 0.00 |
| <i>Chi-square Test (χ^2) for association</i> | | | | |

Table 21. Comparison of the Reject and Retake rate data in the period of Before and After QC program intervention for **Lateral Cephalometry view.**

| Part of examination | Before group | | After group | |
|--|--------------|------------|--------------|------------|
| | No. of exam. | Percentage | No. of exam. | Percentage |
| 2. Lateral Cephalometry | | | | |
| Age (y) | | | | |
| 16 – 30 y | 0 | 0.00 | 0 | 0.00 |
| 31 – 45 y | 2 | 66.67 | 2 | 66.67 |
| 46 – 60 y | 0 | 0.00 | 0 | 0.00 |
| 61 – 75 y | 1 | 33.33 | 1 | 33.33 |
| Gender | | | | |
| Male | 3 | 100.00 | 2 | 66.67 |
| Female | 0 | 0.00 | 1 | 33.33 |
| Weight (kg) | | | | |
| 35 – 54 kg | 1 | 33.33 | 0 | 0.00 |
| 55 – 74 kg | 1 | 33.33 | 3 | 100.00 |
| 75 – 94 kg | 1 | 33.33 | 0 | 0.00 |
| 95 – 114 kg | 0 | 0.00 | 0 | 0.00 |
| Height (cm) | | | | |
| 140-159 cm | 0 | 0.00 | 1 | 33.33 |
| 160-179 cm | 3 | 100.00 | 1 | 33.33 |
| ≥ 180 cm | 0 | 0.00 | 1 | 33.33 |
| Types of reject and retake examination | | | | |
| Position | 0 | 0.00 | 0 | 0.00 |
| Motion | 0 | 0.00 | 0 | 0.00 |
| Technical error | 0 | 0.00 | 0 | 0.00 |
| Selected menu | 0 | 0.00 | 0 | 0.00 |
| High “S” value | 0 | 0.00 | 0 | 0.00 |
| Low “S” value | 0 | 0.00 | 0 | 0.00 |
| Artifacts | 0 | 0.00 | 0 | 0.00 |
| Others | 0 | 0.00 | 0 | 0.00 |
| <i>Chi-square Test (χ^2) for association</i> | | | | |

Table 22. Comparison of the Reject and Retake rate data in the period of Before and After QC program intervention for **C-spine AP view**.

| Part of examination | Before group | | After group | |
|--|--------------|------------|--------------|------------|
| | No. of exam. | Percentage | No. of exam. | Percentage |
| 3. C-spine AP view | | | | |
| Age (y) | | | | |
| 16 – 30 y | 2 | 9.52 | 2 | 9.52 |
| 31 – 45 y | 3 | 14.29 | 3 | 14.29 |
| 46 – 60 y | 9 | 42.86 | 9 | 42.86 |
| 61 – 75 y | 7 | 33.33 | 7 | 33.33 |
| Gender | | | | |
| Male | 5 | 23.81 | 6 | 28.57 |
| Female | 16 | 76.19 | 15 | 71.43 |
| Weight (kg) | | | | |
| 35 – 54 kg | 8 | 38.10 | 11 | 52.38 |
| 55 – 74 kg | 13 | 61.90 | 8 | 38.10 |
| 75 – 94 kg | 0 | 0.00 | 2 | 9.52 |
| 95 – 114 kg | 0 | 0.00 | 0 | 0.00 |
| Height (cm) | | | | |
| 140-159 cm | 10 | 47.62 | 14 | 66.67 |
| 160-179 cm | 11 | 52.38 | 7 | 33.33 |
| ≥ 180 cm | 0 | 0.00 | 0 | 0.00 |
| Types of reject and retake examination | | | | |
| Position | 0 | 0.00 | 0 | 0.00 |
| Motion | 0 | 0.00 | 0 | 0.00 |
| Technical error | 0 | 0.00 | 0 | 0.00 |
| Selected menu | 0 | 0.00 | 0 | 0.00 |
| High “S” value | 0 | 0.00 | 0 | 0.00 |
| Low “S” value | 0 | 0.00 | 0 | 0.00 |
| Artifacts | 0 | 0.00 | 0 | 0.00 |
| Others | 0 | 0.00 | 0 | 0.00 |
| <i>Chi-square Test (χ^2) for association</i> | | | | |

Table 23. Comparison of the Reject and Retake rate data in the period of Before and After QC program intervention for **Chest PA view**.

| Part of examination | Before group | | After group | |
|--|--------------|------------|--------------|------------|
| | No. of exam. | Percentage | No. of exam. | Percentage |
| 4. Chest PA | | | | |
| Age (y) | | | | |
| 16 – 30 y | 111 | 23.47 | 111 | 23.47 |
| 31 – 45 y | 145 | 30.66 | 145 | 30.66 |
| 46 – 60 y | 135 | 28.54 | 135 | 28.54 |
| 61 – 75 y | 82 | 17.34 | 82 | 17.34 |
| Gender | | | | |
| Male | 193 | 40.80 | 202 | 42.71 |
| Female | 280 | 59.20 | 271 | 57.29 |
| Weight (kg) | | | | |
| 35 – 54 kg | 187 | 39.53 | 170 | 35.94 |
| 55 – 74 kg | 241 | 50.95 | 250 | 52.85 |
| 75 – 94 kg | 41 | 8.67 | 50 | 10.57 |
| 95 – 114 kg | 4 | 0.85 | 3 | 0.63 |
| Height (cm) | | | | |
| 140-159 cm | 214 | 45.24 | 203 | 42.92 |
| 160-179 cm | 252 | 53.28 | 264 | 55.81 |
| ≥ 180 cm | 7 | 1.48 | 6 | 1.27 |
| Types of reject and retake examination | | | | |
| Position | 1 | 11.11 | 2 | 33.33 |
| Motion | 1 | 11.11 | 0 | 0.00 |
| Technical error | 2 | 22.22 | 1 | 16.67 |
| Selected menu | 0 | 0.00 | 0 | 0.00 |
| High “S” value | 4 | 44.44 | 0 | 0.00 |
| Low “S” value | 0 | 0.00 | 0 | 0.00 |
| Artifacts | 1 | 11.11 | 3 | 50.00 |
| Others | 0 | 0.00 | 0 | 0.00 |
| <i>Chi-square Test (χ^2) for association</i> | | | | |

Table 24. Comparison of the Reject and Retake rate data in the period of Before and After QC program intervention for **Abdomen AP view**.

| Part of examination | Before group | | After group | |
|--|--------------|------------|--------------|------------|
| | No. of exam. | Percentage | No. of exam. | Percentage |
| 5. Abdomen AP | | | | |
| Age (y) | | | | |
| 16 – 30 y | 4 | 7.84 | 4 | 7.84 |
| 31 – 45 y | 18 | 35.29 | 18 | 35.29 |
| 46 – 60 y | 14 | 27.45 | 14 | 27.45 |
| 61 – 75 y | 15 | 29.41 | 15 | 29.41 |
| Gender | | | | |
| Male | 16 | 31.37 | 27 | 52.94 |
| Female | 35 | 68.63 | 24 | 47.06 |
| Weight (kg) | | | | |
| 35 – 54 kg | 12 | 23.53 | 10 | 19.61 |
| 55 – 74 kg | 32 | 62.75 | 33 | 64.71 |
| 75 – 94 kg | 6 | 11.76 | 8 | 15.69 |
| 95 – 114 kg | 1 | 1.96 | 0 | 0.00 |
| Height (cm) | | | | |
| 140-159 cm | 29 | 54.72 | 16 | 31.37 |
| 160-179 cm | 24 | 45.28 | 35 | 68.63 |
| ≥ 180 cm | 0 | 0.00 | 0 | 0.00 |
| Types of reject and retake examination | | | | |
| Position | 3 | 75.00 | 3 | 100.00 |
| Motion | 1 | 25.00 | 0 | 0.00 |
| Technical error | 0 | 0.00 | 0 | 0.00 |
| Selected menu | 0 | 0.00 | 0 | 0.00 |
| High “S” value | 0 | 0.00 | 0 | 0.00 |
| Low “S” value | 0 | 0.00 | 0 | 0.00 |
| Artifacts | 0 | 0.00 | 0 | 0.00 |
| Others | 0 | 0.00 | 0 | 0.00 |
| <i>Chi-square Test (χ^2) for association</i> | | | | |

Table 25. Comparison of the Reject and Retake rate data in the period of Before and After QC program intervention for **L-S spine AP view**.

| Part of examination | Before group | | After group | |
|--|--------------|------------|--------------|------------|
| | No. of exam. | Percentage | No. of exam. | Percentage |
| 6. L-S spine AP | | | | |
| Age (y) | | | | |
| 16 – 30 y | 5 | 9.09 | 5 | 9.09 |
| 31 – 45 y | 16 | 29.09 | 16 | 29.09 |
| 46 – 60 y | 20 | 36.36 | 20 | 36.36 |
| 61 – 75 y | 14 | 25.45 | 14 | 25.45 |
| Gender | | | | |
| Male | 17 | 30.91 | 19 | 34.55 |
| Female | 38 | 69.09 | 36 | 65.45 |
| Weight (kg) | | | | |
| 35 – 54 kg | 20 | 36.36 | 20 | 36.36 |
| 55 – 74 kg | 30 | 54.55 | 29 | 52.73 |
| 75 – 94 kg | 5 | 9.09 | 6 | 10.91 |
| 95 – 114 kg | 0 | 0.00 | 0 | 0.00 |
| Height (cm) | | | | |
| 140-159 cm | 27 | 49.09 | 27 | 49.09 |
| 160-179 cm | 26 | 47.27 | 27 | 49.09 |
| ≥ 180 cm | 2 | 3.64 | 1 | 1.82 |
| Types of reject and retake examination | | | | |
| Position | 2 | 50.00 | 0 | 0.00 |
| Motion | 0 | 0.00 | 0 | 0.00 |
| Technical error | 0 | 0.00 | 0 | 0.00 |
| Selected menu | 0 | 0.00 | 0 | 0.00 |
| High “S” value | 1 | 25.00 | 0 | 0.00 |
| Low “S” value | 0 | 0.00 | 0 | 0.00 |
| Artifacts | 1 | 25.00 | 0 | 0.00 |
| Others | 0 | 0.00 | 0 | 0.00 |
| <i>Chi-square Test (χ^2) for association</i> | | | | |

Table 26. Comparison of the Reject and Retake rate data in the period of Before and After QC program intervention for **L-S spine Lateral view**.

| Part of examination | Before group | | After group | |
|--|--------------|------------|--------------|------------|
| | No. of exam. | Percentage | No. of exam. | Percentage |
| 7. L-S spine Lat | | | | |
| Age (y) | | | | |
| 16 – 30 y | 4 | 6.67 | 4 | 6.67 |
| 31 – 45 y | 14 | 23.33 | 14 | 23.33 |
| 46 – 60 y | 29 | 48.33 | 29 | 48.33 |
| 61 – 75 y | 13 | 21.67 | 13 | 21.67 |
| Gender | | | | |
| Male | 18 | 30.00 | 21 | 35.00 |
| Female | 42 | 70.00 | 39 | 65.00 |
| Weight (kg) | | | | |
| 35 – 54 kg | 18 | 30.00 | 20 | 33.33 |
| 55 – 74 kg | 34 | 56.67 | 33 | 55.00 |
| 75 – 94 kg | 6 | 10.00 | 7 | 11.67 |
| 95 – 114 kg | 2 | 3.33 | 0 | 0.00 |
| Height (cm) | | | | |
| 140-159 cm | 33 | 55.00 | 30 | 50.00 |
| 160-179 cm | 26 | 43.33 | 29 | 48.33 |
| ≥ 180 cm | 1 | 1.67 | 1 | 1.67 |
| Types of reject and retake examination | | | | |
| Position | 1 | 33.33 | 0 | 0.00 |
| Motion | 0 | 0.00 | 0 | 0.00 |
| Technical error | 0 | 0.00 | 0 | 0.00 |
| Selected menu | 0 | 0.00 | 0 | 0.00 |
| High “S” value | 1 | 33.33 | 0 | 0.00 |
| Low “S” value | 0 | 0.00 | 0 | 0.00 |
| Artifacts | 1 | 33.33 | 0 | 0.00 |
| Others | 0 | 0.00 | 0 | 0.00 |
| <i>Chi-square Test (χ^2) for association</i> | | | | |

Table 27. Comparison of the Reject and Retake rate data in the period of Before and After QC program intervention for **Pelvis AP view**.

| Part of examination | Before group | | After group | |
|--|--------------|------------|--------------|------------|
| | No. of exam. | Percentage | No. of exam. | Percentage |
| 8. Pelvis AP | | | | |
| Age (y) | | | | |
| 16 – 30 y | 2 | 12.50 | 2 | 12.50 |
| 31 – 45 y | 2 | 12.50 | 2 | 12.50 |
| 46 – 60 y | 6 | 37.50 | 6 | 37.50 |
| 61 – 75 y | 6 | 37.50 | 6 | 37.50 |
| Gender | | | | |
| Male | 11 | 68.75 | 9 | 56.25 |
| Female | 5 | 31.25 | 7 | 43.75 |
| Weight (kg) | | | | |
| 35 – 54 kg | 8 | 50.00 | 4 | 25.00 |
| 55 – 74 kg | 7 | 43.75 | 10 | 62.50 |
| 75 – 94 kg | 1 | 6.25 | 2 | 12.50 |
| 95 – 114 kg | 0 | 0.00 | 0 | 0.00 |
| Height (cm) | | | | |
| 140-159 cm | 5 | 31.25 | 4 | 25.00 |
| 160-179 cm | 10 | 62.50 | 12 | 75.00 |
| ≥ 180 cm | 1 | 6.25 | 0 | 0.00 |
| Types of reject and retake examination | | | | |
| Position | 0 | 0.00 | 1 | 100.00 |
| Motion | 0 | 0.00 | 0 | 0.00 |
| Technical error | 0 | 0.00 | 0 | 0.00 |
| Selected menu | 0 | 0.00 | 0 | 0.00 |
| High “S” value | 1 | 100.00 | 0 | 0.00 |
| Low “S” value | 0 | 0.00 | 0 | 0.00 |
| Artifacts | 0 | 0.00 | 0 | 0.00 |
| Others | 0 | 0.00 | 0 | 0.00 |
| <i>Chi-square Test (χ^2) for association</i> | | | | |

APPENDIX B

Table 28. X-ray Machine Calibration Room Number 4

REPORT OF RADIOGRAPHIC SYSTEM PERFORMANCE

| | |
|----------------------|---|
| LOCATION: | BBR 4F King Chulalongkorn Memorial Hospital |
| DATE: | 9/10/2004 |
| ROOM NUMBER: | 4 |
| MANUFACTURE: | Hitachi, Japan; April 1989 |
| MODEL NUMBER | DR-155HM (Tube unit; U-6GE-55T) |
| SERIAL NUMBER | KC12808904 (beam limiting device KC 12003803) |

| | |
|------------|---|
| P | GENERAL MECHANICAL CONDITIONS |
| P | ALL INDICATOR LAMPS AND "BEAM ON INDICATOR" |
| P | DEAD MAN SWITCH |
| F | SOURCE IMAGE DISTANCE INDICATOR (SID) |
| P | MECHANICAL MOTION TEST |
| P | FIELD SIZE INDICATION |
| P | LIGHT VRS RADIATION CONGRUENCE |
| P | CROSS HAIR CENTERING |
| N/A | AUTOMATIC COLLIMATION (PBL) |
| N/A | PHOTO TIMER REPRODUCIBILITY AND DENSITY COMPENSATION |
| P | EXPOSURE REPRODUCIBILITY |
| P | LINEARITY OF EXPOSURE WITH mR/mAs |
| P | TIMER ACCURACY |
| P | BEAM QUALITY (HVL) |
| P | kVp ACCURACY |
| P | ENTRANCE SKIN EXPOSURE (ESE) |

P **PASS**
F **FAIL**
N/A **NOT APPLICABLE**
N/P **NOT PERFORMED**
NOTE **RECOMMENDATION SUGGESTED**

GENERAL CONDITION OF MECHANICAL AND ELECTRICAL COMPONENTS

| | |
|---|--|
| N | Are there any frayed or exposed electrical wires? |
| N | Could the electrical wires interfere with the use of the unit? |
| N | Is there a play in the couch when it is locked? |
| Y | Does it have the freedom of movement it was designed for? |
| Y | Is the couch level in the tube and perpendicular directions? |
| N | Is there a play in the tube when it is locked? |
| Y | Does it have the freedom of movement it was designed for? |
| Y | Does the visual and/or beam-on indicator function properly? |
| Y | Is the "dead-man" switch installed properly? |
| Y | Are all the indicator lamps functioning and properly? |

comments:

SOURCE IMAGE RECEPTOR DISTANCE ACCURACY CHECK

| Allowable limits | 2% of SID | |
|---------------------------|-----------|----|
| Indicated SID | 100 | cm |
| Measured SID | 99.5 | cm |
| SID to table top or Bucky | 106.5 | |
| % Deviation | 0.5 | |
| Pass/fail | PASS | |

Motion and Lock Test

| | |
|---------------------|---|
| Tube longitudinal | Y |
| Tube rotate | Y |
| Tube transverse | Y |
| Tube vertical | Y |
| Tube angulate | Y |
| Collimator jaws | Y |
| Collimator rotation | Y |

comments:

Field Size Indication

The purpose of this test is to ensure that the radiographer can set the optical field size within 2% of SID for all field sizes. It is checked for two selected field sizes.

| | |
|------------|-----|
| SID | 100 |
|------------|-----|

| Field size set | | Measured | | %Deviation | | Pass/Fail |
|----------------|-----------|----------|-----------|------------|-----------|-----------|
| A-C Axis | Perp Axis | A-C Axis | Perp Axis | A-C Axis | Perp Axis | |
| 25 | 18 | 24 | 18 | 1.00 | 0.00 | Pass |
| 30 | 25 | 28 13/16 | 24 13/16 | 1.19 | 0.19 | Pass |

Congruence of Light VS Radiation Filed

The purpose of this test is to verify that the radiation field is aligned with the light field within 2% of SID for all field sizes. It is checked for two selected field sizes.

| Light Field | | Radiation Fld | | %Deviation | | Pass/Fail |
|-------------|-----------|---------------|-----------|------------|-----------|-----------|
| A-C Axis | Perp Axis | A-C Axis | Perp Axis | A-C Axis | Perp Axis | |
| 25 8/16 | 20 8/16 | 25 8/16 | 20 | 0.00 | 0.50 | Pass |
| 30 13/16 | 25 10/16 | 30 8/16 | 25 | 0.31 | 0.63 | Pass |

Cross-hair Centering

The purpose of this test is to verify that the center of optical and radiation fields are within 2% of SID.

| | |
|--------------------------------------|-------------|
| Deviation between the centers | 5/16 |
| % Deviation | 0.31 |

comments:

Positive beam limiting device (PBL) test

| | |
|-----|---|
| N/A | Does the PBL system collimate within 5 seconds? |
| N/A | Does it collimate to larger than the cassette size? |
| N/A | Does its collimate to smaller than the cassette size? |
| N/A | Is there an over ride key? |
| N/A | With the key removed, is PBL automatically activated? |

| Cassette size | | Light Field | | %Deviation | | Pass/Fail |
|---------------|-----------|-------------|-----------|------------|-----------|-----------|
| A-C Axis | Perp Axis | A-C Axis | Perp Axis | A-C Axis | Perp Axis | |
| | | | | | | |
| | | | | | | |

| |
|------------------|
| comments: |
|------------------|

The purpose of this test is to verify that the Co-eff. of Variation of phototimed exposures is within 0.05 and the exposure increases and decreases with the density control function. Use 3.4 mm Cu at approximately 80 kV_p. Select center cell.

| | |
|------------|--|
| Kvp | |
|------------|--|

| Density | mAs/O.D. |
|---------|----------|
| N | N/A |
| N | N/A |
| N | N/A |
| N | N/A |
| -1 | N/A |
| 1 | N/A |

| | |
|---------------------------------|----------------|
| Mean of Normal Exposures | #DIV/0! |
| Standard Deviation | #DIV/0! |
| Coefficient of Variation | #DIV/0! |
| Pass/Fail | #DIV/0! |

Reproducibility of Exposure

The purpose of this test is to verify that radiation exposure at 80 kV_p is reproducible with a CV of 0.05 or less. Select mid current and 1/10 of a second on mA and S or else select about 25 mAs on mAs only option machines. Select SCD=26".

| mA | Sec | mAs |
|-----|------|-----|
| 200 | 3/25 | 24 |

| mR1 | mR2 | mR3 | mR4 |
|------------|------------|------------|------------|
| 169.9 | 171.9 | 174.2 | 176.3 |

| | |
|---------------------------------|-------------|
| Mean Exposure | 173.08 |
| Standard Deviation | 2.777 |
| Coefficient of Variation | 0.016 |
| Pass/fail | Pass |

comments:

mA or mAs Linearity

The purpose of this test is to verify that mR/mAs measured at two adjacent mA stations or mAs settings are linear and retains a COV of less than 0.1. Select around 80 kV_p

| kV_p | mA | Sec | mAs | mR | mR/mAs | COV |
|-----------------------|-----------|------------|------------|-----------|---------------|------------|
| 80 | 200 | 1/20 | 10.0 | 70.5 | 7.05 | |
| 80 | 200 | 1/4 | 54.0 | 358.4 | 6.64 | 0.030 |
| 80 | 200 | 1/2 | 107.0 | 734.9 | 6.87 | 0.017 |

Timer Accuracy

The purpose of this test is to verify that the measured time is within 10% of the set time. A set of three typical times are used for this test.

| Set Time | | Measured | % Dev |
|-----------------|----------------|-----------------|--------------|
| Fraction | Decimal | | |
| 1/20 | 0.0500 | 0.0475 | 5.00 |
| 1/10 | 0.1000 | 0.0975 | 2.50 |
| 1/4 | 0.2500 | 0.2473 | 1.08 |
| 1/2 | 0.5000 | 0.4955 | 0.90 |

comments:

Beam Quality (HVL) Measurement

The purpose of this test is to verify that there is minimum of 2.3 mm of Al HVL in the beam at 80 kV_p.

| Filter Thickness mm of Al | Exposure mR |
|------------------------------|----------------|
| 0.0 | 176.3 |
| 2.0 | 103.4 |
| 3.0 | 88.4 |

50% of open **88.2**

| | | |
|------------|-------------|----------|
| HVL | 3.02 | mm of Al |
|------------|-------------|----------|

kV_p Accuracy and mR/mAs Test

The purpose of this test is to verify that the average kV_p is within 10% of set kV_p and mR/mAs at 40" is within the norms published in NCRP #33

Select SCD of 26"

| Set | kV _p | | mR | mA | Sec | mAs | mR/mAs | % kV _p Deviation |
|------------|-----------------|--|-------|-----|--------|-----|--------|--------------------------------|
| | Measured | | | | | | | |
| 50 | 48.0 | | 54.3 | 200 | 0.1200 | 24 | 2.263 | 4.00 |
| 60 | 55.3 | | 87 | 200 | 0.1200 | 25 | 3.480 | 7.83 |
| 70 | 64.5 | | 134.1 | 200 | 0.1200 | 26 | 5.158 | 7.86 |
| 80 | 75.6 | | 169.9 | 200 | 0.1200 | 25 | 6.796 | 5.50 |
| 90 | 83.8 | | 220.2 | 200 | 0.1200 | 25 | 8.808 | 6.89 |
| 100 | 93.0 | | 280 | 200 | 0.1200 | 25 | 11.200 | 7.00 |
| 110 | 104.7 | | 336.2 | 200 | 0.1200 | 24 | 14.008 | 4.82 |
| 120 | 109.3 | | 391.4 | 200 | 0.1200 | 21 | 18.638 | 8.92 |

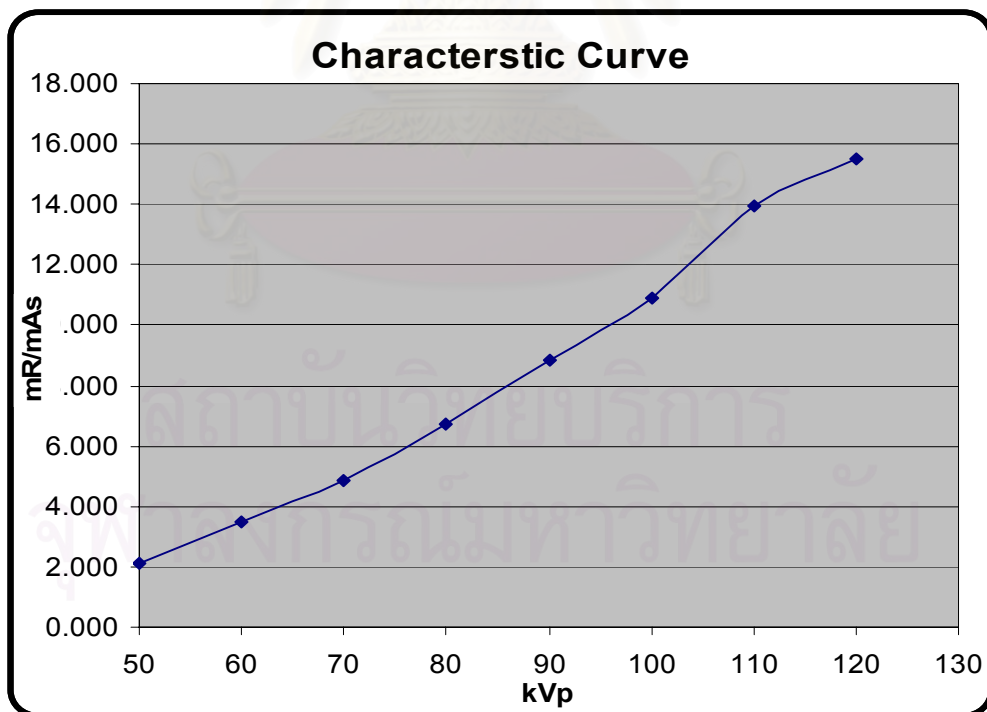
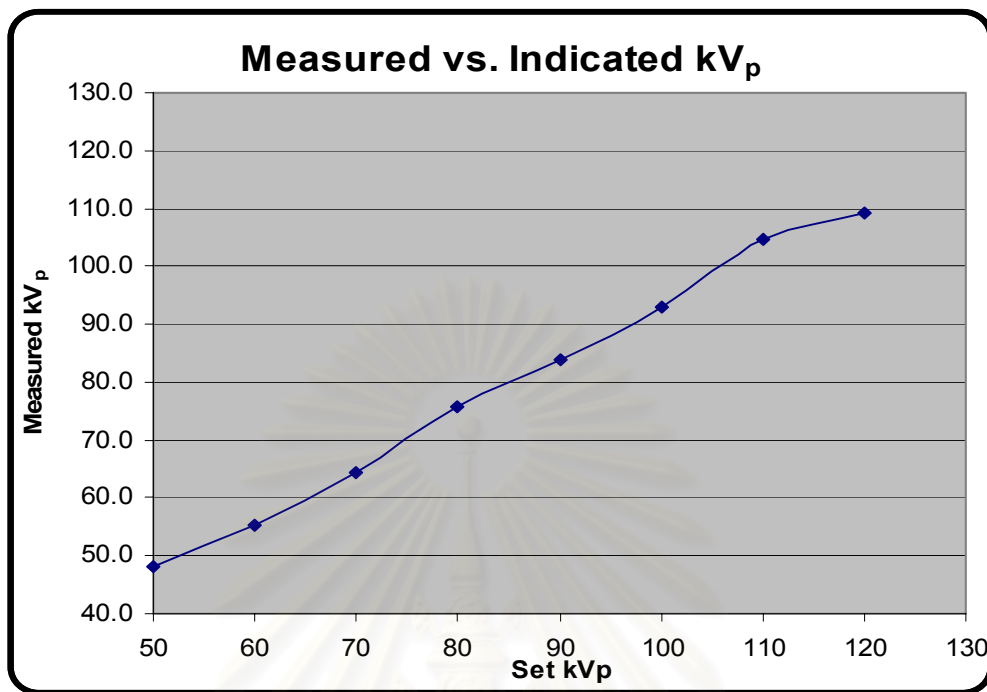


Table 29. X-ray Machine Calibration Room Number 5

REPORT OF RADIOGRAPHIC SYSTEM PERFORMANCE

| | |
|----------------------|---|
| LOCATION: | BBR 4F King Chulalongkorn Memorial Hospital |
| DATE: | 15/10/2004 |
| ROOM NUMBER: | 5 |
| MANUFACTURE: | Hitachi, Japan; April 1989 |
| MODEL NUMBER | DR-155HM April 1989 (Tube unit; U-6GE-55T) |
| SERIAL NUMBER | KC 17714403 JUNE 1994 (from Beam limiting device) |

| | |
|------------|---|
| P | GENERAL MECHANICAL CONDITIONS |
| P | ALL INDICATOR LAMPS AND "BEAM ON INDICATOR" |
| P | DEAD MAN SWITCH |
| N/A | SOURCE IMAGE DISTANCE INDICATOR (SID) |
| P | MECHANICAL MOTION TEST |
| P | FIELD SIZE INDICATION |
| P | LIGHT VRS RADIATION CONGRUENCE |
| P | CROSS HAIR CENTERING |
| N/A | AUTOMATIC COLLIMATION (PBL) |
| N/A | PHOTO TIMER REPRODUCIBILITY AND DENSITY COMPENSATION |
| P | EXPOSURE REPRODUCIBILITY |
| P | LINEARITY OF EXPOSURE WITH mR/mAs |
| P | TIMER ACCURACY |
| P | BEAM QUALITY (HVL) |
| P | kV_p ACCURACY |
| P | ENTRANCE SKIN EXPOSURE (ESE) |

P **PASS**

F **FAIL**

N/A **NOT APPLICABLE**

N/P **NOT PERFORMED**

NOTE **RECOMMENDATION SUGGESTED**

GENERAL CONDITION OF MECHANICAL AND ELECTRICAL COMPONENTS

| | |
|---|--|
| N | Are there any frayed or exposed electrical wires? |
| N | Could the electrical wires interfere with the use of the unit? |
| N | Is there a play in the couch when it is locked? |
| Y | Does it have the freedom of movement it was designed for? |
| Y | Is the couch level in the tube and perpendicular directions? |
| N | Is there a play in the tube when it is locked? |
| Y | Does it have the freedom of movement it was designed for? |
| N | Does the visual and/or beam-on indicator function properly? |
| Y | Is the "dead-man" switch installed properly? |
| Y | Are all the indicator lamps functioning and properly? |

comments:

SOURCE IMAGE RECEPTOR DISTANCE ACCURACY CHECK

| Allowable limits | 2% of SID | |
|---------------------------|-----------|----|
| Indicated SID | 100 | cm |
| Measured SID | 101.0 | cm |
| SID to table top or Bucky | 108.5 | |
| % Deviation | 1.0 | |
| Pass/fail | PASS | |

Motion and Lock Test

| | |
|---------------------|---|
| Tube longitudinal | Y |
| Tube rotate | Y |
| Tube transverse | Y |
| Tube vertical | Y |
| Tube angulate | Y |
| Collimator jaws | Y |
| Collimator rotation | Y |

comments:

Field Size Indication

The purpose of this test is to ensure that the radiographer can set the optical field size within 2% of SID for all field sizes. It is checked for two selected field sizes.

| | |
|------------|-----|
| SID | 100 |
|------------|-----|

| Field size set | | Measured | | %Deviation | | Pass/Fail |
|----------------|-----------|----------|-----------|------------|-----------|-------------|
| A-C Axis | Perp Axis | A-C Axis | Perp Axis | A-C Axis | Perp Axis | |
| 25 | 18 | 25 3/16 | 15 11/16 | 0.19 | 2.31 | Fail |
| 30 | 25 | 30 8/16 | 26 | 0.50 | 1.00 | Pass |

Congruence of Light vs Radiation Filed

The purpose of this test is to verify that the radiation field is aligned with the light field within 2% of SID for all field sizes. It is checked for two selected field sizes.

| Light Field | | Radiation Fld | | %Deviation | | Pass/Fail |
|-------------|-----------|---------------|-----------|------------|-----------|-------------|
| A-C Axis | Perp Axis | A-C Axis | Perp Axis | A-C Axis | Perp Axis | |
| 20 11/16 | 25 8/16 | 20 8/16 | 27 | 0.19 | 1.50 | Pass |
| 25 15/16 | 31 | 26 5/16 | 32 3/16 | 1.00 | 1.19 | Pass |

Cross-hair Centering

The purpose of this test is to verify that the center of optical and radiation fields are within 2% of SID.

| | |
|--------------------------------------|---------------|
| Deviation between the centers | 1 5/16 |
| % Deviation | 1.31 |

comments:

Positive beam limiting device (PBL) test

| | |
|-----|---|
| N/A | Does the PBL system collimate within 5 seconds? |
| N/A | Does it collimate to larger than the cassette size? |
| N/A | Does its collimate to smaller than the cassette size? |
| N/A | Is there an over ride key? |
| N/A | With the key removed, is PBL automatically activated? |

| Cassette size | | Light Field | | %Deviation | | Pass/Fail |
|---------------|-----------|-------------|-----------|------------|-----------|-----------|
| A-C Axis | Perp Axis | A-C Axis | Perp Axis | A-C Axis | Perp Axis | |
| | | | | | | |
| | | | | | | |

| |
|------------------|
| comments: |
|------------------|

The purpose of this test is to verify that the Co-eff. of Variation of phototimed exposures is within 0.05 and the exposure increases and decreases with the density control function. Use 3.4 mm Cu at approximately 80 kV_p. Select center cell.

| | |
|------------|--|
| Kvp | |
|------------|--|

| Density | mAs/O.D. |
|---------|----------|
| N | N/A |
| N | N/A |
| N | N/A |
| N | N/A |
| -1 | N/A |
| 1 | N/A |

| | |
|---------------------------------|----------------|
| Mean of Normal Exposures | #DIV/0! |
| Standard Deviation | #DIV/0! |
| Coefficient of Variation | #DIV/0! |
| Pass/Fail | #DIV/0! |

Reproducibility of Exposure

The purpose of this test is to verify that radiation exposure at 80 kV_p is reproducible with a CV of 0.05 or less. Select mid current and 1/10 of a second on mA and S or else select about 25 mAs on mAs only option machines. Select SCD=26".

| mA | Sec | mAs |
|-----|------|-----|
| 200 | 3/25 | 24 |

| mR1 | mR2 | mR3 | mR4 |
|------------|------------|------------|------------|
| 194.3 | 191.8 | 195.5 | 196.5 |

| | |
|---------------------------------|-------------|
| Mean Exposure | 194.53 |
| Standard Deviation | 2.027 |
| Coefficient of Variation | 0.010 |
| Pass/fail | Pass |

comments:

mA or mAs Linearity

The purpose of this test is to verify that mR/mAs measured at two adjacent mA stations or mAs settings are linear and retains a COV of less than 0.1. Select around 80 kV_p

| kV_p | mA | Sec | mAs | mR | mR/mAs | COV |
|-----------------------|-----------|------------|------------|-----------|---------------|------------|
| 80 | 200 | 1/20 | 11.0 | 78.7 | 7.15 | |
| 80 | 200 | 1/4 | 52.0 | 399.8 | 7.69 | 0.036 |
| 80 | 200 | 1/2 | 104.0 | 820.6 | 7.89 | 0.013 |

Timer Accuracy

The purpose of this test is to verify that the measured time is within 10% of the set time. A set of three typical times are used for this test.

| Set Time | | Measured | % Dev |
|-----------------|----------------|-----------------|--------------|
| Fraction | Decimal | | |
| 1/20 | 0.0500 | 0.0475 | 5.00 |
| 1/10 | 0.1000 | 0.0974 | 2.60 |
| 1/4 | 0.2500 | 0.2473 | 1.08 |
| 1/2 | 0.5000 | 0.4952 | 0.96 |

comments:

Beam Quality (HVL) Measurement

The purpose of this test is to verify that there is minimum of 2.3 mm of Al HVL in the beam at 80 kV_p.

| Filter Thickness mm of Al | Exposure mR |
|------------------------------|----------------|
| 0.0 | 196.4 |
| 2.0 | 115.7 |
| 3.0 | 94.7 |

50% of open

98.2

| | | |
|-----|------|----------|
| HVL | 2.83 | mm of Al |
|-----|------|----------|

kV_p Accuracy and mR/mAs Test

The purpose of this test is to verify that the average kV_p is within 10% of set kV_p and mR/mAs at 40" is within the norms published in NCRP #33

Select SCD of 26"

| Set | kV _p | | mR | mA | Sec | mAs | mR/mAs | % kV _p Deviation |
|-----|-----------------|--|-------|-----|--------|-----|--------|--------------------------------|
| | Measured | | | | | | | |
| 50 | 50.9 | | 56.1 | 200 | 0.1200 | 23 | 2.439 | 1.80 |
| 60 | 57.9 | | 96.5 | 200 | 0.1200 | 24 | 4.021 | 3.50 |
| 70 | 67.8 | | 141.9 | 200 | 0.1200 | 25 | 5.676 | 3.14 |
| 80 | 77.2 | | 194.3 | 200 | 0.1200 | 25 | 7.772 | 3.50 |
| 90 | 86.6 | | 245.9 | 200 | 0.1200 | 25 | 9.836 | 3.78 |
| 100 | 96.9 | | 309.9 | 200 | 0.1200 | 25 | 12.396 | 3.10 |
| 110 | 104.7 | | 363.2 | 200 | 0.1200 | 23 | 15.791 | 4.82 |
| 120 | N/A | | N/A | N/A | N/A | N/A | N/A | N/A |

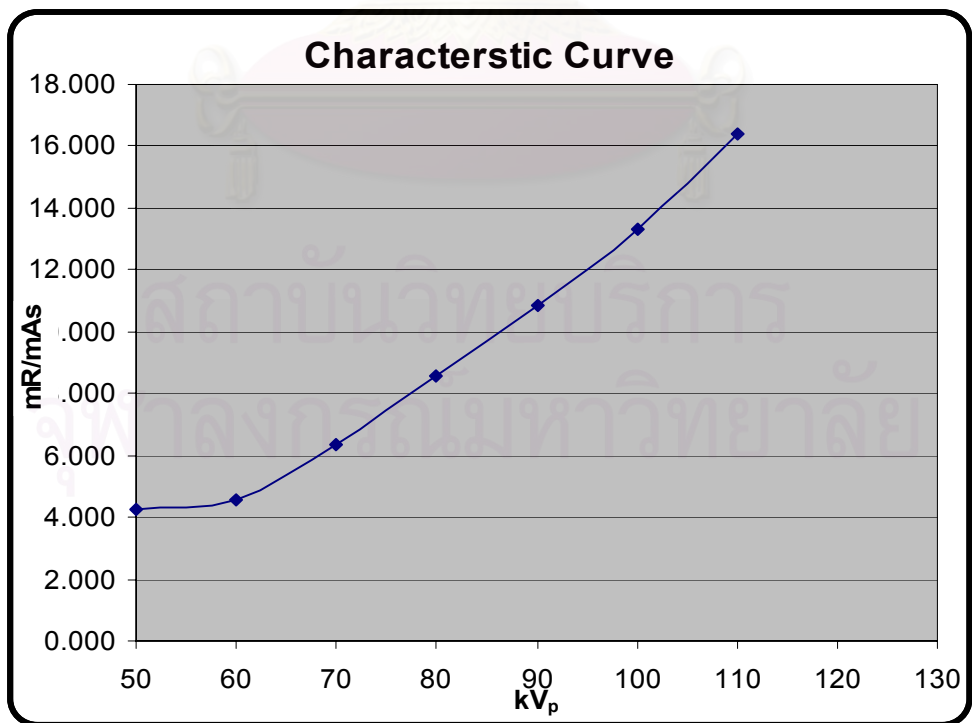
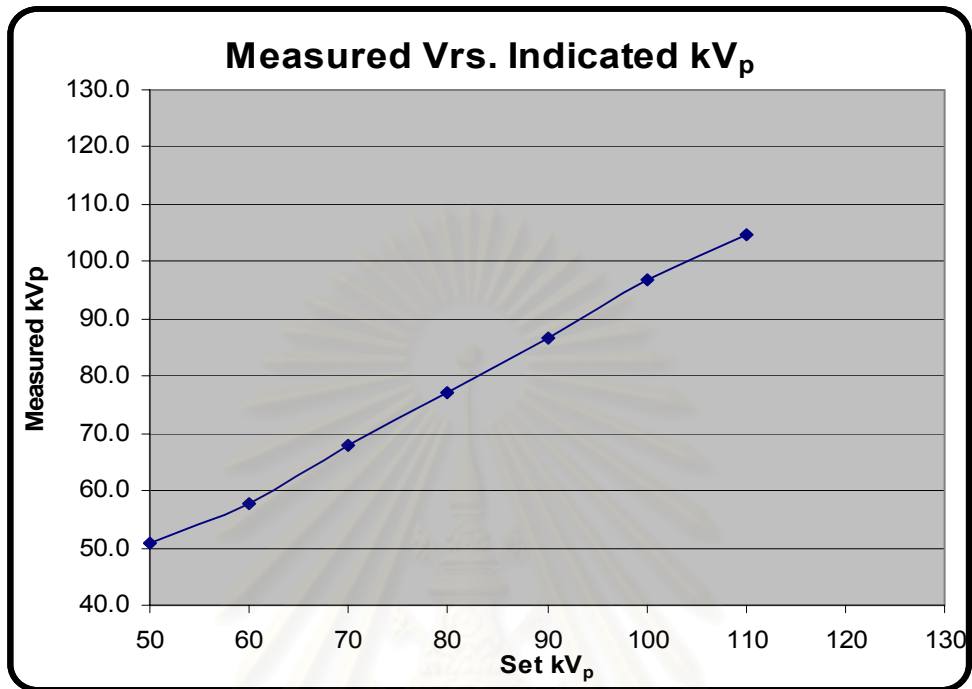


Table 30. Common backscatter factor data for each x-ray energy.

| COMMON BACKSCATTER FACTOR DATA | | | | | | |
|---|---------|---|-------------|------|------|---|
| Backscatter factors (Petoussi-Hens et al, PMB 43:2237-2250, 1998) | | | | | | |
| All for 25 x 25 cm field, ICRU tissue, 2.5 mm Al filtration | | | | | | |
| kVp | HVL | BSF | HVL | BSF | Calc | BSF As Applied |
| 50 | 1.74 | 1.28 | (3 mm Al) | | 1.31 | <i>1.31</i> |
| 60 | 2.08 | 1.32 | | | 1.34 | <i>1.34</i> |
| 70 | 2.41 | 1.36 | 2.64 | 1.38 | 1.38 | 1.38 |
| 80 | 2.78 | 1.39 | 3.04 | 1.41 | 1.41 | 1.41 |
| 90 | 3.17 | 1.42 | 3.45 | 1.44 | 1.44 | 1.44 |
| 100 | 3.24 | 1.42 | 3.88 | 1.46 | 1.46 | 1.46 |
| 110 | 3.59 | 1.44 | | | 1.48 | <i>1.48</i> |
| 120 | | | 4.73 | 1.49 | 1.49 | |
| | Mean | 1.38 | | | 1.40 | |
| Curve Fit Used | | $Y = M0 + M1*x + \dots M8*x^8 + M9*x^9$ | | | | Values in <i>italics</i> are extrapolated or interpolated |
| | | M0 | 1.0684 | | | |
| | | M1 | 0.0052272 | | | |
| | | M2 | -6.7373e-06 | | | |
| | | M3 | -6.2898e-08 | | | |
| R | 0.99967 | | | | | |

Table 31. Normalized the Entrance Skin Dose (uGy/mAs) from backscatter factor and Entrance Surface Air Kerma at 100 cm of Focus to skin distance for large focal spot of Room No. 4.

| Room 4 Large focus | | | | | |
|---------------------------|---------------|-----|--------------|------|---------------------|
| Modified | FCD (cm) | = | 100 | | |
| kVp | Mean ESAK mGy | mAs | ESAK mGy/mAs | BSF | ESD uGy/mAs @100 cm |
| 50 | 0.31 | 40 | 0.00775 | 1.31 | 10.15 |
| 60 | 0.53 | 42 | 0.012619 | 1.34 | 16.91 |
| 70 | 0.79 | 43 | 0.0183721 | 1.38 | 25.35 |
| 80 | 1.07 | 42 | 0.0254762 | 1.41 | 35.92 |
| 90 | 1.34 | 42 | 0.0319048 | 1.44 | 45.94 |
| 100 | 1.73 | 43 | 0.0402326 | 1.46 | 58.74 |
| 110 | 2.04 | 40 | 0.051 | 1.48 | 75.48 |

Table 32. Normalized the Entrance Skin Dose (uGy/mAs) from backscatter factor and Entrance Surface Air Kerma at 100 cm of Focus to skin distance for large focal spot of Room No. 5.

| Room 5 Large focus | | | | | |
|--------------------|-----------|-----|-----------|------|---------------------|
| Modified | FCD (cm) | = | 100 | | |
| kVp | Mean ESAK | mAs | ESAK | BSF | ESD uGy/mAs @100 cm |
| | mGy | | mGy/mAs | | |
| 50 | 0.37 | 37 | 0.01 | 1.31 | 13.10 |
| 60 | 0.63 | 39 | 0.0161538 | 1.34 | 21.65 |
| 70 | 0.93 | 41 | 0.0226829 | 1.38 | 31.30 |
| 80 | 1.17 | 40 | 0.02925 | 1.41 | 41.24 |
| 90 | 1.54 | 40 | 0.0385 | 1.44 | 55.44 |
| 100 | 1.89 | 39 | 0.0484615 | 1.46 | 70.75 |
| 110 | 2.25 | 39 | 0.0576923 | 1.48 | 85.38 |

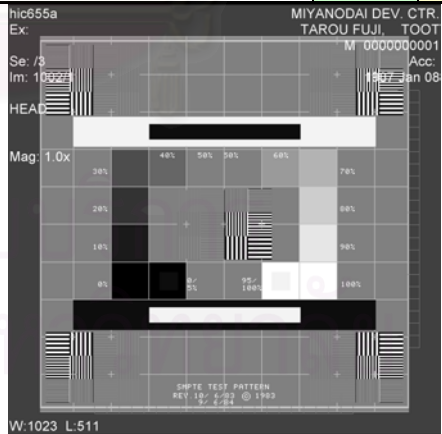
สถาบันวิทยบริการ
จุฬาลงกรณ์มหาวิทยาลัย

Table 33. CR System Calibration

| Result | CR system Calibration Test | Tolerance-The Established Criteria |
|---|--|--|
| P | 1. Monitor & laser printer set-up | The 5% on 0% and 95% on 100% details should be clearly visible. The horizontal and vertical resolutions should not differ by greater than 20%. |
| P | 2. Dark Noise | A uniform artifact free image should be expected. This results in series of bands appearing across the image. |
| P | 3. Erasure cycle efficiency | Absence of a ghost image of the lead block from the first exposure in the re-exposed image. There should be <1% (remedial) difference between the pixel values in the ghosted region and the surrounding areas. A suspension level of <5% is set. |
| P | 4. Sensitivity Index calibration | The indicated exposure should agree with the measured exposure within 20%. |
| P | 5. Sensitivity Index consistency | The variation in the calculated indicated exposures should not differ by greater than 20% between plates. The measurements repeated on the same plate should be used to lay down a baseline for future QA tests. |
| P | 6. Uniformity | The images should not have obvious artifacts. If measuring uniformity from film the maximum variation in optical densities should be less than 10%. Using region of interest analysis, values should be within a range of 10% of each other. |
| P | 7. Scaling errors | The measured distances x and y should agree within 3% of the actual distances. All calculated aspect ratios should be within 1.00 ± 0.03 . |
| P | 8. Blurring | No blurring should be present. If blurring is present on all plates this suggests the reader is at fault, whilst imperfections in individual plates may also lead to blurring. If blurring remains on a region of a plate after cleaning it should not be used clinically. |
| P | 9. Limiting Spatial Resolution | For the 45° angled test object the resolved line pairs per mm should be $>1.2/2p$ where p is the pixel dimension in mm. In the scan and subscan directions the limiting resolution should be $>0.85/2p$. These measurements should be used to set a baseline for future QA tests. |
| P | 10. Threshold Contrast Detail Detectability | The results of this test are used to set a baseline for future QA tests. Results could be compared to those from other similar systems if available. |
| P | 11. Laser beam function | The edge should be continuous across the full length of the image. Stair step characteristics should be uniform across the length of the image. Regions of over or undershoot of the scan lines indicate a timer or laser beam modulation problem. Ruler edges should be straight and continuous without any under- or overshoot of the scan lines in light to dark transitions. |
| F | 12. Moiré Patterns | No Moiré patterns should be visible. If Moiré patterns are visible with a particular grid, it should not be used with the CR plates. The cause of Moiré patterns may be the failure of the motion of moving grids or insufficient grid density. |
| Result: P = PASS, F = FAIL, N/A = NOT APPLICABLE, N/P = NOT PERFORMED NOTE, COMMENT = RECOMMENDATION SUGGESTED | | |

Table 34. Computed Radiography Systems Performance**1. Monitor & laser printer set-up****Density Response - Calibration**

Test Patterns: 1) 24 steps Sensitometric strip image acquired by Wet Fuji laser printer (FLIM-D)
2) HIC-655 workstation generated SMPTE pattern and print-out through FLIM-D.

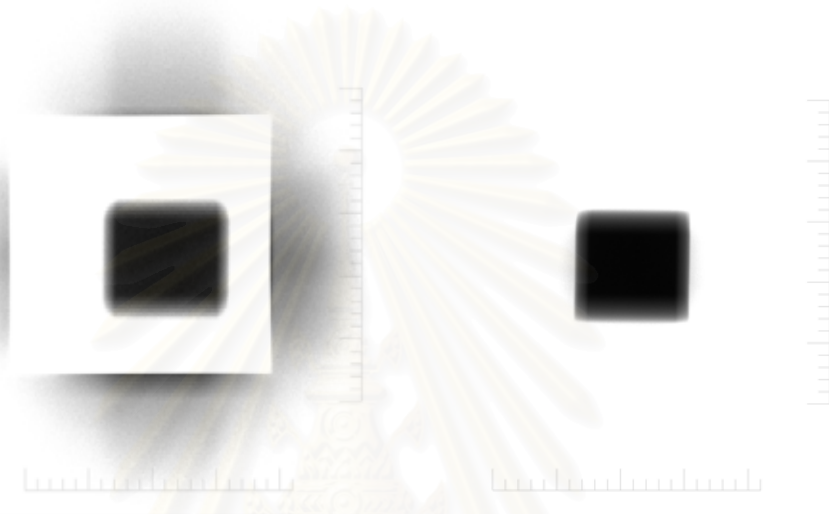
| Step | Printer Setting | | Max Pixel Value | | 1024 |
|---------|------------------|------|--|------|------|
| OD step | C=11, Dmax = 2.7 | | % PV | PV | OD |
| 24 | | 3.17 | 100 | 1020 | 2.36 |
| 23 | | 3.06 | 95 | 972 | 2.22 |
| 22 | | 2.98 | 90 | 920 | 1.99 |
| 21 | | 2.85 | 80 | 816 | 1.79 |
| 20 | 100% | 2.67 | 70 | 716 | 1.6 |
| 19 | 95% | 2.48 | 60 | 612 | 1.4 |
| 18 | | 2.28 | 50 | 508 | 1.18 |
| 17 | 80% | 2.09 | 40 | 408 | 0.97 |
| 16 | 70% | 1.89 | 30 | 304 | 0.76 |
| 15 | 60% | 1.69 | 20 | 204 | 0.56 |
| 14 | | 1.48 | 10 | 100 | 0.37 |
| 13 | | 1.27 | 5 | 48 | 0.3 |
| 12 | 40% | 1.09 | 0 | 0 | 0.24 |
| 11 | 30% | 0.89 |  | | |
| 10 | | 0.72 | | | |
| 9 | | 0.56 | | | |
| 8 | 10% | 0.44 | | | |
| 7 | 5% | 0.34 | | | |
| 6 | | 0.27 | | | |
| 5 | 0% | 0.23 | | | |
| 4 | | 0.2 | | | |
| 3 | | 0.18 | Speed Index #13 | | 1.27 |
| 2 | | 0.17 | Contrast Index # 20 - # 8 | | 2.23 |
| 1 | | 0.16 | | | |

| | |
|-------------|-----|
| Acceptable: | Yes |
|-------------|-----|

| 2. Dark Noise | | | | | | |
|-----------------------|-----------------|------------|------------|---------|---------|---------|
| Menu = TEST | | | | | | |
| SubMenu = Sensitivity | kV _p | Filtration | Focal spot | SID(cm) | S-value | L-value |
| L= 1, EDR = fix 10047 | none | none | none | none | 10048 | 1.00 |

| ID IP | IP size | Mean Pixel Value | Max. Pixel Value | Artifact free? Y / N |
|--------------|----------------|-------------------------|-------------------------|---------------------------------|
| A 08680365 c | 8" x 10" | 387 | 660 | N |
| A 08680396 c | 8" x 10" | 328 | 556 | N |
| A 08680440 c | 8" x 10" | 379 | 476 | N |
| A 08916037 c | 8" x 10" | 277 | 460 | N |
| A 08916068 c | 8" x 10" | 305 | 412 | N |
| A 09200203 c | 8" x 10" | 273 | 372 | N |
| A 09251908 c | 10" x 12" | 359 | 500 | N |
| A 09251953 c | 10" x 12" | 260 | 348 | N |
| A 09251960 c | 10" x 12" | 331 | 508 | N |
| A 09251977 c | 10" x 12" | 292 | 392 | N |
| A 09251991 c | 10" x 12" | 298 | 436 | N |
| A 09252028 c | 10" x 12" | 307 | 424 | N |
| A 09252035 c | 10" x 12" | 282 | 392 | N |
| A 09252158 c | 10" x 12" | 317 | 484 | N |
| A 09252189 c | 10" x 12" | 294 | 472 | N |
| A 09056459 c | 14" x 14" | 204 | 204 | Y |
| A 09056589 c | 14" x 14" | 310 | 456 | N |
| A 09078277 c | 14" x 14" | 275 | 344 | N |
| A 09056381 c | 14" x 14" | 318 | 432 | N |
| A 09056411 c | 14" x 14" | 323 | 444 | N |
| A 09056442 c | 14" x 14" | 290 | 432 | N |
| A 09056466 c | 14" x 14" | 287 | 416 | N |
| A 09256480 c | 14" x 14" | 294 | 404 | N |
| A 09056497 c | 14" x 14" | 278 | 360 | N |
| A 09056510 c | 14" x 14" | 282 | 420 | N |
| A 09233898 c | 14" x 17" | 411 | 824 | N |
| A 09233997 c | 14" x 17" | 284 | 364 | N |
| A 09234000 c | 14" x 17" | 299 | 416 | N |
| A 09234031 c | 14" x 17" | 338 | 472 | N |
| A 09234062 c | 14" x 17" | 343 | 428 | N |
| A 09234079 c | 14" x 17" | 204 | 204 | N |
| A 09234116 c | 14" x 17" | 204 | 204 | Y |
| A 09234123 c | 14" x 17" | 248 | 304 | N |
| A 09234147 c | 14" x 17" | 210 | 216 | N |
| A 09234154 c | 14" x 17" | 354 | 544 | N |
| A 09234178 c | 14" x 17" | 285 | 412 | N |
| A 09234185 c | 14" x 17" | 204 | 204 | Y |
| A 09234208 c | 14" x 17" | 315 | 424 | N |
| A 09234215 c | 14" x 17" | 319 | 576 | N |
| A 09234222 c | 14" x 17" | 233 | 260 | N |
| A 09234239 c | 14" x 17" | 256 | 308 | N |

| 3. Erasure cycle efficiency | | | | | | |
|------------------------------------|-----------------|---------------------------------|------------|-----------------|----------|----------|
| Menu = TEST | | Erasure cycle efficiency | | | | |
| SubMenu = Sensitivity | kV _p | Filtration | Focal spot | Field size (cm) | SCD (cm) | SID (cm) |
| L= 1, EDR = semi | 80 | none | 1.2 mm | 8.5 x 8.5 | 120 | 150 |

**First Exposure**

| FOV | mAs setting | mA/sec/mAs | mR | μGy |
|---------------|-------------|------------|----|-----------------|
| 10 cm x 10 cm | 25 | 26 | 60 | 317.8409 |

Second Exposure

| FOV | mAs setting | mA/sec/mAs | mR | μGy |
|-------------|-------------|------------|----|---------------|
| 9 cm x 9 cm | 0.5 | 0.50 | 1 | 0.7586 |

| | | | |
|--------------|------------|---------|------------------|
| IP Type/Size | ST 14x17 | | |
| IP S.N. | A 09234079 | Object: | 1.0 mm square Pb |

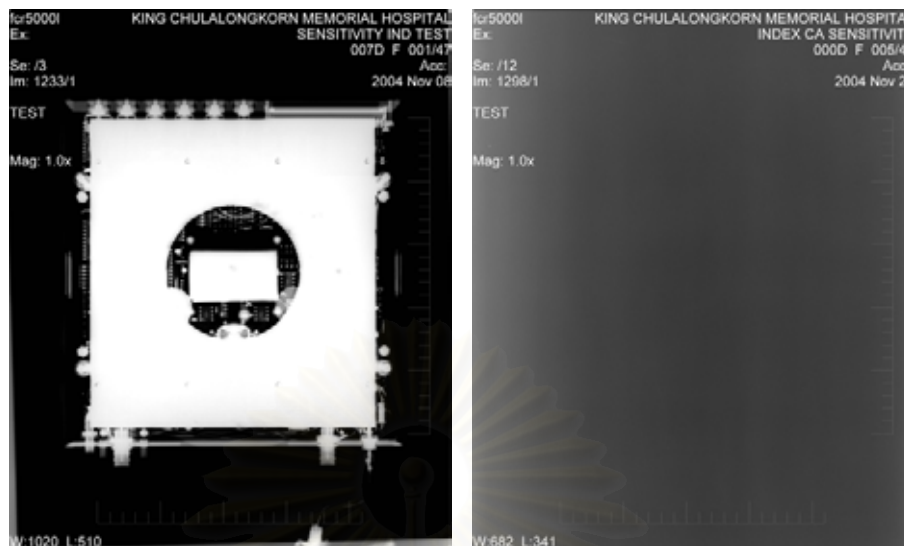
| | |
|---|-------------|
| Is the image free of any "ghost" image after erasure? | Yes* |
|---|-------------|

| | |
|-------------|-------------|
| Acceptable: | Yes* |
|-------------|-------------|

| | | | |
|----------------------------------|------------------------|-----------------|--|
| Farmer ionization chamber | | model 2670 type | |
| Chamber size | 0.6 | cc | |
| range | 2 | | |
| sensitivity | 40 | Gy/ μ C | |
| Measurement unit | pC | | |
| Correction factor; $N_D =$ | 4.203×10^{-7} | Gy/C | (100 kV _p , HVL = 4.0 mmAl) |
| Temperature | 25 | °C | |
| Pressure | 760 | PSI | |
| Victoreen 4000M+ | | | |
| Chamber size | 8.5 x 8.5 | cm ² | |
| range | 50 - 85 | kV _p | |
| filter | W / Al | | |
| Mode | Radio /High | | |
| Measurement unit | mR | | |
| SID | 150 cm | | |

| Radiation dose | Field size | SCD | kV _p | mAs | Time (sec.) | Measurement | | | |
|----------------|-------------|-----|-----------------|-----|-------------|-------------|--------|--------|--------|
| | | | | | | #1 | #2 | #3 | #4 |
| μ Gy | measurement | cm | | | | | | | |
| 1 | 10" x 12" | 100 | 75 | 32 | 0.02 | 0.1093 | 0.1279 | 0.1116 | 0.1081 |
| | 14" x 17" | 100 | 75 | 32 | 0.02 | 0.1105 | 0.1105 | 0.0947 | 0.0988 |
| 4 | 10" x 12" | 120 | 75 | 50 | 0.02 | 0.107 | 0.1128 | 0.114 | |
| | 14" x 17" | 120 | 75 | 50 | 0.02 | 0.1407 | 0.1465 | 0.1616 | |
| 10 | 10" x 12" | 120 | 80 | 125 | 0.01 | 0.2047 | 0.2628 | 0.1924 | 0.193 |
| | 14" x 17" | 120 | 80 | 125 | 0.01 | 0.3056 | 0.2628 | 0.2616 | |
| 12 | 10" x 12" | 120 | 75 | 50 | 0.03 | 0.3674 | 0.3337 | 0.3779 | |
| | 14" x 17" | 120 | 75 | 50 | 0.03 | 0.3849 | 0.4256 | 0.4221 | |
| 50 | 10" x 12" | 120 | 80 | 200 | 0.02 | 1.558 | 1.6203 | 1.5209 | 1.5593 |
| | 14" x 17" | 120 | 80 | 125 | 0.03 | 1.643 | 1.5907 | 1.5977 | 1.5593 |

| Radiation dose | | calc. μ Gy | nom. μ Gy | Measurement mR at SCD | | | | average mR | nom.mR |
|----------------|------------|----------------|---------------|-----------------------|-----|-------|-----|------------|----------|
| μ Gy | average pC | at SCD | at SID | #1 | #2 | #3 | #4 | | at SID |
| 1 | 0.114225 | 4.800877 | 2.133723 | 2.3 | 2.3 | 2.4 | 2.4 | 2.35 | 1.044444 |
| | 0.103625 | 4.355359 | 1.935715 | 2.3 | 2.3 | 2.4 | 2.4 | 2.35 | 1.044444 |
| 4 | 0.1112667 | 4.676538 | 2.992984 | 2.5 | 2.5 | 2.322 | 2.5 | 2.4555 | 1.57152 |
| | 0.1496 | 6.287688 | 4.02412 | 2.5 | 2.5 | 2.322 | 2.5 | 2.4555 | 1.57152 |
| 10 | 0.213225 | 8.961847 | 5.735582 | 3 | 3.1 | 2.8 | 2.8 | 2.925 | 1.872 |
| | 0.2766667 | 11.6283 | 7.442112 | 3 | 3.1 | 2.8 | 2.8 | 2.925 | 1.872 |
| 12 | 0.3596667 | 15.11679 | 9.674746 | 3.7 | 3.7 | 3.5 | 3.7 | 3.65 | 2.336 |
| | 0.4108667 | 17.26873 | 11.05198 | 3.7 | 3.7 | 3.5 | 3.7 | 3.65 | 2.336 |
| 50 | 1.564625 | 65.76119 | 42.08716 | 9.2 | 9.2 | 9.3 | 9.4 | 9.275 | 5.936 |
| | 1.597675 | 67.15028 | 42.97618 | 9 | 9 | 9.1 | 9 | 9.025 | 5.776 |



4. Sensitivity Index calibration

| | | | | | | | |
|-----------------------|--------------------------------------|---------------|------------|------------|------------|----------|----------|
| Menu = TEST | Sensitivity Index calibration | | | | | | |
| SubMenu = Sensitivity | kV _p | mA/sec/mAs | Filtration | Focal spot | Time delay | SID (cm) | SCD (cm) |
| L= 1, EDR = semi | 80 | 125/0.01/1.25 | None | 1.2 mm | ~ 6 mins. | 150 | 120 |

| IP Type | IP SN | mAs | mR-meter | mR-IP | S | S (1mR) | PV | mR =200/S |
|---------------------|------------|------|----------|-------|-----|---------|--------|-----------|
| ST 10x12 | A 09251953 | 1.25 | 2.925 | 1.87 | 171 | 320 | 521.12 | 1.17 |
| ST 10x12 | A 09252158 | 1.25 | 2.925 | 1.87 | 171 | 320 | 516.64 | 1.17 |
| ST 14x17 | A 09234079 | 1.25 | 2.925 | 1.87 | 179 | 335 | 468.8 | 1.12 |
| ST 14x17 | A 09234116 | 1.25 | 2.925 | 1.87 | 179 | 335 | 479.3 | 1.12 |
| Mean: | | | | | | 328 | 496.47 | 1.14 |
| Standard Deviation: | | | | | | 8.65 | 26.30 | 0.03 |

| | |
|-------------|------------|
| Acceptable: | Yes |
|-------------|------------|

| IP SN | Pixel value | | | | | Average | Standard |
|------------|-------------|-------------|------------|------------|-------------|---------|-----------|
| | Center | Upper Right | Upper Left | Lower Left | Lower Right | PV | Deviation |
| A 09251953 | 523.2 | 508.8 | 524 | 530.4 | 519.2 | 521.12 | 7.971951 |
| A 09252158 | 523.2 | 512.8 | 522.4 | 501.6 | 523.2 | 516.64 | 9.489362 |
| A 09234079 | 519.2 | 406.4 | 447.2 | 460 | 511.2 | 468.8 | 46.8393 |
| A 09234116 | 518.4 | 492 | 424.5 | 448 | 513.6 | 479.3 | 41.38031 |

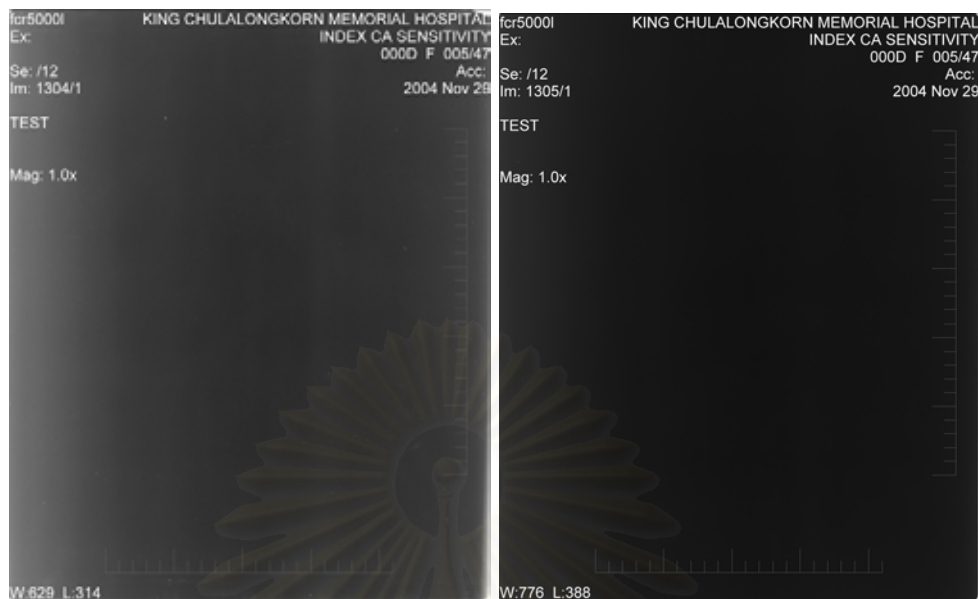


| 5. Sensitivity Index consistency | | | | | | | |
|----------------------------------|-------------------------------|---------------|------------|------------|------------|----------|----------|
| Menu = TEST | Sensitivity Index consistency | | | | | | |
| SubMenu = Sensitivity | kV _p | mAs | Filtration | Focal spot | Time delay | SID (cm) | SCD (cm) |
| L= 1, EDR = semi | 80 | 125/0.01/1.25 | None | 1.2 mm | None | 150 | 120 |

| study No. | Cassette | Cassette Serial Number | Defect Free? (Y/N) | Exposure Index (S-value) | Nom. μ Gy | Average Pixel Value | Standard Deviation |
|-----------|-----------|------------------------|--------------------|--------------------------|---------------|---------------------|--------------------|
| | Type/Size | | | | | | |
| A 292 | ST 14x17 | A 09234208 | Y | 159 | 7.4421 | 491.73 | 30.15368 |
| A 293 | ST 14x17 | A 09234222 | Y | 159 | 7.4421 | 494.53 | 30.8163 |
| A 294 | ST 14x17 | A 09234253 | Y | 156 | 7.4421 | 484.4 | 34.02809 |
| A 295 | ST 14x17 | A 09054062 | Y | 159 | 7.4421 | 491.2 | 28.23079 |
| A 285 | ST 10x12 | A 09251960 | Y | 145 | 5.7356 | 512.53 | 11.35684 |
| A 286 | ST 10x12 | A 09251915 | Y | 152 | 5.7356 | 521.2 | 5.838569 |
| A 288 | ST 10x12 | A 09252028 | Y | 156 | 5.7356 | 517.73 | 8.361286 |
| A 290 | ST 10x12 | A 09251953 | Y | 156 | 5.7356 | 520.00 | 8.844333 |

| study No. | Pixel value | | | | | Average | Standard |
|-----------|-------------|-------------|------------|------------|-------------|---------|-----------|
| | Center | Upper Right | Upper Left | Lower Left | Lower Right | PV | Deviation |
| A 292 | 520.67 | 498.00 | 450.00 | 472.67 | 517.33 | 491.73 | 30.15 |
| A 293 | 524.00 | 498.00 | 449.33 | 480.67 | 520.67 | 494.53 | 30.82 |
| A 294 | 514.67 | 492.67 | 435.33 | 465.33 | 514.00 | 484.40 | 34.03 |
| A 295 | 521.33 | 490.00 | 452.67 | 476.67 | 515.33 | 491.20 | 28.23 |
| A 285 | 516.67 | 494.00 | 512.00 | 524.67 | 515.33 | 512.53 | 11.36 |
| A 286 | 520.67 | 516.00 | 516.00 | 523.33 | 530.00 | 521.20 | 5.84 |
| A 288 | 518.67 | 504.67 | 518.00 | 528.00 | 519.33 | 517.73 | 8.36 |
| A 290 | 522.00 | 506.00 | 518.67 | 523.33 | 530.00 | 520.00 | 8.84 |

Acceptable: **Yes**



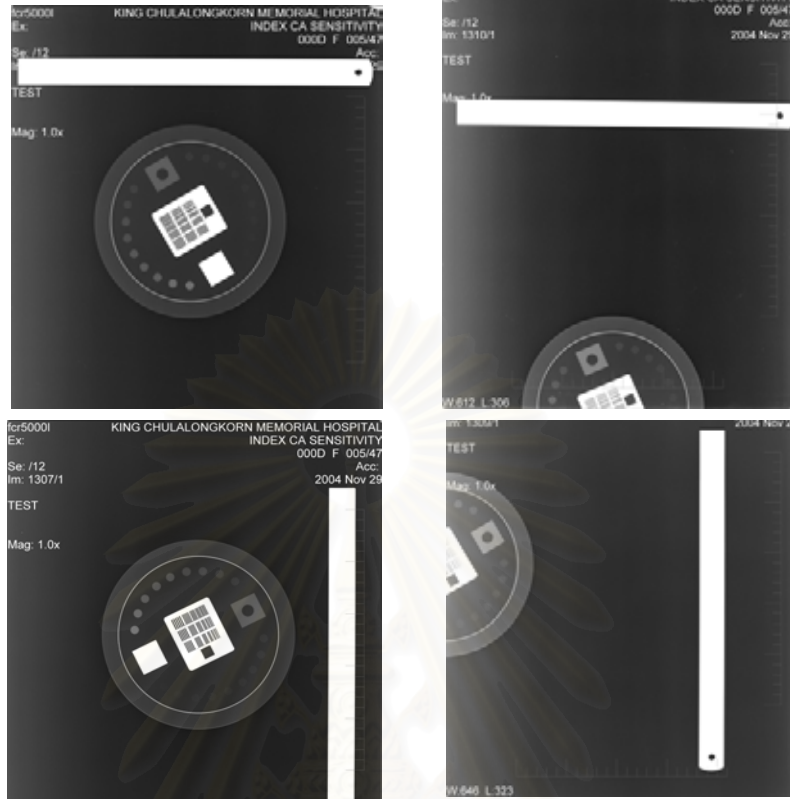
| 6.Uniformity | #1 - #3 | Uniformity | #4- #5 |
|-------------------|---------|-------------------------|--------|
| Menu = TEST | | Menu = TEST | |
| SubMenu = AVE 1.0 | | SubMenu = AVE 2.0 | |
| L= 1, EDR = semi | | L= 2, EDR = fix "S" 200 | |

| UNIFORMITY | | | | | | | | |
|-----------------|------------|------------|------------|----------|----------|---------|-----|----------|
| kV _p | Filtration | Focal spot | Time delay | SID (cm) | SMD (cm) | Nom. mR | mAs | mR-meter |
| 80 | None | 1.2 mm | ~ 6 min | 150 | 120 | 5 | 1 | 1.5 |

| Study No. | Cassette | | Cassette Serial Number | Defect Free? (Y/N) | Sensitivity value | Latitude value | Average Pixel Value | Standard Deviation |
|-----------|-----------|----------|------------------------|--------------------|-------------------|----------------|---------------------|--------------------|
| | Type/Size | | | | | | | |
| #1 | A 302 | ST 14x17 | A 09234116 | Y | 84 | 1.00 | 493.72 | 27.07 |
| #2 | A 303 | | A 09234079 | Y | 82 | 1.00 | 494.72 | 23.53 |
| #3 | A 304 | | A 09234062 | Y | 80 | 1.00 | 484 | 19.23 |
| #4 | A 305 | | A 09234079 | Y | 200 | 2.00 | 700.32 | 13.35 |
| #5 | A 306 | | A 09234062 | Y | 200 | 2.00 | 695.36 | 11.77 |

| Study No. | | Pixel value | | | | | | Average | SD |
|-----------|-------|-------------|-------|-------|-------|-------|--------|---------|----|
| | | UR | UL | LL | LR | C | | | |
| #1 | A 302 | 499.2 | 468 | 459 | 510.4 | 532 | 493.72 | 27.07 | |
| #2 | A 303 | 504.8 | 457.6 | 470.4 | 512.8 | 528 | 494.72 | 23.53 | |
| #3 | A 304 | 492.8 | 455.2 | 457.6 | 503.2 | 511.2 | 484 | 19.23 | |
| #4 | A 305 | 704.8 | 680.8 | 684.8 | 712 | 719.2 | 700.32 | 13.35 | |
| #5 | A 306 | 705.6 | 676 | 677.6 | 705.6 | 712 | 695.36 | 11.77 | |

Acceptable: **Yes**

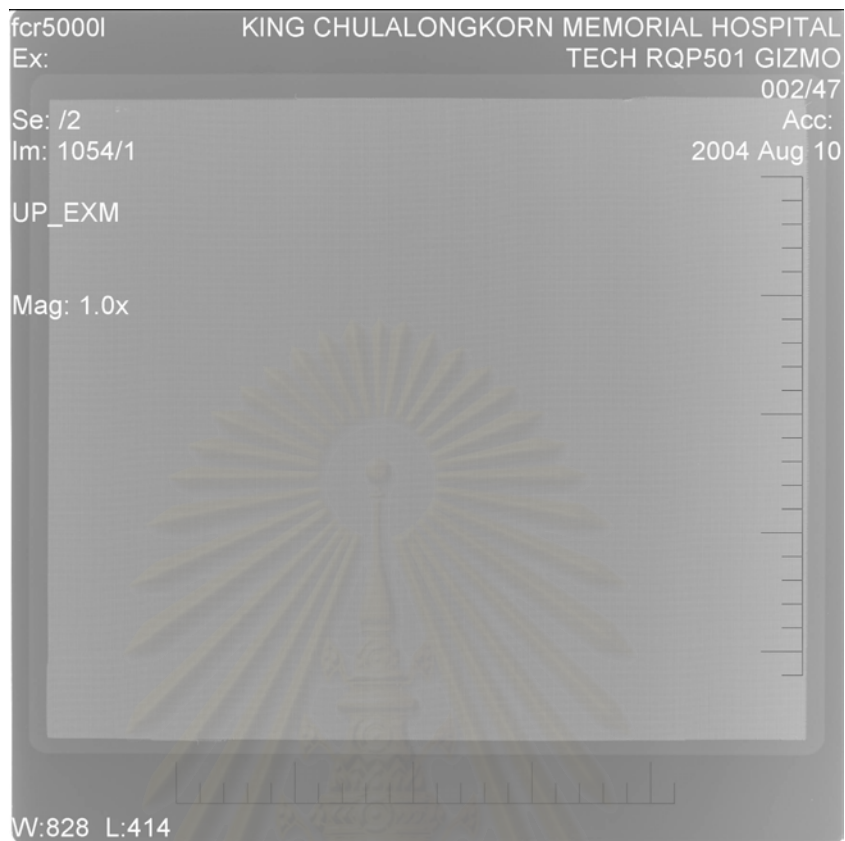


| |
|-------------------------|
| 7. Scaling error |
| Menu = TEST |
| SubMenu = Sensitivity |
| L = 1, EDR = semi |

| Scaling error | | | | | | | | |
|---------------|-----------------|------------|-----------------|------------|----------|-----|-----------|-----------|
| IP No. | kV _p | Filtration | Focal spot (mm) | Time delay | SID (cm) | mAs | S - value | Nom. mR |
| A 09234079 | 50/ 200/ 0.05 | None | 1.2 | None | 150 | 9 | 210/1.00 | 0.61 |
| A 09234062 | 50 | None | 1.2 | None | 150 | 9 | 200/1.00 | 0.64 |
| A 09234079 | 50 | None | 1.2 | None | 150 | 9 | 100/1.00 | 1.28 |
| A 09234062 | 50 | None | 1.2 | None | 150 | 9 | 98/1.00 | 1.3061224 |

| IP No. | x -distance | y - distance | x / y ratio |
|------------|-------------|--------------|-------------|
| A 09234079 | 18.22 | 18.19 | 1.0014657 |
| A 09234079 | 18.09 | 18.18 | 0.9950495 |

| | |
|-------------|------------|
| Acceptable: | Yes |
|-------------|------------|



8. Blurring

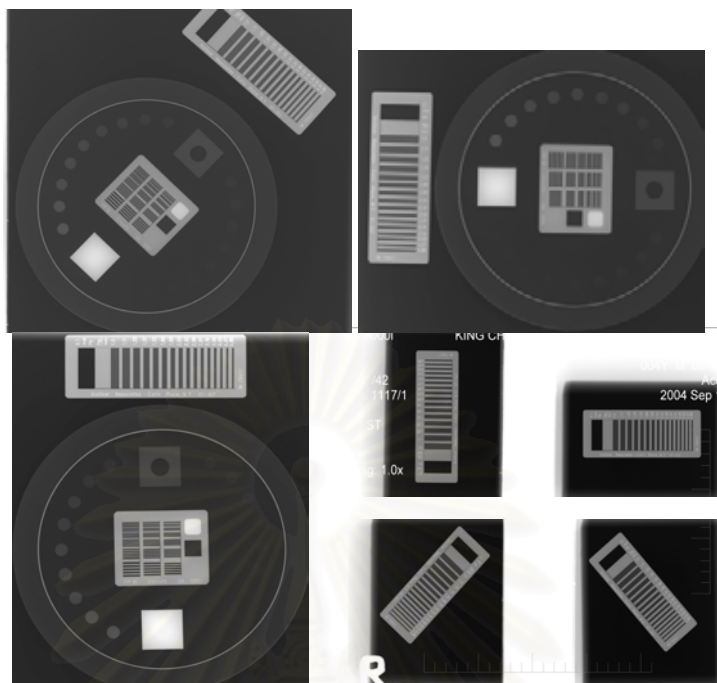
Menu = TEST

SubMenu = Sensitivity

L = 1, EDR = semi

| Blurring | | | | | | | | | |
|-----------|------------|-----------------|------------|-----------------|------------|----------|-----------|---------|-------------------------|
| Study No. | IP No. | kV _p | Filtration | Focal spot (mm) | Time delay | SID (cm) | S - value | Nom. mR | Fine mesh uniform (Y/N) |
| A 1259 | A 09234185 | 50 | None | 1.2 | None | 180 | 449 | 0.45 | Y |
| A 1260 | A 09234116 | 50 | None | 1.2 | None | 180 | 439 | 0.46 | Y |
| A 1261 | A 09234079 | 50 | None | 1.2 | None | 180 | 449 | 0.45 | Y |

Acceptable: **Yes**



9. Limiting Spatial Resolution

Menu = TEST

SubMenu = AVE 2.0

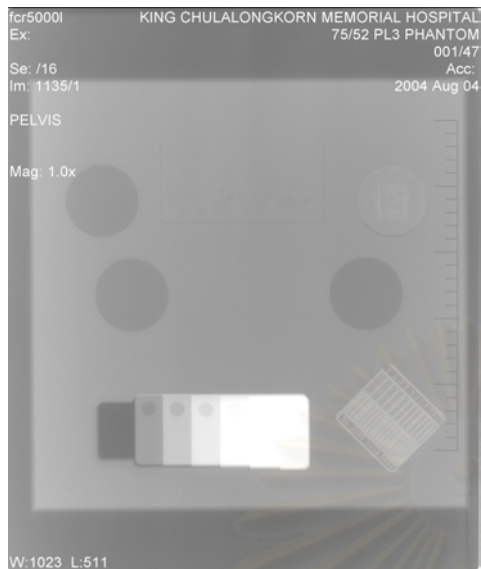
L= 2, EDR = fix 200

Display Condition: Max zoom and Contrast on the HIC display.

| Limiting Spatial Resolution | | | | | | | Display Condition: |
|-----------------------------|-----------------|------------|------------|---------|------|--|--------------------|
| study No. | kV _p | Filtration | Focal spot | SID(cm) | mAs | | |
| # 1 | 50 | none | 1.2 | 180 | ~ 10 | Max zoom 180 % and Contrast on the HIC display. | |
| # 2 | 50 | none | 1.2 | 180 | ~ 10 | | |
| # 3 | 50 | none | 1.2 | 180 | ~ 10 | | |

| IP | | Pixel Size | Nyquist frequency | Expected | Laser scan | Plate scan | Laser scan | Plate scan |
|-----------|------------|------------|-------------------|----------|------------|------------|------------|------------|
| Type/Size | S.N. | (mm) | (lp/mm) | Response | lp/mm | lp/mm | % diff | % diff |
| ST 14x17 | A 09234079 | 0.17 | 2.94 | 2.5 | 2.58 | 2.48 | 0.03 | -0.01 |
| ST 14x17 | A 09234116 | 0.17 | 2.94 | 2.5 | 2.58 | 2.48 | 0.03 | -0.01 |
| ST 14x17 | A 09234062 | 0.17 | 2.94 | 2.5 | 2.58 | 2.48 | 0.03 | -0.01 |
| ST 14x17 | A 09234079 | 0.17 | 2.94 | 2.5 | 2.58 | 2.48 | 0.03 | -0.01 |
| ST 10x12 | A 09252189 | 0.12 | 4.17 | 3.3 | 3.13 | 3.27 | -0.05 | -0.01 |
| ST 10x12 | A 09251960 | 0.12 | 4.17 | 3.3 | 3.13 | 3.27 | -0.05 | -0.01 |

Acceptable: **Yes**



10. TCDD

Menu = TEST

SubMenu = Sensitivity

L= 1, EDR = semi

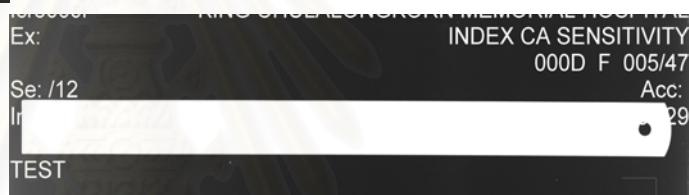
| study No. | IP No. | kV _p | mAs | Filtration (mmAl) | Focal spot (mm) | Time delay | SID (cm) | S - value | Nom. μ Gy |
|-----------|------------|-----------------|-----|-------------------|-----------------|------------|----------|-----------|---------------|
| A 004 | A 09234079 | 75 /100 /0.02 | 2.0 | 5 | 1.2 | None | 150 | 365 | 4.77 |
| A 005 | A 09234079 | 75 /50/0.01 | 0.5 | 5 | 1.2 | None | 150 | 1236 | 1.41 |
| A 006 | A 09234079 | 75 /200 /0.04 | 9.0 | 5 | 1.2 | None | 150 | 132 | 13.18 |

| Soft copy visualize | | zoom 150% |
|----------------------|---------------------|-----------|
| High contrast object | Low contrast object | lp/mm |
| 9 | 8 | 15 |
| 9 | 7 | 15 |
| 9 | 8 | 16 |

Acceptable: **Yes**



| |
|--------------------------------|
| 11. Laser beam function |
| Menu = TEST |
| SubMenu = Sensitivity |
| L= 1, EDR = semi |
| IP Type/Size 3 IPs |



| IP | IP | kV _p | Filtration | Focal spot | SID (cm) | Nom. μ Gy | mAs | Magnify |
|-----------|------------|-----------------|------------|------------|----------|---------------|-----|---------|
| Type/Size | S.N. | 80 | none | 1.2 | 150 | 50 | | x 10 |
| ST 14x17 | A 09234062 | 125/0.03 | Y | 1.2 | 150 | 42.9762 | 4 | 400% |
| ST 14x17 | A 09234079 | 125/0.03 | Y | 1.2 | 150 | 42.9762 | 4 | 400% |
| ST 14x17 | A 09234062 | 125/0.03 | Y | 1.2 | 150 | 42.9762 | 4 | 400% |
| ST 10x12 | A 09252158 | 200/0.02 | Y | 1.2 | 150 | 42.0872 | 5 | 400% |
| ST 10x12 | A 09251953 | 200/0.02 | Y | 1.2 | 150 | 42.0872 | 5 | 400% |
| ST 10x12 | A 09252158 | 200/0.02 | Y | 1.2 | 150 | 42.0872 | 5 | 400% |

| | |
|-------------------------------------|-----|
| Ruler edge straight and continuous? | Yes |
| Beam jitters absent? | Yes |
| Signal dropouts absent? | Yes |

Acceptable: **Yes**



12. Moiré Patterns

Menu = TEST

SubMenu = Contrast

L= 1, EDR = Semi

| kV _p | Filtration | Focal spot | SID (cm) | Nom. μ Gy | mAs |
|-----------------|------------|------------|----------|---------------|--------|
| 70 | 1.5 mmCu | 1.2 mm | 150 | 10 | varies |

| Grid direction | Study No. | IP Type/Size | Stationary Grid | | | | S-value |
|----------------|-----------|--------------------------------|-----------------|--------------------------------|------------|---|---------|
| | | | Grid ratio | | Grid freq. | | |
| | | | 12:1 | | 80 | | |
| | | Grid Direction with Laser scan | | Grid Direction with Plate scan | | | |
| | | Perpend | Parallel | Perpend | Parallel | | |
| longitudinal | A 013 | ST 14x17 70/250/0.1/25 mAs | Y | Y | Y | Y | 762 |
| horizontal | A 014 | ST 14x17 70/250/0.1/25 mAs | Y | Y | Y | Y | 649 |
| longitudinal | A 015 | ST 10x12 70/200/0.2/42mAs | Y | Y | Y | Y | 745 |
| horizontal | A 016 | ST 10x12 70/200/0.2/42mAs | Y | Y | Y | Y | 762 |

Acceptable: **No**

| Table 35. Image Display Device Constancy Test Report (regular test) | | |
|--|---|--|
| Image display device | Model: TOTOKU; Japan | Serial No. |
| | Marker: Fuji Photo Film Co.,Ltd. | Category: <input type="checkbox"/> A <input type="checkbox"/> B <input type="checkbox"/> C |
| | Type: <input checked="" type="checkbox"/> Black-and-white <input type="checkbox"/> Color <input type="checkbox"/> CRT <input checked="" type="checkbox"/> LCD | |
| Installed at | Out-patient diagnostic radiology (PPR. Building 4 th floor) King Chulalongkorn Memorial Hospital, Thai Red Cross Society | |
| Luminance meter | Model: 352 | Serial No. 56073 |
| | Maker: GAMMEX-RMI BMBH; Germany | |
| Test date: December 8, 2004 | Tested by: Petcharleeya Suwanpradit/ Assoc.Prof.Dr. Anchali Krisanachinda | |
| Objective: <input type="checkbox"/> Routine constancy test <input checked="" type="checkbox"/> First constancy test (for determination of baseline values) | | |
| 1. Visual inspection of viewing condition | Reflected luminance spot: <input checked="" type="checkbox"/> None <input type="checkbox"/> Present | |
| | Light source within visual field: <input type="checkbox"/> None <input checked="" type="checkbox"/> Present | |
| | Judgment: <input checked="" type="checkbox"/> PASS <input type="checkbox"/> FAIL <input type="checkbox"/> Not executed. | |
| 2. Measurement of reflected luminance | Reflected luminance = 23.2 L x at 1 meter from monitor | |
| | Judgment: <input type="checkbox"/> PASS <input type="checkbox"/> FAIL <input type="checkbox"/> Not executed <input type="checkbox"/> Baseline values are used. | |
| 3. Measurement of luminance uniformity | Center luminance = 50.5 cd/m ² | |
| | Upper left luminance = 45.7 cd/m ² , Upper left luminance = 90.50 % | |
| | Upper right luminance = 45.7 cd/m ² , Upper right luminance = 90.50 % | |
| | Lower left luminance = 49.0 cd/m ² , Lower left luminance = 97.03 % | |
| | Lower right luminance = 46.8 cd/m ² , Upper right luminance = 92.67 % | |
| | Judgment: <input type="checkbox"/> PASS <input type="checkbox"/> FAIL <input type="checkbox"/> Not executed <input type="checkbox"/> Baseline values are used. | |

| Table 36. Viewbox Constancy Test Report | |
|---|---|
| Installed at: <i>Film Reading Room</i> | Out-patient diagnostic radiology (PPR. Building 4 th floor) King Chulalongkorn Memorial Hospital, Thai Red Cross Society |
| 1. Visual inspection of viewing condition | Reflected luminance spot: <input checked="" type="checkbox"/> None <input type="checkbox"/> Present Light source within visual field: <input type="checkbox"/> None <input checked="" type="checkbox"/> Present Judgment: <input checked="" type="checkbox"/> PASS <input type="checkbox"/> FAIL <input type="checkbox"/> Not executed. |
| 2. Measurement of reflected luminance | Reflected luminance = 137 L x at 1 meter from viewbox Judgment: <input type="checkbox"/> PASS <input type="checkbox"/> FAIL <input type="checkbox"/> Not executed <input type="checkbox"/> Baseline values are used. |
| 3. Measurement of luminance uniformity | Viewbox No.1 Center luminance = 898 cd/m² Upper left luminance = 583 cd/m² , Upper left luminance = 64.92% Upper right luminance = 650 cd/m² , Upper right luminance = 72.38% Lower left luminance = 698 cd/m² , Lower left luminance = 77.73% Lower right luminance = 722 cd/m² , Upper right luminance = 80.40% Viewbox No.2 Center luminance = 1314 cd/m² Upper left luminance = 1002 cd/m² , Upper left luminance = 76.26% Upper right luminance = 960 cd/m² , Upper right luminance = 73.06% Lower left luminance = 1062 cd/m² , Lower left luminance = 80.82% Lower right luminance = 1089 cd/m² , Upper right luminance = 82.88% Judgment: <input type="checkbox"/> PASS <input type="checkbox"/> FAIL <input type="checkbox"/> Not executed <input type="checkbox"/> Baseline values are used. |
| Installed at: <i>Film Checking Room</i> | Out-patient diagnostic radiology (PPR. Building 4 th floor) King Chulalongkorn Memorial Hospital, Thai Red Cross Society |
| 1. Visual inspection of viewing condition | Reflected luminance spot: <input checked="" type="checkbox"/> None <input type="checkbox"/> Present Light source within visual field: <input type="checkbox"/> None <input checked="" type="checkbox"/> Present Judgment: <input checked="" type="checkbox"/> PASS <input type="checkbox"/> FAIL <input type="checkbox"/> Not executed. |
| 2. Measurement of reflected luminance | Reflected luminance = 137 L x at 1 meter from viewbox Judgment: <input type="checkbox"/> PASS <input type="checkbox"/> FAIL <input type="checkbox"/> Not executed <input type="checkbox"/> Baseline values are used. |
| 3. Measurement of luminance uniformity | Viewbox No.1 Center luminance = 898 cd/m² Upper left luminance = 583 cd/m² , Upper left luminance = 64.92% Upper right luminance = 650 cd/m² , Upper right luminance = 72.38% Lower left luminance = 698 cd/m² , Lower left luminance = 77.73% Lower right luminance = 722 cd/m² , Upper right luminance = 80.40% Viewbox No.2 Center luminance = 1314 cd/m² Upper left luminance = 1002 cd/m² , Upper left luminance = 76.26% Upper right luminance = 960 cd/m² , Upper right luminance = 73.06% Lower left luminance = 1062 cd/m² , Lower left luminance = 80.82% Lower right luminance = 1089 cd/m² , Upper right luminance = 82.88% Judgment: <input type="checkbox"/> PASS <input type="checkbox"/> FAIL <input type="checkbox"/> Not executed <input type="checkbox"/> Baseline values are used. |

APPENDIX C

Table 37. Approaches to Reference Levels (September 2001)

| Document | Exam Type: Measured Quantity | Selection | Purpose |
|---|---|--|---|
| ICRP 73 (1996) Radiological Protection and Safety in Medicine. ICRP Publication 73. International Commission on Radiological Protection (1996) | Diagnostic radiology (common exams & broadly defined types of equipment); easily measured quantity (for radiology, absorbed dose in air or in tissue-equivalent material at surface of a simple standard phantom or representative patient) | professional medical bodies; percentile point on observed distribution for patients; specific to country or region | advisory: form of investigation level, identify unusually high levels; in principle, lower level also; not for regulatory or commercial purposes; not a dose constraint; not linked to limits or constraints |
| IAEA (1996) International Basic Safety Standards Protection against Ionizing Radiation and for the Safety of Radiation Sources, Safety Series No. 115, International Atomic Energy Agency (1996) | <u>Radiographs</u> ESD in mGy (for film-screen combinations with relative speed 200; reduce by factor of 2 to 3 for film speed 400-600) | derived from wide- scale surveys for typical adults | corrective actions if doses fall substantially below levels with no useful information or medical benefit or if doses exceed levels. |
| EC (1999a) (General) Guidance on DRLs for Medical Exposures Radiation Protection 109 Directorate General, Environment, Nuclear Safety and Civil Protection. European Commission (1999) | <u>radiographs</u> : ESD in mGy | <u>radiography</u> : 3rd quartile values from; European surveys. | x-ray examinations : groups of standard-sized patients or phantoms, broadly defined types of equipment ;levels expected not to be exceeded when good and normal practice is applied; when consistently exceeded, review procedures and equipment |
| AAPM (1999) (General, U.S.) Reference Values Applications and Impact in Radiology. American Association of Physicists in Medicine Task Group (November 1999 Draft) | <u>radiographs</u> : ESAK in mGy (ESE in mR) ; measurements in air, no <u>phantom</u> | derived from 75th or 80th percentile of U.S. survey data | non-regulatory: to assist medical professionals in evaluating exposure levels; if exceeded, facility investigates reason; reduce, if possible without sacrificing image quality. |
| Note 2: Nordic (1996). Nordic Guidance Levels for Patient Doses in Diagnostic Radiology. Report on Nordic Radiation Protection Co-operation No. 5 (Denmark, Finland, Iceland, Norway and Sweden) SSK (2000). | | | |

Table 38. Listing of Dose Reference Levels (DRL; September 2001)

| Medical Imaging Task | (General U.S.) CRCPD 1988 | (General U.K.) IPSM 1992 | (BSS) IAEA 1996 | (General) EC 1990,1996a, 1999a | (General,U.S.) AAPM 1999 | (General) NRPB 1999 |
|--|----------------------------------|--------------------------------|-----------------------|--------------------------------------|--|---------------------------|
| Radiographs [values are ESD in mGy, except as noted for CRCPD, AAPM and NRPB] [NOTE: CRCPD entries were converted from ESE in mR (x 0.00876) to ESAK in mGy] | | | | | | |
| -AP Dental | [ESAK in mGy] | | 5 | | [ESAK in mGy] | |
| -Dental Cephalometry | 0,3 | | | | 0,25 | |
| -PA or AP Skull | | 5 | 5 | 5 | | 5, 1.5 |
| -LAT Skull | 1.3, 0.6 | 3 | 3 | 3 | | 3, 1 |
| -AP Cervical Spine | 1.2, 0.8 | | | | 1,25 | |
| - PA Chest | 0.1, 0.04 no grid | 0,3 | 0,4 | 0,3 | 0,25 | 0,3 |
| | 0.2, 0.1 grid | | | | | |
| - AP Abdomen | 4.3, 2.6 | 10 | 10 | | 4,5 | 10, 6 |
| - AP or PA Lumbar Spine | 3.9, 3.1 | 10 | 10 | 10 | 5 | 10, 5 |
| - LAT Lumbar Spine (lumbo-sacral joint) | [two film speeds: 200, then 400] | 30 40 | 30 40 | 30 40 | | 30, 12 40, 24 |
| - AP Pelvis | | 10 | 10 | 10 | | 10, 4 |
| [NOTE: EC 1999a gives values for several other countries. EC 1999a and SSK 2000 give a set of values for children.] | | | | | | |
| List of Symbols and Acronyms: ESD - entrance surface dose (includes backscatter) ESD rate - entrance surface dose rate (includes backscatter) ESAK - entrance surface air kerma (free-in-air) PED - patient entrance dose (free-in-air) ESE - entrance skin exposure (free-in-air) | | | | | AP - anterioposterior PA – posteroanterior LAT – lateral | |

APPENDIX D

Table 39. Image Quality Grading Forms

| | |
|--|------------|
| Chest pa | 1 |
| Patient identification | 106229/29 |
| Positioning criteria | |
| 1. Performed at full inspiration (as assessed by the position of the ribs above the diaphragm-- either 6 anteriorly or 10 posteriorly) and with suspended respiration. | 1 |
| 2. Symetrical reproduction of the thorax, as shown by the central position of a spinous process between the medial ends of the clavicles. | 1 |
| 3. Medial border of the scapulae to be outside the lung fields. | 0.5 |
| 4. Reproduction of the whole rib cage above the diaphragm. | 0.5 |
| Total: | 3 |
| Image quality | |
| 1. Visually sharp reproduction of the vascular pattern of the lungs, particularly the peripheral vessels. | 1 |
| 2. Visually sharp reproduction of the trachea and proximal bronchi | 0.5 |
| 3. Visually sharp reproduction of the borders of the heart and the aorta | 1 |
| 4. Visually sharp reproduction of the diaphragm and lateral costophrenic angles | 1 |
| 5. Visualization of the retrocardiac lung and the mediastinum. | 0.5 |
| 6. Visualization of the spine through the heart shadow. | 0.5 |
| Important image details **: Small round details in the whole lung, including the retrocardiac areas: High contrast: 0.7 mm; low contrast: 2 mm diameter | 1 |
| High contrast: 0.7 mm; low contrast: 2 mm diameter high contrast: 0.3 mm; low contrast: 2 mm in width | 1 |
| Total: | 6.5 |
| Rate image noise (1-5 scale ***) | 3 |
| Rate overall diagnostic image quality (1-5 scale ***) | 5 |

สถาบันวิทยบริการ
จุฬาลงกรณ์มหาวิทยาลัย

| | |
|---|-----------|
| Lumbar Spine ap/pa | 1 |
| Patient identification | 106229/29 |
| Image quality | |
| 1. Visually sharp reproduction of the upper and lower-plate surfaces, represented as lines in the centred beam area | 0.5 |
| 2. Visually sharp reproduction of the pedicles | 1 |
| 3. Reproduction of the intervertebral joints | 0.5 |
| 4. Reproduction of the spinous and transverse processes | 0.5 |
| 5. Visually sharp reproduction of the cortex and trabecular structures | 0.5 |
| 6. Reproduction of the adjacent soft tissues, particularly the psoas shadows | 0.5 |
| 7. Reproduction of the sacro-iliac joints | 0.5 |
| Image details at 3rd lumbar vertebral body: details with 0.3 - 0.5 mm in width clearly visible ** | 0.5 |
| Total: | 4.5 |
| Rate image noise (1-5 scale ***) | 2 |
| Rate overall diagnostic image quality (1-5 scale ***) | 3 |

| | |
|---|----------|
| Abdomen ap | 1 |
| Patient identification | 77507/43 |
| Positioning criteria | |
| 1. Image includes the area from the upper border of the pubic symphysis to the diaphragm | 0.5 |
| 2. Vertebral column in the center of the radiograph | 1 |
| 3. Ribs, pelvis, and hips equidistant to the edge of the radiograph | 1 |
| 4. Spinous processes in the center of the vertebral column | 1 |
| 5. Iliac wings symmetric | 1 |
| 6. Ischial spines symmetric | 1 |
| Total | 5.5 |
| Image Quality | |
| 1. No motion | 1 |
| 2. Sharp visualisation of ribs and gas bubble margins | 1 |
| 3. Visualisation of lateral abdominal wall and the peritoneal fat layer | 1 |
| 4. Visualisation of lower margin of liver and spleen, kidneys, the lateral borders of psoas muscles | 1 |
| 5. Visualisation of kidneys | 1 |
| 6. Visualisation of the lateral borders of psoas muscles | 1 |
| 7. Visualisation of ribs and transverse processes of lumbar vertebrae | 1 |
| 8. Markers indicating either upright or supine position | 1 |
| Total | 8 |
| Rate image noise (1-5 scale ***) | |
| Rate overall diagnostic image quality (1-5 scale ***) | |

| | |
|--|-----------|
| Lumbar Spine lat | 1 |
| Patient identification | 106229/29 |
| 1. Visually sharp reproduction of the upper and lower-plate surfaces, represented as lines with the resultant visualization of the intervertebral spaces | 0.5 |
| 2. Full superimposition of the posterior vertebral edges | 1 |
| 3. Reproduction of the pedicles and intervertebral foramina | 1 |
| 4. Visualization of the spinous processes | 1 |
| 5. Visually sharp reproduction of the cortex and trabecular structures | 0.5 |
| 6. Visually sharp reproduction of the vertebral bodies in the thoracolumbar area | 0.5 |
| Important image details**: Image details at 3rd lumbar vertebral body, ventral edge: 0.5 mm in width clearly visible | 0.5 |
| Total: | 5 |
| Rate image noise (1-5 scale ***) | 2 |
| Rate overall diagnostic image quality (1-5 scale ***) | 4 |

สถาบันวิทยบริการ
จุฬาลงกรณ์มหาวิทยาลัย

Table 40. Exposure factors chart

| Exam Part | Average BMI | Average Body Part Thickness (cm) | kVp | mA | Time (s) | mAs | FFD | Grid |
|---------------|-------------|----------------------------------|-----|-----|----------|-----|-----|------|
| Skull PA(PNS) | 16-25 | 15 - 19 | 70 | 200 | 0.16 | 32 | 100 | Yes |
| | | 20 - 23 | 75 | 200 | 0.20 | 32 | 100 | Yes |
| | 26-35 | 15 - 19 | 70 | 200 | 0.20 | 40 | 100 | Yes |
| | | 20 - 23 | 75 | 200 | 0.20 | 40 | 100 | Yes |
| Ceph lat | 16-25 | 13 - 17 | 75 | 10 | 1.00 | 10 | 150 | No |
| | | 18 - 22 | 78 | 10 | 1.00 | 10 | 150 | No |
| | 26-35 | 13 - 17 | 75 | 10 | 1.00 | 10 | 150 | No |
| | | 18 - 22 | 78 | 10 | 1.00 | 10 | 150 | No |
| C spine AP | 16-25 | 7 --11 | 66 | 200 | 0.06 | 12 | 180 | No |
| | | 12 -- 16 | 68 | 200 | 0.07 | 14 | 180 | No |
| | 26-35 | 7 --11 | 68 | 200 | 0.06 | 12 | 180 | No |
| | | 12 -- 16 | 70 | 200 | 0.07 | 14 | 180 | No |
| Chest PA | 16-25 | 14 - 17 | 68 | 200 | 0.04 | 8 | 180 | No |
| | | 18 - 21 | 70 | 200 | 0.05 | 10 | 180 | No |
| | | 22 - 25 | 73 | 250 | 0.05 | 13 | 180 | No |
| | | 26 - 29 | 75 | 250 | 0.06 | 15 | 180 | No |
| | | 30 - 33 | 78 | 250 | 0.06 | 15 | 180 | No |
| | 26-35 | 14 - 17 | 68 | 250 | 0.04 | 10 | 180 | No |
| | | 18 - 21 | 70 | 250 | 0.05 | 13 | 180 | No |
| | | 22 - 25 | 75 | 250 | 0.06 | 15 | 180 | No |
| | | 26 - 29 | 80 | 250 | 0.06 | 15 | 180 | No |
| | | 30 - 33 | 80 | 250 | 0.07 | 18 | 180 | No |
| Abdomen AP | 16-25 | 14 - 17 | 75 | 200 | 0.20 | 40 | 100 | Yes |
| | | 18 - 21 | 75 | 200 | 0.25 | 50 | 100 | Yes |
| | | 22 - 25 | 75 | 200 | 0.25 | 50 | 100 | Yes |
| | | 26 - 29 | 78 | 200 | 0.25 | 50 | 100 | Yes |
| | | 30 - 33 | 78 | 200 | 0.32 | 66 | 100 | Yes |

| Exam Part | Average BMI | Average Body Part Thickness (cm) | kVp | mA | Time (s) | mAs | FFD | Grid |
|---------------|-------------|----------------------------------|-----|-----|----------|-----|-----|------|
| Abdomen AP | 26-35 | 14 - 17 | 70 | 200 | 0.25 | 50 | 100 | Yes |
| | | 18 - 21 | 75 | 200 | 0.05 | 50 | 100 | Yes |
| | | 22 - 25 | 75 | 200 | 0.32 | 66 | 100 | Yes |
| | | 26 - 29 | 80 | 200 | 0.32 | 66 | 100 | Yes |
| | | 30 - 33 | 80 | 200 | 0.40 | 80 | 100 | Yes |
| L-S spine AP | 16-25 | 14 - 17 | 75 | 200 | 0.20 | 40 | 100 | Yes |
| | | 18 - 21 | 75 | 200 | 0.25 | 50 | 100 | Yes |
| | | 22 - 25 | 75 | 200 | 0.25 | 50 | 100 | Yes |
| | | 26 - 29 | 78 | 200 | 0.25 | 50 | 100 | Yes |
| | | 30 - 33 | 80 | 200 | 0.32 | 66 | 100 | Yes |
| | 26-35 | 14 - 17 | 70 | 200 | 0.25 | 50 | 100 | Yes |
| | | 18 - 21 | 75 | 200 | 0.25 | 50 | 100 | Yes |
| | | 22 - 25 | 75 | 200 | 0.32 | 66 | 100 | Yes |
| | | 26 - 29 | 80 | 200 | 0.32 | 66 | 100 | Yes |
| | | 30 - 33 | 80 | 200 | 0.40 | 80 | 100 | Yes |
| L-S spine lat | 16-25 | 14 - 17 | 85 | 200 | 0.32 | 65 | 100 | Yes |
| | | 18 - 21 | 85 | 200 | 0.40 | 80 | 100 | Yes |
| | | 22 - 25 | 85 | 200 | 0.50 | 100 | 100 | Yes |
| | | 26 - 29 | 85 | 200 | 0.50 | 100 | 100 | Yes |
| | | 30 - 33 | 90 | 250 | 0.50 | 125 | 100 | Yes |
| | 26-35 | 14 - 17 | 85 | 200 | 0.32 | 65 | 100 | Yes |
| | | 18 - 21 | 85 | 200 | 0.40 | 80 | 100 | Yes |
| | | 22 - 25 | 85 | 200 | 0.50 | 100 | 100 | Yes |
| | | 26 - 29 | 87 | 250 | 0.50 | 125 | 100 | Yes |
| | | 30 - 33 | 93 | 250 | 0.63 | 159 | 100 | Yes |
| Pelvis AP | 16-25 | 14 - 21 | 70 | 200 | 0.20 | 40 | 100 | Yes |
| | | 22 - 30 | 75 | 200 | 0.25 | 50 | 101 | Yes |
| | 26-35 | 14 - 21 | 70 | 200 | 0.20 | 40 | 102 | Yes |
| | | 22 - 30 | 75 | 200 | 0.25 | 50 | 103 | Yes |

APPENDIX E

ข้อมูลสำหรับผู้ป่วย (Patient Information Sheet)

การศึกษาทางห้องปฏิบัติการ: การควบคุมคุณภาพของระบบคอมพิวเตอร์ควบคุมการแสดงผลภาพรังสี

เรียน ผู้ป่วยทุกท่าน

ท่านเป็นผู้ที่ได้เข้ารับบริการการถ่ายภาพทางรังสีทั่วไปของหน่วยงานเอกซเรย์ผู้ป่วยนอก ตึก ภปร. ชั้น 4 ท่านเป็นผู้ได้รับเชิญจากนักรังสีการแพทย์ นักฟิสิกส์การแพทย์และรังสีแพทย์ให้เข้าร่วมการศึกษาวิจัยถึงปริมาณรังสีที่ท่านจะได้รับ รวมถึงการประเมินคุณภาพของภาพรังสีภายหลังจากเข้ารับบริการการถ่ายภาพทางรังสีทั่วไป ก่อนที่ท่านจะตกลงเข้าร่วมการศึกษาดังกล่าว ขอเรียนให้ท่านทราบถึงเหตุผลและรายละเอียดของการศึกษาวิจัยในครั้งนี้

ในปัจจุบันนี้ การเข้ารับบริการการถ่ายภาพทางรังสีทั่วไป ณ หน่วยงานเอกซเรย์ผู้ป่วยนอก ตึก ภปร. ชั้น 4 ได้มีการนำเครื่องมือที่มีเทคโนโลยีสูงเข้ามาช่วยในการบริการการถ่ายภาพทางรังสีทั่วไปแก่ผู้ป่วย คือเครื่อง Computed Radiography (CR) ทำให้การบริการเป็นไปด้วยความรวดเร็วยิ่งขึ้น สามารถปรับแต่งคุณภาพของภาพรังสีให้พอเหมาะแก่การวินิจฉัยโรคมายังขึ้นสามารถบริหารจัดการข้อมูลภาพเข้าสู่โครงข่ายคอมพิวเตอร์ของภายในฝ่ายรังสีวิทยาและภายในโรงพยาบาลจุฬาลงกรณ์ สภากาชาดไทยได้ ซึ่งจะเป็นประโยชน์ต่อท่านเมื่อเข้ารับบริการการตรวจวินิจฉัยและรักษากับโรงพยาบาลฯ ในอนาคต

ในการนำเครื่อง CR มาใช้งานการถ่ายภาพทางรังสีทั่วไปนี้ ทั้งนักรังสีการแพทย์ นักฟิสิกส์การแพทย์และรังสีแพทย์ คาดหวังว่าจะสามารถลดปัญหาการถ่ายภาพรังสีซ้ำอันเนื่องมาจากความบกพร่องของเครื่องมือและอุปกรณ์ร่วม ซึ่งย่อมเป็นการลดปริมาณรังสีที่ผู้ป่วยจะได้รับให้น้อยลง ลงไว้ซึ่งคุณภาพของภาพรังสีที่ยังเป็นที่ยอมรับของรังสีแพทย์และแพทย์ผู้ทำการตรวจรักษา มีการใช้ปริมาณรังสีเท่าที่จำเป็น ซึ่งเป็นมาตรการป้องกันอันตรายจากรังสีโดยตรงที่ทุกคนและทุกหน่วยงานที่เกี่ยวข้องกับรังสีตระหนักเป็นอย่างดี ดังนั้น จึงเกิดแนวคิดในการควบคุมคุณภาพของเครื่อง Computed Radiography (CR) และอุปกรณ์ร่วม เพื่อป้องกันปัญหาและข้อบกพร่องที่จะเกิดกับเครื่อง อันจะส่งผลถึงการใช้ปริมาณรังสีและการสร้างคุณภาพของภาพรังสี รวมทั้งจัดการ- ปรับปรุงแก้ไขให้เครื่องอยู่ในมาตรฐาน

ดังนั้น เพื่อให้มาตรการการถ่ายภาพรังสีมีมาตรฐาน สามารถบรรลุเป้าหมายดังกล่าวในการให้บริการถ่ายภาพรังสีทั่วไปแก่ท่านทุกครั้ง นักรังสีการแพทย์จำเป็นต้องได้รับข้อมูลเกี่ยวกับท่านก่อนการถ่ายภาพรังสีทั่วไปอันได้แก่ การตรวจสอบอายุ ชั่งน้ำหนัก วัดส่วนสูง และวัดความหนาบริเวณกึ่งกลางของส่วนของร่างกายที่แพทย์ผู้ทำการรักษาต้องการให้เข้ารับบริการการถ่ายภาพทางรังสีทั่วไป

หากท่านตกลงที่จะเข้าร่วมการศึกษาวิจัยนี้ จะมีข้อปฏิบัติร่วมดังนี้

- ท่านผู้เข้าร่วมการศึกษานี้ เป็นผู้ป่วยที่ต้องมีคำร้องขอเข้ารับการวินิจฉัยด้วยภาพรังสีทั่วไปจากแพทย์ผู้ตรวจท่านนั้น เป็นผู้ได้รับเกียรติที่ผ่านเกณฑ์การคัดเลือกกลุ่มตัวอย่างตามแบบฟอร์มโครงการงานวิจัยที่ได้รับอนุมัติจากคณะกรรมการพิจารณาจริยธรรมแล้ว รวมทั้งสิ้นอย่างน้อย 1,384 การตรวจ ภายในช่วงระยะเวลา 3 เดือนของการเก็บข้อมูล
- ท่านจะเสียค่าตรวจวินิจฉัยด้วยภาพรังสีเฉพาะในส่วนของการถ่ายภาพรังสีที่แพทย์ผู้ตรวจส่งตรวจท่านนั้น ต้องไม่มีค่าใช้จ่ายใดๆ เพิ่มเติมจากค่าตรวจปกติทั้งสิ้น
- การศึกษานี้เป็นการเก็บข้อมูลที่เป็นในการกำหนดปริมาณรังสีแก่ผู้ป่วยที่เข้ารับการวินิจฉัยด้วยภาพรังสีที่พึงปฏิบัติตามปกติวิสัยของการถ่ายภาพรังสีทั่วไป
- การศึกษานี้เป็นการเก็บข้อมูลความบกพร่องที่อาจเกิดขึ้นบนภาพรังสี มิได้เป็นการให้หรือละเว้นการให้สิ่งใดแก่ผู้เข้าร่วมการศึกษานี้
- การศึกษานี้เป็นความพยายามเพิ่มคุณภาพและมาตรฐาน อีกทั้งช่วยยืดอายุการใช้งานเครื่องมือและอุปกรณ์ร่วมในการถ่ายภาพรังสีทั่วไป
- ก่อนการถ่ายภาพรังสีทั่วไปทุกครั้ง ท่านจะได้รับทราบข้อมูลของการถ่ายภาพทางรังสีทั่วไปจากนักรังสีการแพทย์ที่ทำการเก็บข้อมูลตามความเป็นจริง อันได้แก่ ส่วนของร่างกายที่จะได้รับการถ่ายภาพรังสี จำนวนภาพรังสีที่เกิดขึ้น และวิธีการปฏิบัติตัวระหว่างการรับบริการการถ่ายภาพรังสี
- ในระหว่างการถ่ายภาพรังสีทั่วไป ท่านต้องปฏิบัติตามคำแนะนำของนักรังสีการแพทย์ผู้ปฏิบัติงาน เพื่อป้องกันการถ่ายภาพรังสีซ้ำ
- กรณีที่จำเป็นต้องทำการถ่ายภาพรังสีทั่วไปซ้ำ อันเนื่องมาจากสาเหตุใดๆก็ตาม นักรังสีการแพทย์ผู้ปฏิบัติงานจะต้องชี้แจงเหตุผลตามความเป็นจริงแก่ท่านทุกครั้งก่อนทำการถ่ายภาพรังสีทั่วไปซ้ำ
- การเข้าร่วมการศึกษานี้ เป็นไปโดยสมัครใจ ท่านอาจปฏิเสธที่จะเข้าร่วมการศึกษานี้ โดยไม่กระทบต่อการให้บริการการตรวจวินิจฉัยที่ท่านจะได้รับจากนักรังสีการแพทย์ นักฟิสิกส์การแพทย์และรังสีแพทย์ หรือผู้ให้บริการท่านอื่นๆ

ประการสำคัญที่ท่านควรทราบ คือ

ผลของการศึกษานี้จะใช้สำหรับวัตถุประสงค์ทางวิชาการเท่านั้น

ขอรับรองว่าจะไม่มีการเปิดเผยชื่อของท่านตามกฎหมาย

หากท่านมีปัญหาคหรือข้อสงสัยประการใด กรุณาติดต่อ นางเพชรลิข์ สุวรรณประดิษฐ์ สาขาวิชา
 ฉายาเวชศาสตร์ ภาควิชารังสีวิทยา คณะแพทยศาสตร์ จุฬาลงกรณ์มหาวิทยาลัย โทรฯ 02-
 2564417 หรือ 02-9851000 ซึ่งยินดีให้คำตอบแก่ท่านทุกเมื่อ

ขอขอบพระคุณในความร่วมมือของท่านมา ณ ที่นี้

ใบยินยอมเข้าร่วมการศึกษา (Consent form)

Study No.

เลขที่ผู้ป่วย..... ชื่อ และ นามสกุล

ข้าพเจ้าได้รับทราบจากนักรังสีการแพทย์ผู้ทำการเก็บข้อมูลตามความเป็นจริง ซึ่งได้ลงนามด้านท้ายของหนังสือนี้ ถึงวัตถุประสงค์และวิธีการเข้าร่วมการศึกษานี้เป็นที่เรียบร้อยแล้ว

ข้าพเจ้ายินดีให้นำข้อมูลภาพรังสีและข้อมูลที่ทำเป็นในการวิเคราะห์ของข้าพเจ้า แก่นักรังสีการแพทย์ผู้ทำการเก็บข้อมูล เพื่อประโยชน์ในการศึกษาวิจัยครั้งนี้ ได้แก่

อายุ.....ปี น้ำหนัก.....กิโลกรัม ส่วนสูง.....ซม
ความหนาบริเวณกึ่งกลางของส่วนของร่างกายที่ได้รับการถ่ายภาพรังสี.....ซม

ข้าพเจ้ายินดีเข้าร่วมการศึกษานี้โดยสมัครใจ โดยไม่มีการบังคับหรือให้อามิสสินจ้างใดๆ และข้าพเจ้าอาจปฏิเสธการเข้าร่วมการศึกษานี้เมื่อใดก็ได้ โดยไม่จำเป็นต้องแจ้งเหตุผล

ข้าพเจ้าได้รับทราบและเข้าใจข้อมูลจากนักรังสีการแพทย์ผู้ให้บริการถ่ายภาพรังสี จะปฏิบัติตามคำแนะนำขณะเข้ารับบริการถ่ายภาพรังสีทั่วไปตามใบคำร้องขอของแพทย์ผู้ส่งตรวจ และยอมรับฟังเหตุผลของการถ่ายภาพรังสีซ้ำ หากเกิดกรณีสุดวิสัยแห่งความบกพร่องของภาพรังสีทุกประการ

สุดท้ายนี้ ข้าพเจ้ายินดีเข้าร่วมการศึกษานี้ ภายใต้เงื่อนไขที่ระบุไว้ข้างต้น

...../...../.....254.....

เอกซเรย์ผู้ป่วยนอก ตึก ภปร. ชั้น 4-วันที่/ เดือน / ปี ()

ลงนามผู้ป่วย หรือผู้ปกครองโดยชอบด้วยกฎหมาย

.....

(นางฉวี ฤชาพันธ์)

(นายบุญชัย นิตยสุภาภรณ์)

พยาน

นักรังสีการแพทย์ผู้ทำการเก็บข้อมูล

.....

()

(นางเพ็ชรลีย์ สุวรรณประดิษฐ์)

นักรังสีการแพทย์ผู้ให้บริการถ่ายภาพรังสี

ผู้ทำการศึกษาวิจัย

VITAE

Name: Mrs. Petcharleeya SUWANPRADIT

Date of birth: November 9, 1964

Place of birth: Banpong, Ratchburi, Thailand

Qualification:

- Bachelor of Science (Health Education), Bansomdejchaopraya Teachers' College, 1993.
- Bachelor of Science (Radiological Technology), Ramkhamhaeng University, 1997.

Job experiences:

- Radiological Technologist of Department of Radiology, King Chulalongkorn Memorial Hospital, Thai Red Cross Society for 18 years.
- Lecturer in Radiological Technique subject for Radiological Technology Students of King Chulalongkorn Memorial Hospital, Thai Red Cross Society for 8 years.
- JICA's trainee in Radiological technology field for twice in Nagoya and Osaka, Japan, 1995 and 2001.

Present position: Radiological Technologist of Department of Radiology, King Chulalongkorn Memorial Hospital, Thai Red Cross Society.

King Chulalongkorn Memorial Hospital, Thai Red Cross Society's Grant had been supported for Master Degree of Science (Medical Imaging), Department of Radiology, Faculty of Medicine, Chulalongkorn University.

สถาบันวิทยบริการ
จุฬาลงกรณ์มหาวิทยาลัย